

January
-
August
2017

Effects of sterol-O-acyl transferase 1 (SOAT1) inhibitors in canine adrenocortical cells: *in vitro* investigation

Master research internship of G.J. van Staalduinen BSc (4068491)

Under the supervision of:

K. Sanders, DVM PhD candidate

S. Galac, DVM PhD

UTRECHT UNIVERSITY | Faculty of Veterinary Medicine, Department of Clinical Sciences of Companion Animals, Yalelaan 104, 3584 CM, Utrecht, the Netherlands

Abstract

Current medical treatment options in dogs with cortisol-secreting adrenocortical adenomas (ACAs) and adrenocortical carcinomas (ACCs) are limited. Therefore, there is a strong need of new medical therapies. Recently, sterol-O-acyl-transferase 1 (SOAT1) inhibitors Sandoz 58-035 (S035) and ATR-101 regained attention. By inhibiting SOAT1, free cholesterol and fatty acids accumulate, leading to endoplasmic reticulum stress (ER-stress). ER-stress activates the unfolded protein response (UPR), ultimately leading to apoptosis and thereby decreased steroidogenesis. Inhibition of SOAT1 could thus be an interesting therapy option in dogs with cortisol-secreting adrenocortical tumors (ATs), but can only be useful if canine ATs express SOAT1.

The aim of this study was to determine whether the use of SOAT1 inhibitors could have potential in the treatment of canine ATs. Quantitative real-time polymerase chain reaction (RT-qPCR) and immunohistochemistry (IHC) revealed SOAT1 expression at the mRNA and protein level in all ACAs and ACCs. Expression did not significantly differ between the groups, although expression was more variable in ACCs. After 24 hours, the cortisol concentration, determined by radioimmunoassay (RIA), of ACTH-stimulated normal adrenocortical cells (n=4) incubated with mitotane or ATR-101 decreased. The cortisol concentrations at the maximum compound concentration (100 μ M mitotane, 100 nM ATR-101) were 32.9% \pm 54.2 and 28.8% \pm 31.2, respectively. S035 did not decrease the cortisol concentration of ACTH-stimulated normal adrenocortical cells. The cortisol concentrations of mitotane and ATR-101 incubated ACC cells (n=1) were decreased (8.5% and 65.5%, respectively). S035 did not reduce the cortisol concentration of ACC cells. Mitotane and ATR-101 increased apoptosis of non-stimulated normal adrenocortical cells (n=2), determined by the Caspase-Glo[®] 3/7 Assay, with 476.0% \pm 132.5 and 433.5% \pm 19.7, respectively. S035 had little effect on apoptosis of normal adrenocortical cells. In non-stimulated ACC cells (n=1), mitotane, S035 and ATR-101 increased apoptosis (842.7%, 372.8% and 571.0%, respectively). After 6 hours, the UPR seemed to be activated in mitotane incubated non-stimulated and ACTH-stimulated ACC cells. The UPR was activated to some extent in S035 and ATR-101 incubated non-stimulated and ACTH-stimulated ACC cells (n=1).

Current study has brought important preliminary data on SOAT1 inhibitors in dogs. It will serve as a solid base for further studies about SOAT1 inhibitors in humans and dogs, which we are setting up in cooperation with the Endocrine research group from the Medical Center from Würzburg, Germany.

Keywords: ATR-101, dogs, endoplasmic reticulum stress, mitotane, Sandoz 58-035, sterol-O-acyl transferase 1, unfolded protein response.

Abbreviations

ACA(s)	Adrenocortical adenoma(s)
ACC(s)	Adrenocortical carcinoma(s)
AT(s)	Adrenocortical tumor (s)
ATF4	Activating transcription factor 4
ATF6(n)	Activating transcription factor 6 (nucleus)
ACTH	Adrenocorticotrophic hormone
BAX	BCL-2 associated X
BCL-2	B-cell lymphoma 2
BAK	BCL-2 homologous antagonist killer
Casp3	Caspase 3
CHOP	CCAAT/enhancer-binding protein homologous protein
CYP17	17 α -hydroxylase
EDEM1	ER degradation enhancing α -mannosidase like protein 1
ERAD	ER-associated protein degradation
ERP72	ER protein 72
ER	Endoplasmic reticulum
ER-stress	Endoplasmic reticulum stress
(p)-eIF2α	(Phosphorylated) eukaryotic initiation factor 2 α
GRP78	Glucose-regulated protein 78kDa
Herp	Homocysteine-induced endoplasmic reticulum protein
HERPUD1	Homocysteine inducible endoplasmic reticulum protein with ubiquitin like domain 1
IRE1	Inositol-requiring protein 1
NA(s)	Normal adrenal(s)
PERK	Protein kinase RNA (PKR)-like ER kinase
p58^{ipk}	DnaJ heat shock protein family member C3
SCAP	SREBP cleavage activating protein
SOAT1/2	Sterol-O-acyl transferase 1/2
SREBF1/2	Sterol regulatory element-binding transcription factor 1/2
SREBP1/2	Sterol regulatory element-binding protein 1/2

S035	Sandoz 58-035
s/uXBP1	Spliced/unspliced X-box binding protein 1
UPR	Unfolded protein response
zF	Zona fasciculata
zG	Zona glomerulosa
zR	Zona reticularis

Contents

Abstract	1
Abbreviations	2
Chapter 1: Introduction	6
Paragraph 1.1: The adrenal glands.....	6
Paragraph 1.2: Cushing’s Syndrome.....	6
Paragraph 1.3: SOAT1 inhibition	8
Paragraph 1.4: ER-stress and the UPR.....	9
Paragraph 1.5: SREBPs.....	11
Paragraph 1.6: SOAT1 inhibitors’ mechanism of action.....	11
Chapter 2: Aim of the study	13
Chapter 3: Materials and methods	14
Paragraph 3.1: SOAT1 expression	14
Paragraph 3.1.1: Animals and tissues.....	14
Paragraph 3.1.2: Histopathology.....	14
Paragraph 3.1.3: RT-qPCR.....	14
Paragraph 3.1.4: Western Blot	15
Paragraph 3.1.5: IHC.....	15
Paragraph 3.1.6: Statistics	16
Paragraph 3.2: In vitro studies	16
Paragraph 3.2.1: Animals	16
Paragraph 3.2.2: Cell suspensions	16
Paragraph 3.2.3: Compounds.....	17
Paragraph 3.2.4: Cortisol and protein measurements	17
Paragraph 3.2.5: Viability, cytotoxicity and apoptosis	17
Paragraph 3.2.6: Lipidomics	18
Paragraph 3.2.7: Fluorescent imaging of lipid droplets	18
Paragraph 3.2.8: RT-qPCR.....	19
Paragraph 3.2.9: Western Blot	20
Paragraph 3.2.10: Statistics	20
Chapter 4: Results	21
Paragraph 4.1: SOAT1 expression	21
Paragraph 4.1.1: Western Blot	21
Paragraph 4.1.2: SOAT1 mRNA and protein expression	21

Paragraph 4.2: In vitro studies	28
Paragraph 4.2.1: Cortisol concentration	28
Paragraph 4.2.2: Viability, cytotoxicity and apoptosis	32
Paragraph 4.2.3: Lipidomics	37
Paragraph 4.2.4: Lipid droplets	38
Paragraph 4.2.5: ER-stress and the UPR.....	39
Chapter 5: Discussion and Conclusion	44
Paragraph 5.1: SOAT1 expression	44
Paragraph 5.2: In vitro studies	45
Paragraph 5.2.1: Steroidogenesis.....	45
Paragraph 5.2.2: Viability and apoptosis.....	46
Paragraph 5.2.3: SOAT1 and cholesterol esterification	47
Paragraph 5.2.4: ER-stress and the UPR.....	48
Acknowledgements	51
References.....	52
Appendix	59
Appendix 1: Animals.....	59
Appendix 2: SOAT1 protein expression.....	63
Appendix 2.1: ACAs	63
Appendix 2.2: ACCs.....	68
Appendix 2.3: Control tissues.....	72
Appendix 3: Primers	73
Appendix 4: Absolute data	75
Appendix 4.1: Pilot study 1.....	75
Appendix 4.2: Pilot study 2.....	78
Appendix 4.3: Follow-up cortisol.....	79
Appendix 4.4: ApoTox-Glo™ Triplex Assay	82
Appendix 4.5: Follow-up apoptosis and viability	83
Appendix 5: Lipidomics.....	86

Chapter 1: Introduction

Paragraph 1.1: The adrenal glands

The bilateral adrenal glands are situated craniomedial to the corresponding kidneys and are composed of the medulla, the cortex and a capsule. The enclosing mesenchymal capsule, consisting of fibroblasts and myofibroblast, contains an arterial plexus. Arterials derived from the plexus, together with nerves, travel to the underlying cortex via trabeculae. Underneath the capsule, the outermost zona of the mesodermal cortex is localized: the zona glomerulosa (zG).¹⁻⁴

The zG consists of small, lipid-poor cells arranged in clusters. The zG cells are responsible for the production of mineralocorticoids (e.g. aldosterone) and cannot produce cortisol or androgens, since zG cells lack 17 α -hydroxylase activity. Secretion of aldosterone is influenced by the renin-angiotensin system and potassium and influences blood pressure by regulating the amount of sodium retention by the kidneys.¹⁻⁴

Beneath the zG, a thick layer of lipid-rich cells arranged in columns, the zona fasciculata (zF), is visible. The zF produces mainly glucocorticoids, but also a small number of androgens. In dogs, the end product of the glucocorticoid pathway is cortisol. Cortisol affects metabolism, cardiovascular system and immune system.¹⁻⁴ The synthesis and release of cortisol is dependent on a negative feedback loop involving adrenocorticotropic hormone (ACTH), secreted by the anterior lobe of the pituitary, and corticotropin-releasing hormone, secreted by the hypothalamus. Corticotropin-releasing hormone increases ACTH secretion resulting in increased cortisol secretion by the adrenals. Cortisol inhibits the secretion of ACTH and corticotropin-releasing hormone: the hypothalamic-pituitary-adrenal axis.⁴

Lastly, the innermost zona, the zona reticularis (zR), contains columns of cells with granular cytoplasm. The zR cells produce mainly androgens (e.g. androstenedione) and to a lesser extent cortisol. Together, the zF and zR function as a single unit in the cortisol production.¹⁻⁴

Adjacent to the zR lies the medulla, which contains epithelial cells surrounded by venous sinusoids. The neuroectodermal cells of the medulla produce catecholamines (norepinephrine and epinephrine).¹⁻⁴

Paragraph 1.2: Cushing's Syndrome

Cushing's syndrome (hypercortisolism) is one of the most common endocrinopathies in middle-aged and older dogs. There is no gender or obvious breed predilection. Small breed dogs show a slight predilection. About 80-85% of cases are ACTH-dependent, most often the result of excessive secretion of ACTH by a pituitary corticotroph adenoma. In the remaining cases, hypercortisolism is ACTH-independent, the result of excessive secretion of glucocorticoids by an adrenocortical adenoma (ACA) or an adrenocortical carcinoma (ACC).⁴

The clinical signs of dogs suffering from hypercortisolism are due to the actions of glucocorticoids: increased gluconeogenesis, lipogenesis and protein breakdown. Possible clinical signs are polyphagia, centripetal obesity, muscle atrophy, alopecia and skin atrophy, polyuria and polydipsia.^{4,5} Other clinical signs may develop secondary due to mass-occupying effects of a pituitary tumor or adrenocortical tumor (AT). A pituitary tumor may cause neurologic signs such as inappetence, anorexia, stupor, circling, aimless wandering, pacing, ataxia and behavioral alterations. ACCs may cause retroperitoneal hemorrhage, blood loss anemia and abdominal pain due to invasion of the caudal vena cava, the phrenico abdominal vein or both. ACCs could also initiate the development of a thrombus, subsequently leading to ascites or paresis.⁵

The diagnosis of hypercortisolism involves demonstration of an increased cortisol production and decreased sensitivity to glucocorticoid feedback using the intravenous low-dose dexamethasone suppression test or urinary corticoid to creatinine ratios combined with the high-dose dexamethasone

suppression test. ACTH measurements and diagnostic imaging are additional techniques to discriminate between ACTH-dependent or ACTH-independent hypercortisolism.^{4,5}

ACTH-independent hypercortisolism is treated by adrenalectomy or medical therapy. When there are no visible metastases and there is no extensive vascular invasion, surgically removing the unilateral AT is the treatment of choice. Adrenalectomy is the treatment of choice, because the unilateral AT will be removed and the clinical signs of hypercortisolism will resolve.^{4,6} However, surgery is invasive and can only be performed at specialized institutions.^{7,8} The affected adrenal is usually removed via a ventral midline or paracostal approach.⁸ Laparoscopic adrenalectomy is another method to remove ATs, although less frequently performed.⁹ Advantages of laparoscopic adrenalectomy compared to open adrenalectomy are lower perioperative death, shorter surgical time, shorter hospitalization time and rapid discharge from the hospital after surgery.¹⁰ At the time of anesthesia, substitution of cortisol is indicated, because the remaining adrenal is atrophic and not or almost not producing cortisol. Subsequently, the dosage cortison acetate is decreased over a period of 6 till 8 weeks after surgery, after which the remaining adrenal is solely responsible for cortisol production. In case of bilateral adrenalectomy, lifelong substitution of glucocorticoids, mineralocorticoids and salt is indicated.^{6,8}

In case of visible metastases, extensive vascular invasion, recurrence or incomplete removal of an AT, hypercortisolism is managed medically.^{4,6} Currently, there are two types of drugs: the adrenocorticolytic drug Lysodren® (mitotane) and the adrenocorticostatic drug Vetoryl® (trilostane). Adrenocorticolytic drugs destroy adrenocortical cells, which is responsible for the steroidogenesis reducing effect. Adrenocorticostatic drugs interfere with steroidogenesis, remaining adrenocortical cells intact.⁴

The exact mechanism of action of the adrenocorticolytic drug mitotane is unknown and is currently the focus of research.¹¹ After and while mitotane therapy, substitution of glucocorticoids, mineralocorticoids and salt is indicated, because adrenocortical (tumor) cells are (being) destroyed.¹²⁻¹⁴ Mitotane causes extensive adverse effects in dogs. Symptoms of mitotane intoxication are, for example, anorexia, vomiting, lethargy, weakness, diarrhea and ataxia.¹³⁻¹⁵ Therefore, the veterinarian has to give clear instructions to the owners regarding recognizing and responding to intoxication signs. In case of intoxication signs, mitotane therapy is discontinued, while substitution therapy is continued. Mitotane is potentially toxic to humans and thus should not be administered to dogs living in households in which there is a pregnant woman or are young children.⁴

The second medical treatment option is trilostane.^{4,6} Trilostane is a competitive inhibitor of the 3 β -hydroxysteroid dehydrogenase/isomerase system and 11 β -hydroxylase. The 3 β -hydroxysteroid dehydrogenase/isomerase system and 11 β -hydroxylase are important in catalyzing steroidogenic reactions, ultimately resulting in the formation of aldosterone, cortisol and androstenedione. Trilostane only inhibits steroid hormone synthesis, thereby improving clinical signs, but does not affect tumor growth.¹⁶ Therefore, trilostane therapy is classified as palliative. In contrast to mitotane, trilostane is usually well tolerated¹⁷, but there is a marked variation in the optimal dose. This obligates regular check-ups and dose adjustments, in order to avoid trilostane overdose, which may potentially lead to a life threatening cortisol and mineralocorticoid deficiency.^{12,16,18} Trilostane is not toxic to humans and can thus be easily administered.¹⁶

In the light of the limitations of mitotane and trilostane, a new adrenal-specific, nontoxic and AT destroying medical therapy is warranted.

Paragraph 1.3: SOAT1 inhibition

Currently, research is focused on clarifying the mechanism of action of mitotane in order to develop structurally related compounds. A tumor destroying medical therapy similar to mitotane, but with less extensive side effects is warranted. Research into the mechanism of action of mitotane, revealed that sterol-O-acyl-transferase 1 (SOAT1) inhibition is part of the mechanism of action of mitotane.¹¹

SOAT, an enzyme localized in the endoplasmic reticulum (ER) membranes, also known as acyl-coenzyme A: cholesterol O-acyltransferase, catalyzes the conversion of free cholesterol and fatty acids to cholesteryl esters, using ATP and coenzyme A as cofactors. Cholesterol esters are visible as lipid droplets in the adrenocortical cell: the storage form of cholesterol.^{19,20} Cholesterol esterification, resulting in a decreased amount of free cholesterol, is very important, because free cholesterol is toxic to (adrenocortical) cells.²¹

There are two types of SOAT: SOAT1 and SOAT2, encoded by the SOAT1 and SOAT2 genes.²⁰ SOAT1 is expressed in almost every tissue. The adrenocortical SOAT1 expression is high, while SOAT2 is (almost) not expressed. SOAT2 is highly expressed in the intestines and liver.²²

Cholesterol, stored in lipid droplets by the action of SOAT1, is the precursor molecule for adrenal steroidogenesis. Hormone sensitive lipase deesterifies esterified cholesterol preceding entering the mitochondria via steroidogenic acute regulatory protein.^{23,24} Within the mitochondria, cholesterol is processed by cytochrome P450 side chain cleavage into pregnenolone. Via several steroidogenic enzymes, pregnenolone is converted into aldosterone, cortisol and androstenedione: the end products of adrenocortical steroidogenesis.²⁵

Incubating the human adrenocortical cell line NCI-H295R and liver cancer cell line HepG2 with mitotane, resulted in a time- and dose-dependent increase of free cholesterol and fatty acids and in a decrease of cholesteryl esters in the human adrenocortical cell line NCI-H295R, but not in the human liver cancer cell line HepG2.¹¹ These results suggested that mitotane, specifically acting on adrenocortical cells, is a SOAT1 inhibitor, because SOAT1 normally creates cholesteryl esters using free cholesterol and fatty acids. Similar to mitotane, Sandoz 58-035 (S035), a compound that has been used for years in order to specifically inhibit SOAT1²¹, decreased cholesteryl esters and increased free cholesterol in the NCI-H295R cell line.¹¹ With SOAT1 inhibition being part of the mechanism of action of mitotane, LaPensee *et al.* 2016 researched whether ATR-101 was capable of inhibiting SOAT1. ATR-101 increased free cholesterol and decreased cholesteryl esters in the NCI-H295R cell line, indicating that ATR-101 is a SOAT1 inhibitor (figure 1).²⁶

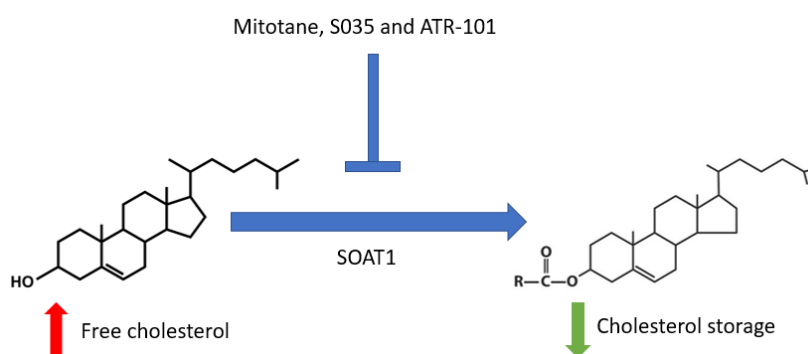


Figure 1: Inhibition of sterol-O-acyl transferase 1 (SOAT1) by mitotane, Sandoz 58-035 (S035) and ATR-101. SOAT1 normally esterifies free cholesterol into cholesteryl esters, which is the storage form of cholesterol in the adrenal gland. Inhibition of SOAT1 by mitotane, S035 and ATR-101 leads to an increased level of toxic free cholesterol. Adapted from Sbiere *et al.* 2015 and LaPensee *et al.* 2016.^{11,26}

SOAT1 inhibitors mitotane, S035 and ATR-101 of course require their target enzyme SOAT1 in order to increase free cholesterol levels. Sbierra *et al.* 2015 determined SOAT1 protein expression by means of immunohistochemistry (IHC) in human ACAs, ACCs and metastases. SOAT1 protein expression in ACAs was strong, while SOAT1 protein expression of ACCs was more variable. SOAT1 protein expression in metastases was low.¹¹

Paragraph 1.4: ER-stress and the UPR

In order to understand the complete mechanism of action of mitotane, S035 and ATR-101, the role of endoplasmic reticulum stress (ER-stress) and the unfolded protein response (UPR) first needs to be elucidated.

The ER is a cell organelle that is important in protein synthesis, protein modification, lipid metabolism and calcium storage. ER-stress is a condition characterized by the accumulation of unfolded proteins in the ER lumen. In response to accumulation of proteins, the cell initiates the UPR.²⁷ The UPR consists of two phases: the adaptive phase and the apoptotic phase.

In the adaptive phase, the UPR is responsible for reducing the number of polypeptides entering the ER, increasing the expression of ER-chaperones that enhance protein folding, initiating a system to eliminate misfolded proteins called ER-associated protein degradation (ERAD) and expanding the ER. The goal of the adaptive phase is to restore ER homeostasis.^{27,28}

ER-stress is sensed by three transmembrane signal transducers: activating transcription factor 6 (ATF6), inositol-requiring protein 1 (IRE1) and protein kinase RNA (PKR)-like ER kinase (PERK).²⁷ The luminal domain of ATF6 is bound to glucose-regulated protein 78kDa (GRP78). Upon ER-stress, GRP78 dissociates and ATF6 is transported to the Golgi Apparatus of the cell.²⁹ Within the Golgi Apparatus, ATF6 is cleaved by site-1 protease and site-2 protease.³⁰ The resulting ATF6 nucleus (ATF6n) is now able to enter the nucleus and functions like a transcription factor for ER-chaperon GRP78, ER-co-chaperon DnaJ heat shock protein family member C3 (p58^{ipk}), folding enzymes like ER protein 72 (ERP72) and ERAD component homocysteine-induced endoplasmic reticulum protein (Herp).³¹⁻³³ In addition, ATF6 is responsible for the transcription of unspliced X-box binding protein (uXBP1). After uXBP1 transcription, IRE1 is able to splice uXBP1 mRNA (figure 2).^{34,35}

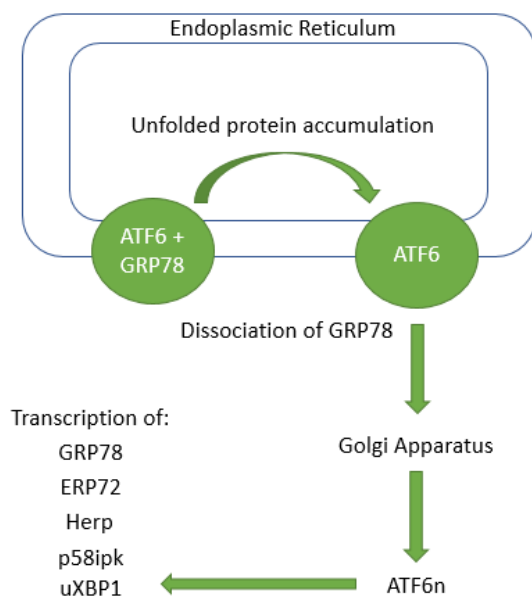


Figure 2: The activating transcription factor 6 (ATF6) pathway of the unfolded protein response. Upon accumulation of unfolded proteins, glucose regulated protein 78 (GRP78) dissociates and after cleavage of ATF6 in the Golgi Apparatus, ATF6 nucleus (ATF6n) regulates the transcription of GRP78, ER protein 72 (ERP72), homocysteine-induced endoplasmic reticulum protein (Herp), DnaJ heat shock protein family member C3 (p58^{ipk}) and unspliced X-box binding protein 1 (uXBP1). Adapted from Ye *et al.* 2000, Yoshida *et al.* 2001, Okada *et al.* 2002, Shen *et al.* 2002, Yamamoto *et al.* 2002, Yoshida *et al.* 2003 and Adachi *et al.* 2008.²⁹⁻³⁵

IRE1 becomes active upon GRP78 dissociation in response to unfolded proteins.³⁶ Consequently, IRE1 gains RNase activity by auto phosphorylation. The RNase activity of IRE1 is responsible for the splicing of uXBP1. Splicing involves deleting an intron of 26 nucleotides resulting in spliced XBP1 (sXBP1).^{35,37,38} sXBP1 is a transcription factor which initiates the transcription of different UPR target genes, for example GRP78 and ER degradation enhancing α -mannosidase like protein 1 (EDEMI) (figure 3).³⁹ The transcription of EDEMI, an ERAD component, is solely dependent on sXBP1³⁴ and the transcription of GRP78 could also be induced by ATF6 (as described previously).

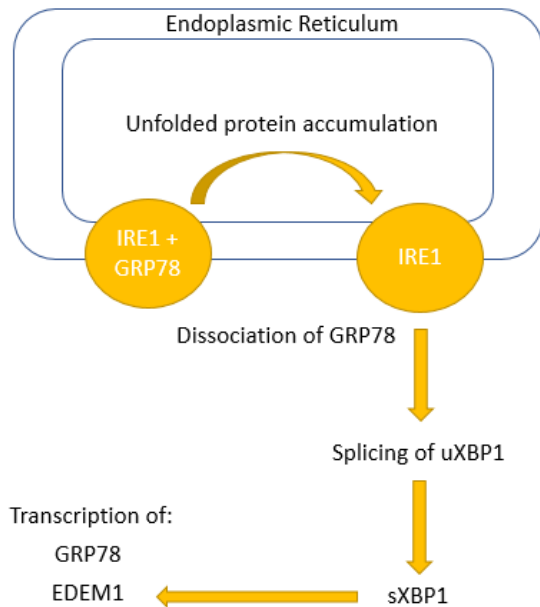


Figure 3: The inositol-requiring protein 1 (IRE1) pathway of the unfolded protein response. Upon accumulation of unfolded proteins, glucose regulated protein 78 (GRP78) dissociates and IRE1 gains RNase activity in order to splice unspliced X-box binding protein (uXBP1). The resulting spliced XBP1 (sXBP1) regulates transcription of GRP78 and ER degradation enhancing α -mannosidase like protein 1 (EDEMI). Adapted from Bertolotti et al. 2000, Yoshida et al. 2001, Calton et al. 2002, Lee et al. 2002, Lee et al. 2003 and Yoshida et al. 2003.³⁴⁻³⁹

GRP78 is normally, i.e. amongst non-ER-stress conditions, bounded to PERK. Upon ER-stress, GRP78 dissociates from PERK.³⁶ Via auto phosphorylation, PERK becomes active and phosphorylates eukaryotic initiation factor 2 alpha (eIF2 α) at serine 51. Phosphorylated eIF2 α (p-eIF2 α) decreases protein synthesis and initiates transcription of activating transcription factor 4 (ATF4).⁴⁰ ATF4 is responsible for the select transcription of ER-chaperons and ERAD components. ATF4 also upregulates the expression of genes involved in amino acid metabolism and redox control (figure 4).^{27,41}

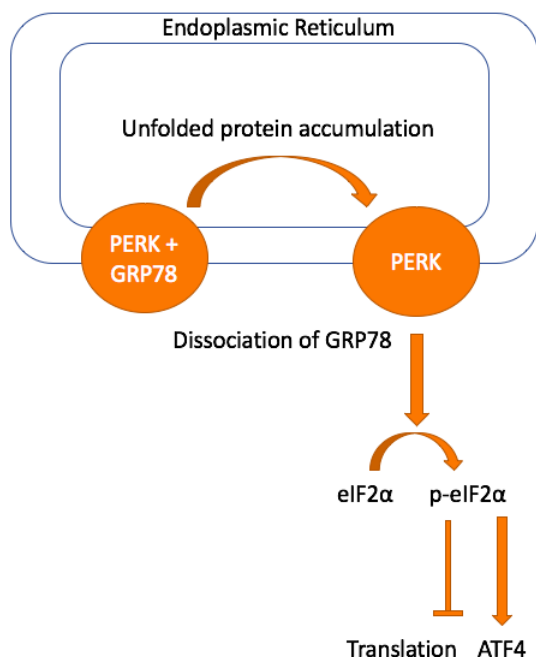


Figure 4: The protein kinase RNA (PKR)-like ER kinase (PERK) pathway of the unfolded protein response. Upon accumulation of unfolded proteins, glucose regulated protein 78 (GRP78) dissociates and PERK phosphorylates eukaryotic initiation factor 2 alpha (eIF2 α). Phosphorylated eIF2 α (p-eIF2 α) reduces protein translation and transcribes ATF4. Adapted from Harding et al. 1999, Bertolotti et al. 2002, Harding et al. 2003 and Brewer et al. 2014.^{27,36,40,41}

Despite the efforts of the UPR, homeostasis cannot always be restored, resulting in the initiation of the apoptotic phase. ATF4 induces the transcription of CCAAT/enhancer-binding protein homologous protein (CHOP).⁴²⁻⁴⁴ ATF6 could also induce the transcription of CHOP.^{32,45} CHOP decreases B-cell lymphoma 2 (BCL-2) expression, thereby releasing several pro-apoptotic factors important for the initiation of BCL-2 associated X/BCL-2 homologous antagonist killer (BAX/BAK) mediated permeabilization of the mitochondrial membrane. Due to the permeabilization, cytochrome c is released. Cytochrome c triggers caspase activation and apoptosis.^{27,46}

Paragraph 1.5: SREBPs

In addition to ER-stress and the UPR, sterol regulatory element-binding transcription proteins (SREBPs) might also play a role in the mechanism of action of SOAT1 inhibitors mitotane, S035 and ATR-101.

There are three SREBPs: SREBP1a, SREBP1c and SREBP2. The SREBPs are encoded by two genes: sterol regulatory element-binding transcription factor 1 and 2 (SREBF1 and SREBF2). SREBPs are transcription factors of enzymes involved in lipid and cholesterol synthesis. All SREBPs are inactive transcription factors, which are, together with SREBP cleavage activating protein (SCAP), connected to the ER membrane, forming the SREBP-SCAP complex. The SREBP-SCAP complex has a sterol-sensing domain. If sterols, like cholesterol, are present, SREBP-SCAP interacts with insulin-induced protein 1 and 2. If the number of sterols decreases, insulin-induced proteins release and SCAP brings SREBP to the Golgi Apparatus. Here, SREBP is cleaved by site-1 and site-2 proteases. The amino-terminus is then able to enter the nucleus and functions like a transcription factor. SREBP1 activates genes involved in lipid metabolism. SREBP2 activates genes involved in cholesterol metabolism (figure 5).⁴⁷

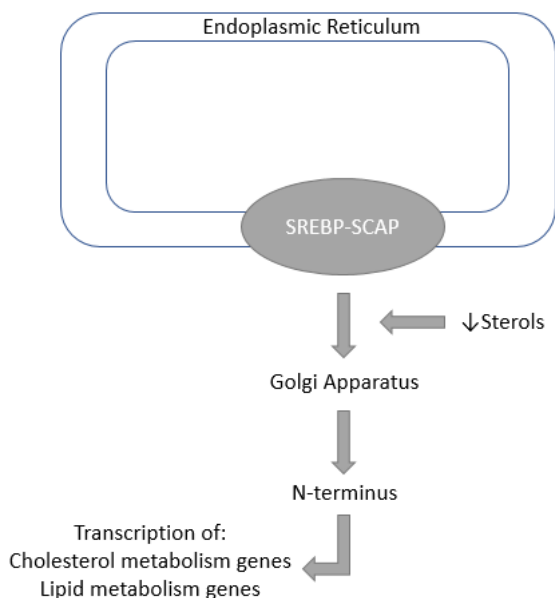


Figure 5: The sterol regulatory element-binding transcription protein (SREBP) and SREBP cleavage activating protein (SCAP) complex. When the level of sterols decreases, the SREBP-SCAP complex is released from the ER membrane. SCAP brings SREBP to the Golgi Apparatus where it is cleaved. Its N-terminus functions like a transcription factor for genes involved in cholesterol and lipid metabolism. Adapted from Xiaoping *et al.* 2012.⁴⁷

Paragraph 1.6: SOAT1 inhibitors' mechanism of action

Current proposed mechanism of action of mitotane, S035 and ATR-101 is represented in figure 6. Inhibition of SOAT1 results in an increase of free cholesterol and fatty acids. The increased amount of free cholesterol causes ER-stress. ER-stress initiates the UPR, which ultimately leads to apoptosis. Cortisol production decreases due to apoptosis, because less cells are left to produce cortisol. In addition, downregulation of SREBF and SREBF-dependent genes could decrease cortisol production.

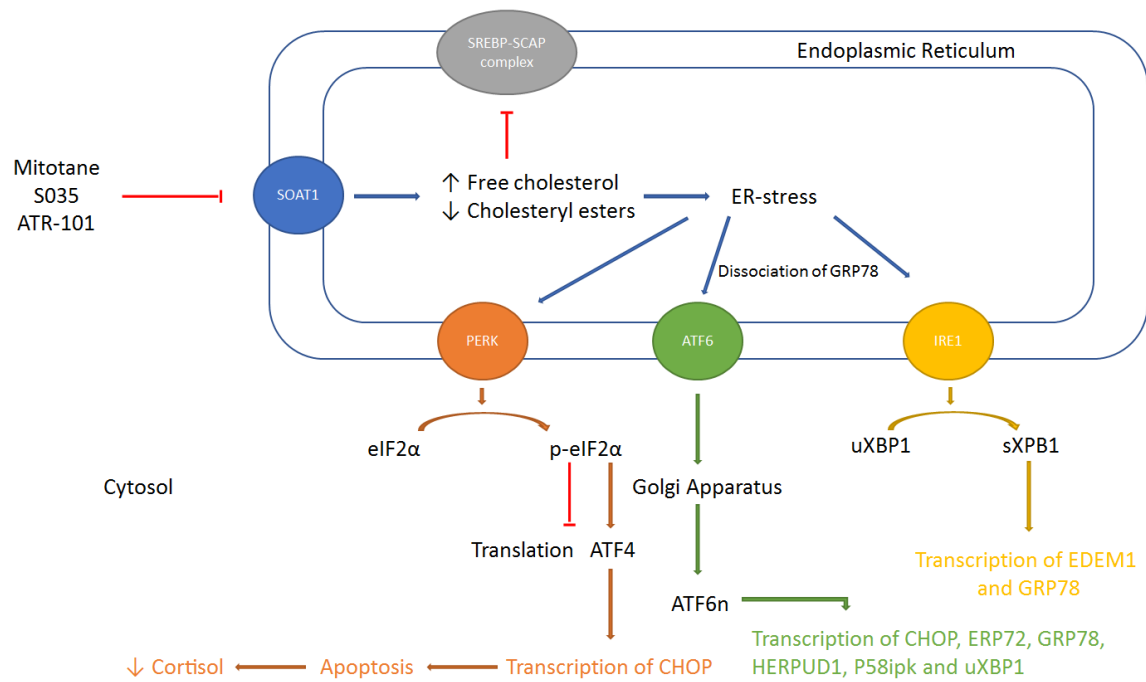


Figure 6: Hypothesized mechanism of action of mitotane, Sandoz 58-035 (S035) and ATR-101. Mitotane, S035 and ATR-101 inhibit sterol-O-acyl transferase 1 (SOAT1), resulting in increased free cholesterol levels. Free cholesterol prevents the release of sterol regulatory element-binding proteins (SREBPs), thereby inhibiting the transcription of genes involved in cholesterol metabolism. In addition, free cholesterol causes endoplasmic reticulum stress (ER-stress). Unfolded proteins activate the three pathways of the unfolded protein response (UPR). Whenever homeostasis cannot be restored, apoptosis is initiated resulting in decreased cortisol production. ATF4 = activating transcription factor 4, ATF6(n) = activating transcription factor 6 (nucleus), CHOP = CCAAT/enhancer-binding protein homologous protein, EDEM1 = ER degradation enhancing α -mannosidase like protein 1, (p-)eIF2 α = (phosphorylated) eukaryotic initiation factor 2 alpha, ERP72 = ER protein 72, GRP78 = glucose-regulated protein 78, HERPUD1 = homocysteine inducible endoplasmic reticulum protein with ubiquitin like domain 1, IRE1 = inositol-requiring protein 1, PERK = protein kinase RNA (PKR)-like ER kinase, p58^{ipk} = DnaJ heat shock protein family member C3, SCAP = SREBP cleavage activating protein, sXBP1 = spliced X-box binding protein 1, uXBP1 = unspliced X-box binding protein 1. Adapted from Brewer *et al.* 2014, LaPensee *et al.* 2016 and Sbiera *et al.* 2015.^{11,26,27}

Chapter 2: Aim of the study

The aim of this study was to evaluate whether SOAT1 inhibitors S035 and ATR-101 could represent a new medical therapy for canine cortisol-secreting ATs. Therefore, we first determined SOAT1 mRNA and protein expression of NAs, ACAs, ACCs and metastases. Thereafter, we studied the effect of SOAT1 inhibitors *in vitro*. Adrenocortical cells cultures were incubated with various concentrations of SOAT1 inhibitors and we studied their effect on cortisol production, apoptosis and viability.

Chapter 3: Materials and methods

Paragraph 3.1: SOAT1 expression

Paragraph 3.1.1: Animals and tissues

Healthy dogs and dogs with ACTH-independent hypercortisolism were incorporated in this study. The normal adrenals (NAs) were obtained from 16 dogs which were euthanized for reasons unrelated to this study. The median age was 691 days (inter quartile range (IQR) = 1024). The owners of the dogs with ACTH-independent hypercortisolism gave permission to the use of the ATs and metastases for research purposes. The ATs were obtained from 71 dogs with ACTH-independent hypercortisolism. The metastases were obtained from three of these dogs. The median age at the time of adrenalectomy was 3751 days (IQR = 861). Adrenalectomy was performed at the Department of Clinical Sciences of Companion Animals of the Faculty of Veterinary Medicine, Utrecht University, the Netherlands. The study was approved by the Ethical Committee of the Faculty of Veterinary Medicine.

Suspicion of hypercortisolism was based on history, physical examination and routine laboratory findings. The diagnosis hypercortisolism was confirmed by a urinary corticoid: creatinine ratio above 8.3×10^{-6} in two successive morning urine samples collected at home. After collection of the second urine sample, three doses of 0.1 mg dexamethasone per kg body weight were administered every 8 hours. The third urine sample was collected the following morning. When the urinary corticoid: creatinine ratio of the third urine sample was suppressed by less than 50% of the mean of the first two samples and basal plasma ACTH concentration was less than 15 ng/L, ACTH-independent hypercortisolism was confirmed. The unilateral ATs were visualized using abdominal ultrasonography or computed tomography.⁴⁸

In addition to evaluating the SOAT1 protein expression in NAs, ACAs, ACCs and metastases, we evaluated the SOAT1 protein expression in two pituitaries, which were obtained from two healthy dogs.

Information about dog breeds and gender of the dogs of which the NAs, ACAs, ACCs and metastases for RT-qPCR and IHC were obtained from, is presented in appendix 1 table 13 and 14, respectively.

To test our anti-SOAT1-antibody, protein was isolated from one testis, one pituitary, one NA and two ACCs. The ACCs were obtained from a 2541 days old castrated female Miniature Wirehaired Dachshund and a 3254 days old castrated female Briard diagnosed with ACTH-independent hypercortisolism as described previously. The dogs of which the testis, pituitary and NA were obtained from were healthy.

Paragraph 3.1.2: Histopathology

ATs were characterized as ACAs or ACCs according to the histopathologic criteria of Labelle *et al.* 2004.⁴⁹ Typical characteristics of an ACA were hematopoiesis, fibrin thrombi and cytoplasmic vacuolization. Typical characteristics of an ACC were a size larger than 2 cm in diameter, peripheral fibrosis, capsular invasion, trabecular growth pattern, hemorrhage, necrosis and single-cell necrosis.

Paragraph 3.1.3: RT-qPCR

RNA was isolated using RNeasy Mini Kit (QIAGEN, Venlo, the Netherlands) according to manufacturer's protocol and measured using Nanodrop 1000 (Isogen Life Science, Utrecht, the Netherlands) with accessory program Nanodrop 1000 operating software v3.8.1. cDNA was synthesized using 1000 ng RNA and the iScript™ cDNA Synthesis Kit (Bio-Rad, Veenendaal, the Netherlands) and thermal cycler Dyad Disciple Cyler (Bio-Rad) with accessory program MJ Research cyler v2.0. To correct for differences in cDNA content, hypoxanthine-guanine phosphoribosyltransferase (HPRT), ribosomal protein S5 (RPS5), succinate dehydrogenase complex subunit A (SDHA), signal recognition particle

receptor (SRPR) and tyrosine 3-monooxygenase/tryptophan 5-monooxygenase (YWHAZ) were used as reference genes.^{50,51} iQ™ SYBR Green Supermix (Bio-Rad) was used to detect RT-qPCR reactions performed in a CFX384 Touch™ Real-Time PCR Detection System (Bio-Rad). Data were analyzed in CFX Manager™ software v3.1 (Bio-Rad) and processed according to the $2^{-\Delta\Delta Ct}$ method.⁵²

Paragraph 3.1.4: Western Blot

To determine the specificity of our polyclonal rabbit anti-SOAT1 antibody (orb100781, Biorbyt, Bioconnect BV, Huissen, the Netherlands) we performed a Western Blot. Protein samples were diluted to 2 µg/µL using milli Q (mQ). 2 µg/µL protein samples were 1:1 diluted using sample buffer and heated at 95°C for 2 minutes. The protein samples and Precision Plus Protein™ Standard dual color (Bio-Rad) were loaded onto a 7.5% Criterion™ TGX™ Precast Gel (Bio-Rad). Gel electrophoresis (100-150V) was performed using a Criterion™ Cell electrophoresis (Bio-Rad) until sufficient separation of the bands. Blotting was performed in a Criterion™ Blotter (Bio-Rad) at 100 V for 1 hour. The membrane was blocked using 4% ECL blocking solution (GE Healthcare, Amersham, United Kingdom) in Tris-buffered saline 0.1% Tween (TBST0.1%) for 60 minutes and incubated with 1:100 diluted primary antibody in 4% bovine serum albumin (BSA) in TBST0.1% overnight. The next day, the membrane was washed three times for 5 minutes in TBST0.1% after which the membrane was ready to be incubated with our 1:10000 diluted polyclonal anti-rabbit secondary horseradish peroxidase (HRP) labeled antibody (65-6120, Thermo Fisher Scientific, Breda, the Netherlands) for 60 minutes. The secondary antibody was dissolved in 4% BSA in TBST0.1%. After washing three times for 5 minutes using TBST0.1%, the membrane was placed on a copier sheet and incubated with ECL substrate solution (GE Healthcare). ChemiDoc™ (Bio-Rad) and Image Lab v5.1 were used to observe the results.

Paragraph 3.1.5: IHC

All tissues were fixed in 4% paraformaldehyde (PFA) for 24-48 hours and paraffin-embedded. NAs were used as positive control tissue and colon, liver and muscle were used as negative control tissue. Pieces of 5 µm were cut and mounted on SuperFrost plus microscope slides (Menzel-Gläser, Braunschweig, Germany). The slides were deparaffinized and rehydrated in a series of xylene and ethanol. In order to retrieve antigens, slides were treated with Tris-EDTA buffer in a water bath at 98°C for 15 minutes. After cooling down, slides were incubated with 0.75% glycine in phosphate buffered saline (PBS) for 30 minutes to reduce background staining. Slides were rinsed with PBS for 10 minutes and with PBS 0.1% Tween for 5 minutes after which slides were incubated with 3% BSA in PBS 0.1% Tween to reduce background staining. Slides were incubated with 1:150 diluted primary anti-SOAT1 antibody (orb100781) or a negative rabbit IgG control (X0720, Vector laboratories, Burlingame, CA, USA) and stored at 4°C overnight. The primary antibody and the negative IgG control were diluted in 3% BSA in PBS 0.1% Tween. The next day, slides were rinsed with PBS 0.1% Tween four times for 10 minutes. Endogenous peroxidases were blocked using 3% H₂O₂ in PBS 0.1% Tween after which slides were rinsed with PBS 0.1% Tween three times for 5 minutes. HRP-labeled anti-rabbit secondary antibody (K4003, DAKO, Agilent Technologies, Amstelveen, the Netherlands) was added for 1 hour. After rinsing with PBS three times for 10 minutes, antibody was visualized with the diaminobenzidine (DAB) substrate kit for peroxidase (K3468, DAKO, Agilent Technologies). A 1:4 diluted hematoxylin was used as a nuclear counterstain. Slides were dehydrated in a series of ethanol and xylene. Cover slips were mounted using Vectamount Mounting Medium (H-5000, Vector laboratories). A semi quantitative H-score for SOAT1 protein expression was calculated by multiplying the area of positive staining with the staining intensity grading score (table 1). The microscope Olympus BX60 with a Leica DFC450 C digital camera (Leica Microsystems B.V., Amsterdam, the Netherlands) and the accessory program Leica Application Suite v4.7.1 (Leica Microsystems B.V.) were used to score the slides.

Table 1: Semi quantitative H-score. A semi quantitative H-score was calculated as following. Slides showed different intensity of staining throughout the slide. Therefore, the percentage of the slide showing a certain intensity was multiplied by the score. In this way, the whole slide (100%) was scored. The total score was multiplied by the number coupled to the total percentage of the slide that was stained. For example, a slide was stained for 50% very strongly positive, for 30% weakly positive and for 20% there was no staining. 80% of the whole slide was stained. This resulted in the following score: $((0.5 \times 4) + (0.3 \times 1) + (0.2 \times 0)) \times 4 = 9.2$.

H-score		% Area with positive staining	
0	No staining	0	< 5% of the sample
1	Weakly positive	1	5 - 25% of the sample
2	Mildly positive	2	25 - 50% of the sample
3	Highly positive	3	50 – 75% of the sample
4	Very strongly positive	4	> 75% of the sample

Paragraph 3.1.6: Statistics

A statistical analysis of mRNA (fold change) and protein expression (H-score) of SOAT1 in NAs, ACAs and ACCs was performed. Normality was analyzed with the Shapiro-Wilk test. Due to the non-normal distribution of the samples, the Kruskal-Wallis test was used to check for differences between the expression of SOAT1 at the mRNA and protein level in NAs, ACAs and ACCs. A p-value of <0.05 was considered significant. Data are reported in median (IQR). IBM® SPSS® Statistics v24.0.0.1 was used to analyze SOAT1 mRNA and protein expression data. The evaluation of SOAT1 protein expression in NAs, ACAs, ACCs, metastases and pituitaries will also be descriptive.

Paragraph 3.2: *In vitro* studies

Paragraph 3.2.1: Animals

Healthy dogs and one dog with ACTH-independent hypercortisolism, diagnosed as described previously (paragraph 3.1.1), were incorporated in this study. The 10 dogs of which the NAs were obtained from were euthanized for reasons unrelated to this study. Two dogs were Beagles and eight dogs were mixed breed dogs. Four dogs were intact females and the remaining six dogs were intact males. The median age was 468 days (IQR = 87). The owners of the 4206 days old castrated female Cairn Terrier with ACTH-independent hypercortisolism gave permission to the use of the AT for research purposes. Adrenalectomy was performed at the Department of Clinical Sciences of Companion Animals of the Faculty of Veterinary Medicine, Utrecht University, the Netherlands. The AT was characterized as an ACC based on the criteria as described previously (paragraph 3.1.2). The study was approved by the Ethical Committee of the Faculty of Veterinary Medicine. An overview of which NA is used for which experiment and in which experiments the ACC was incorporated, is presented in appendix 1 table 15.

Paragraph 3.2.2: Cell suspensions

NAs and the ACC were collected in ice-cold Hanks Balanced Salt Solution (HBSS; Gibco, Invitrogen, Breda, the Netherlands) with 2% Penicillin-Streptomycin (P/S; Gibco). After removal of surrounding tissues and medulla, the NAs were cut into pieces and digested in a collagenase solution (1 % D-(+)-glucose monohydrate (Sigma-Aldrich, Zwijndrecht, the Netherlands), 0.2% BSA (Sigma-Aldrich), 0.75 mg DNase (Sigma-Aldrich), 45 mg collagenase 1A (Sigma-Aldrich) and 1% P/S in Leibowitz L15 (Gibco)) in a CELLSTAR® T75 tissue culture flask (Greiner Bio-One, Alphen aan den Rijn, the Netherlands) for 60-75 minutes at 37°C while shaking. Tumor tissue was selected and digested in the collagenase solution. Every 15-20 minutes, the suspension was pipetted up and down using pipette tips with a wider and smaller opening. After 60-75 minutes, the suspension was filtered through a 100 µm and a 70 µm EASYstrainer™ (Greiner Bio-One) after which Leibowitz 15 containing 2% fetal calf serum (FCS; Gibco) and 0.2% P/S was added 1:1. 3% BSA was added on the bottom of a tube after which the suspension was centrifuged at 190 relative centrifugal force (RCF) at 4°C for 10 minutes. The pellets were dissolved in Leibowitz L15 with 10% FCS and 1% P/S and centrifuged again. The newly formed pellets were

dissolved in adrenal medium (1% P/S, 1% Insulin-Transferrin-Selenium (Gibco), 0.125% BSA, 2.5% Nu Serum (Corning, Amsterdam, the Netherlands) in Dulbecco's Modified Eagle Medium F-12 (Gibco)). Cells were diluted using 0.16% trypan blue (Gibco) to count cells. The cells were counted using a Bürker-Türk counting chamber (W. Schreck, Hofheim/TS). Cells were seeded in Primaria™ 6-, 24- and 96-wells plates (Corning) and in a coated 12 Well Chamber, removable (Ibidi, Planegg, Germany) at a density of 1.0×10^5 cells/mL. The protocol for coating chamber slides is described in paragraph 3.2.7. The cells were left to attach for 4-7 days at 37°C in a humidified atmosphere of 95% air and 5% CO₂, after which the culture medium was refreshed before the cells were incubated with the compounds.

Paragraph 3.2.3: Compounds

Mitotane (25925-1G-F, Sigma-Aldrich) and S035 (S9318-5MG, Sigma-Aldrich) were dissolved in dimethyl sulfoxide (DMSO; Merck KGaA, Darmstadt, Germany) at 30 mM. 10 µM ATR-101 in 96% ethanol stock was a generous gift of Dr. Kroiss, University of Würzburg, Germany. Compounds were diluted to desired compound concentrations while keeping DMSO and ethanol end concentrations at a constant level of 0.33% and 0.96%, respectively. DMSO and ethanol were used as vehicle controls. To mimic hypercortisolism, 100 nM synthetic ACTH [1-24] (Synacthen®, Sigma-Tau BV, Utrecht, the Netherlands) was added.

Paragraph 3.2.4: Cortisol and protein measurements

Paragraph 3.2.4.1: Pilot studies

In our first pilot study, we incubated normal adrenocortical cells with 0 and 100 µM mitotane or S035 for 6 and 24 hours. Medium was removed for cortisol measurements. Cortisol concentrations were determined using radioimmunoassay (RIA) according to Meijer *et al.* 1978.⁵³ After medium removal, cells were washed twice using PBS. Fresh PBS was added and cells were scraped using a cell scraper (Greiner Bio-One). The obtained suspension was transferred to Eppendorf cups and stored at -20°C (protein samples) or -70°C (lipid samples) until performing protein measurements and lipidomics.

The Quick Start™ Bradford Protein Assay (Bio-Rad) was performed according to manufacturer's protocol. The DTX 880 Multimode Detector (Beckman Coulter, Woerden, the Netherlands) and accessory program Anthos Multimode Detectors v2.0.0.13 were used to measure absorbance (595Ex).

The protocol for lipidomics is outlined in paragraph 3.2.6.

In our second pilot study, we wanted to determine concentration dependent effects of mitotane, S035 and ATR-101. Normal adrenocortical cells were incubated with 0, 1, 2, 5, 10, 20, 50 and 100 nM ATR-101 or 0, 1, 2, 5, 10, 20, 50 and 100 µM mitotane or S035 for 6 hours. After 6 hours, medium was collected for cortisol measurements and wells were washed twice using PBS. PBS was added to the wells and the plates were stored at -20°C until the Quick Start™ Bradford Protein Assay was performed.

Paragraph 3.2.4.2: Follow-up experiments

We incubated normal adrenocortical cells and ACC cells with 0, 1, 2, 5, 10, 20, 50 and 100 nM ATR-101 or 0, 1, 2, 5, 10, 20, 50 and 100 µM mitotane or S035 for 24 hours. After 24 hours, medium was collected for cortisol measurements and wells were washed twice using PBS. PBS was added to the wells and the plates were stored at -20°C until the Quick Start™ Bradford Protein Assay was performed.

Paragraph 3.2.5: Viability, cytotoxicity and apoptosis

Paragraph 3.2.5.1: ApoTox-Glo™ Triplex Assay

To determine if the ApoTox-Glo™ Triplex Assay (Promega, Leiden, the Netherlands) was a suitable test to evaluate the effects of all three compounds on cell viability, cytotoxicity and apoptosis, we tested the assay. We incubated normal adrenocortical cells with 0, 20, 50 and 100 µM mitotane for 24 hours.

After 24 hours, the ApoTox-Glo™ Triplex Assay was performed according to manufacturer's protocol. Fluorescence was measured by Infinite 200 (Tecan Life Sciences, Giessen, the Netherlands) and accessory program Tecan I-control v.1.11.1.0. Fluorescence was measured at 400Ex/505Em (viability) and at 485Ex/520Em (cytotoxicity). Luminescence (apoptosis) was measured by the DTX 880 Multimode Detector. An integration time of 1 second was used.

Because ATR-101 was dissolved in 96% ethanol, we wanted to study the effects of several ethanol concentrations on normal adrenocortical cells. We incubated normal adrenocortical cells with 0.1, 0.25, 0.5, 1 and 2% ethanol for 24 hours. Normal adrenocortical cells incubated without ethanol were used as a control.

Paragraph 3.2.5.2: Follow-up experiments

Regarding our follow-up experiments (alamarBlue® and Caspase-Glo® 3/7 assay), we incubated normal adrenocortical cells with 0, 10, 20, 50 and 100 nM ATR-101 or 0, 10, 20, 50 and 100 µM mitotane or S035 for 24 hours. In contrast to the normal adrenocortical cells, we performed the Caspase-Glo® 3/7 Assay in ACC cells incubated with 0, 50 and 100 nM ATR-101 or 0, 50 and 100 µM mitotane or S035. The alamarBlue® Assay (Thermo Fisher Scientific) was performed identical to how the assay was performed in normal adrenocortical cells.

After 22 hours, 10 µL alamarBlue® reagent was added per well and the cells were placed back in the incubator. After 24 hours of incubation, fluorescence (535Ex/595Em) was measured using DTX 880 Multimode Detector after which the Caspase-Glo® Reagent was added. The cells were left at room temperature for one hour, after which luminescence was measured using DTX 880 Multimode Detector. An integration time of 1 second was used.

Paragraph 3.2.6: Lipidomics

Based on protein concentrations, determined by the Quick Start™ Bradford Protein Assay, we determined the amount of sample containing 1 µg protein and consummated this volume to 800 µL using PBS. Lipids were extracted according to Bligh and Dyer 1959⁵⁴ and separated in a neutral (triacylglycerol, cholesteryl esters, retinols and cholesterol) and phospholipid fraction.⁵⁵ The neutral lipid fraction was dissolved in methanol/chloroform (1/1, v/v) and separated using a Kinetex/HALO C8-e column (2.6 micron, 150 x 3.0 mm; Phenomenex, Utrecht, the Netherlands). A methanol/water (5/5, v/v) to methanol/isopropanol (8/2, v/v) gradient was created at a constant flow rate of 0.6 ml/min. High performance liquid chromatography (HPLC) was performed on a 1290 Infinity LC system (Agilent Technologies) at 40°C. Mass spectrometry (MS) of neutral lipids was performed using atmospheric pressure chemical ionization (APCI) on a Orbitrap Fusion (Thermo Fisher Scientific).⁵⁶ Data were analyzed using XCMS v1.52.0. Lipid extraction and HPLC-MS were performed at the Department of Biochemistry and Cell Biology of the Faculty of Veterinary Medicine Utrecht, Utrecht University, the Netherlands.

Paragraph 3.2.7: Fluorescent imaging of lipid droplets

We used 4,4-difluoro-2,3,5,6-bis-tetramethylene-4-bora-3a,4a-diaza-s-indacene (LD540) dye to stain lipid droplets. We combined this dye with 4',6-diamidino-2-phenylindole (DAPI) nuclear staining. A 12 Well Chamber, removable (Ibidi) was coated with rat tail collagen type I (Ibidi) diluted in 17.5 mM acetic acid at 5 µg/cm² for at least 1 hour, after which the chamber slide was rinsed using DMEMF12 and was ready to be seeded with normal adrenocortical cells. The chamber slide was incubated with 0, 50 and 100 µM mitotane or S035 for 24 hours. After 24 hours, medium was removed and the cells were fixed with 4% PFA at room temperature for 45 minutes. Thereafter, wells were quenched and permeabilized using 20 mM ammonium chloride, 2% BSA, 5% normal goat serum and 0.1% Triton X-100 in PBS. After 10 minutes, the solution was removed and replaced by 2% BSA. The chamber slide was stored at 4°C overnight. The next day, the chamber slide was washed twice for 5 minutes using PBS. LD450 was diluted 1:1000 and DAPI 1:4000. Both dyes were diluted using PBS. The LD540 and

DAPI staining were added and after 15 minutes of incubation the chamber slide was washed three times for 5 minutes using PBS. Thereafter, mQ was added and the silicone gasket was removed. The slide was mounted with FluorSave mounting medium (Merck Millipore, Amsterdam, the Netherlands) and a coverslip. All these steps were performed in the dark. The microscope Olympus BX60 with a Leica DFC450 C digital camera was used to observe the results.

Paragraph 3.2.8: RT-qPCR

The relative mRNA expressions of ATF4, BAX, BCL-2, caspase 3 (Casp3), CHOP, 17 α -hydroxylase (CYP17), EDEM1, ERP72, GRP78, homocysteine inducible endoplasmic reticulum protein with ubiquitin like domain 1 (HERPUD1), p58^{ipk}, SOAT1, steroidogenic factor 1 (SF1), SREBF1, SREBF2, sXBP1 and uXBP1 were determined using RT-qPCR. ACC cells were incubated with 0 and 100 nM ATR-101 or 0 and 100 μ M mitotane or S035 for 6 and 24 hours. RT-qPCR was performed as described in paragraph 3.1.3. 250 or 500 ng RNA was used to synthesize cDNA and ribosomal protein S19 (RPS19), SDHA, SRPR and YWHAZ were used as reference genes.

Paragraph 3.2.8.1: Primers

The mRNA sequences of genes of interest were obtained from National Center for Biotechnology Information (NCBI) GenBank database. Primers were designed using Perl-primer software v1.1.21 according the parameters in the Bio-Rad iCycler manual. PCR-products of the primer pairs were checked for secondary structure formation with mfold web server v3.6 (<http://unafold.rna.albany.edu/?q=mfold>). It was checked if our selected primer pair yielded only our gene of interest using NCBI primer Basic Local Alignment Search Tool (BLAST) (<https://blast.ncbi.nlm.nih.gov/Blast.cgi>). Primers were ordered from Eurogentec (Seraing, Belgium). Normal adrenocortical cells were incubated with 0, 12.5, 25, 50 and 100 μ M mitotane for 24 hours to induce ER-stress. RNA was isolated, cDNA was synthesized and RT-qPCR was performed as described previously (paragraph 3.1.3), although this time 500 ng RNA was used to synthesize cDNA. Reactions of each primer set were optimized by performing the reactions under gradually increasing annealing temperatures (56-66°C). Primer specificity was confirmed by melting curve analysis, electrophoresis and product sequencing. CFX Manager™ v3.1 (Bio-Rad) was used to analyze the melting curve. Primer pairs with an efficiency of 95-105% and a $R^2 > 0.99$ were deemed appropriate. To visualize our PCR-products on gel electrophoresis, loading dye (Promega) was added to our PCR-products. A 100 bp DNA ladder (Promega) and Gel Doc 2000 (Bio-Rad) with accessory program Quantity One v4.3.0 (Bio-Rad) were used to evaluate product sizes. The PCR-products were purified using Shrimp alkaline phosphatase/Exonuclease I (New England Biolabs® Inc, Leiden, the Netherlands) in a C1000 Touch™ Thermal Cycler (Bio-Rad). Purified PCR-products were amplified with the BigDye® Terminator v3.1 Cycle Sequencing Kit (Applied Biosystems, Foster City, CA, USA) in a GeneAmp® PCR system 9700 (Applied Biosystems). Amplified PCR-products were filtered on a Sephadex G-50 Superfine (GE Healthcare, Amersham, United Kingdom) loaded MultiScreen_{HTS} HV Filter Plate (Merck Millipore, Amsterdam, the Netherlands) in a MicroAmp® Optical 96-wells reaction plate (Applied Biosystems) and sequenced using the ABI Prism 3100 Genetic Analyzer (Applied Biosystems) with accessory program 3130 Series Data Collection Software v4. The sequencing data were compared to the NCBI database using BLAST. All primer sequences, annealing temperatures (Ta), accession numbers and product lengths are presented in appendix 3 table 16.

Paragraph 3.2.9: Western Blot

To evaluate the protein expression of the UPR components, we determined the specificity of antibodies against eIF2 α , p-eIF2 α , CHOP and ATF6. We incubated normal adrenocortical cells with 0, 10, 20, 50 and 100 μ M mitotane for 24 hours to induce ER-stress. Protein was isolated from the normal adrenocortical cells and from normal adrenocortical cells incubated with mitotane. Western Blot was performed as described previously (paragraph 3.1.4). A 12% Criterion™ TGX™ Precast Gel (Bio-Rad) was used. Detailed information about our antibodies and used dilutions is presented in table 2.

Table 2: Western Blot antibodies. ATF6 = activating transcription factor 6, CHOP = CCAAT/enhancer-binding protein homologous protein, (p-)eIF2 α = (phosphorylated) eukaryotic initiation factor 2 alpha.

Antibody	Source	Company	Product number	Dilution
Anti-ATF6	Mouse monoclonal antibody	Novus Biologicals, Abdingdon, United Kingdom	NBP1-40256	1:1500
Anti-CHOP	Mouse monoclonal antibody	Cell Signaling, Leiden, the Netherlands	2895	1:500
Anti-eIF2α	Rabbit monoclonal antibody	Cell Signaling	5324	1:1000
Anti-p-eIF2α	Rabbit polyclonal antibody	Cell Signaling	9721	1:600
HRP labeled anti-mouse	Goat polyclonal IgG	R&D Systems, Abdingdon, United Kingdom	HAF007	1:20000
HRP labeled anti-rabbit	Goat polyclonal IgG	Thermo Fisher Scientific	65-6120	1:20000

Paragraph 3.2.10: Statistics

Statistics were performed in our follow-up studies of cortisol and viability. Normality was checked using Shapiro-Wilk test. Due to the non-normal distribution of the follow-up cortisol samples, the Friedman test was used to check for differences between cortisol production at different compound concentrations. A p-value of <0.05 was considered significant. Post hoc analysis with Wilcoxon signed-rank tests was conducted with a Bonferroni correction applied, resulting in a significance level set at p <0.007. The follow-up viability data were normally distributed. Therefore, the One-Way ANOVA was used to check for differences between viability at different compound concentrations. A p-value of <0.05 was considered significant. Data are reported relative to the DMSO (mitotane and S035) or ethanol (ATR-101) control in mean \pm standard deviation. The principal component analysis was used in our lipidomic study.

Chapter 4: Results

Paragraph 4.1: SOAT1 expression

Paragraph 4.1.1: Western Blot

To immunohistochemically evaluate the SOAT1 protein expression, we tested an anti-SOAT1-antibody. Protein expression of SOAT1 (55 kDa) was present in all tissues tested. However, in the pituitary several proteins did cross react.

SOAT1 protein expression was the strongest in the pituitary, followed by the testis and the NA. In the ACCs SOAT1 protein expression was very low (figure 7).

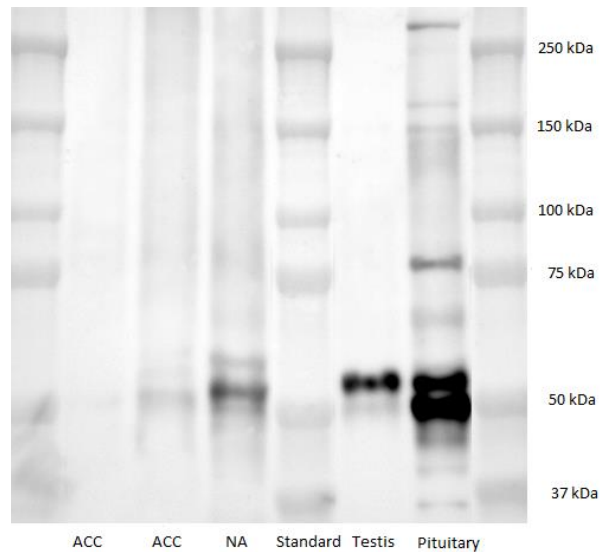


Figure 7: Western Blot of sterol-O-acyl transferase 1 (SOAT1). SOAT1 protein (55 kDa) was present in all tissues tested. The expression of SOAT1 protein was the strongest in the pituitary, followed by the testis, normal adrenal (NA) and adrenocortical carcinomas (ACCs), respectively.

Paragraph 4.1.2: SOAT1 mRNA and protein expression

SOAT1 mRNA was detectable with RT-qPCR in all NAs, ACAs and ACCs tested. Expression was more variable in ACCs. Median fold changes were 1.1 (IQR = 0.5), 1.2 (IQR = 1.0) and 1.6 (IQR = 1.4), respectively. No significant differences ($p = 0.077$) were found between NAs, ACAs and ACCs (figure 8). The median fold change of SOAT1 mRNA expression in metastases was 0.8 (IQR = 0.7).

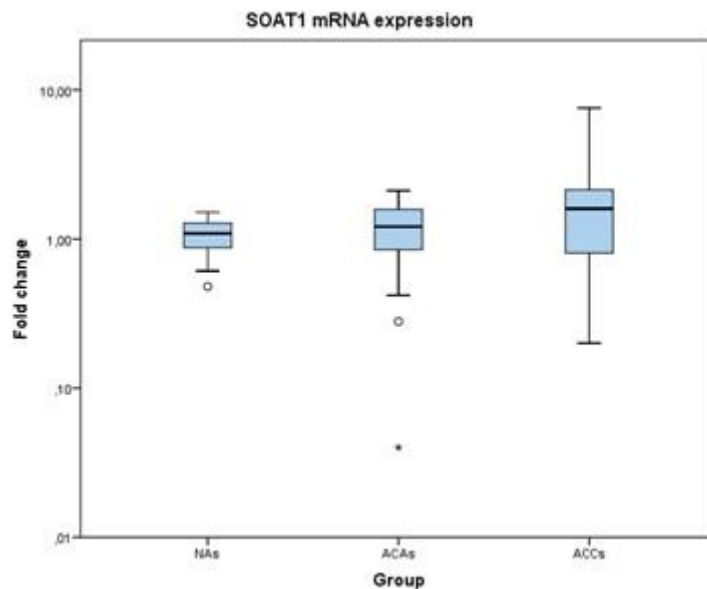


Figure 8: Sterol-O-acyl transferase 1 (SOAT1) mRNA expression. Expression of SOAT1 mRNA in normal adrenals (NAs), adrenocortical adenomas (ACAs) and adrenocortical carcinomas (ACCs). The SOAT1 mRNA expression was more variable in ACCs. No significant difference was found between NAs, ACAs and ACCs.

SOAT1 protein was detectable with IHC in all NAs, ACAs and ACCs (figure 9). In NAs, SOAT1 protein expression was present in all zones. The medulla stained negative. Some nonspecific staining was observed in the capsule (figure 10 and 11). ACAs and ACCs were characterized by heterogeneous SOAT1 protein expression (figure 12 and 13). The ACCs showed more variable expression and three ACCs had low to absent SOAT1 protein expression (H-score lower than one). To illustrate the variable SOAT1 protein expression of ACCs, two ACCs with a high and low H-score are presented in figure 13. Median H-scores of NAs, ACAs and ACCs were 5.8 (IQR = 3.5), 5.2 (IQR = 2.4) and 5.3 (IQR = 5.8), respectively. No significant differences ($p = 0.927$) were found in protein expression between NAs, ACAs and ACCs.

The SOAT1 protein expression of metastases was heterogeneous. One part of the liver metastasis stained stronger than the other part (figure 14). The H-score of SOAT1 protein expression in the liver metastasis was 5.0. The H-score of SOAT1 protein expression in the lung metastasis was 3.6 (figure 15).

Additional histologic pictures of NAs, ACAs and ACCs with varying SOAT1 expression are presented in appendix 2.

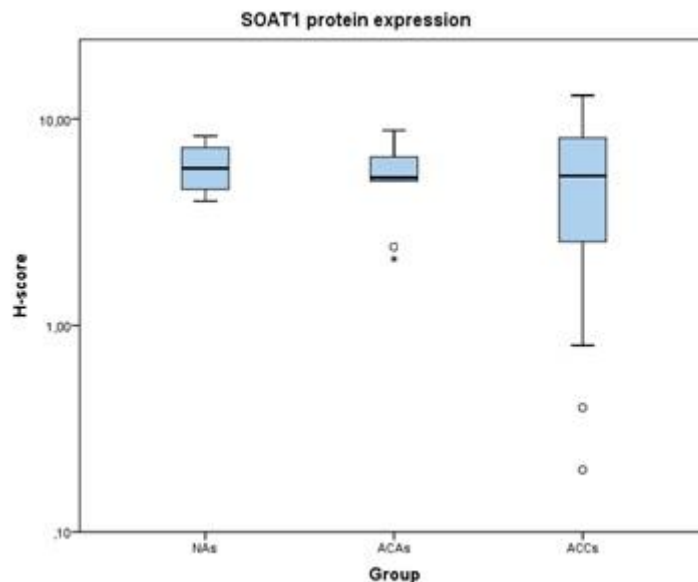


Figure 9: Sterol-O-acyl transferase 1 (SOAT1) protein expression. Expression of SOAT1 protein in normal adrenals (NAs), adrenocortical adenomas (ACAs) and adrenocortical carcinomas (ACCs). The SOAT1 protein expression was more variable in ACCs. No significant difference was found between NAs, ACAs and ACCs.

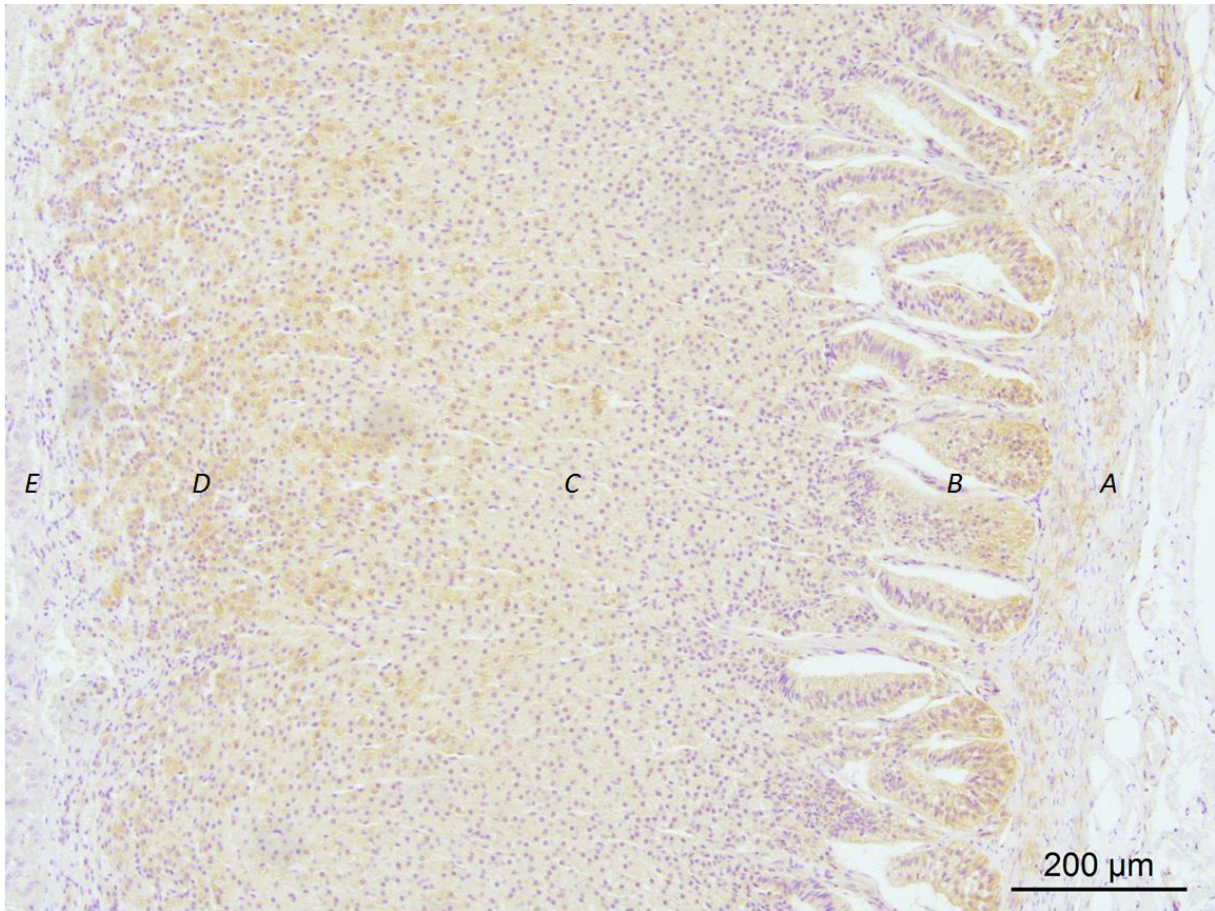


Figure 10: Sterol-O-acyl transferase 1 (SOAT1) protein expression of a normal adrenal (NA). A NA with an H-score of 6.4. SOAT1 protein was expressed in all zones. A = capsule, B = zona glomerulosa, C = zona fasciculata, D = zona reticularis, E = medulla. Scale bar represents 200 μM.

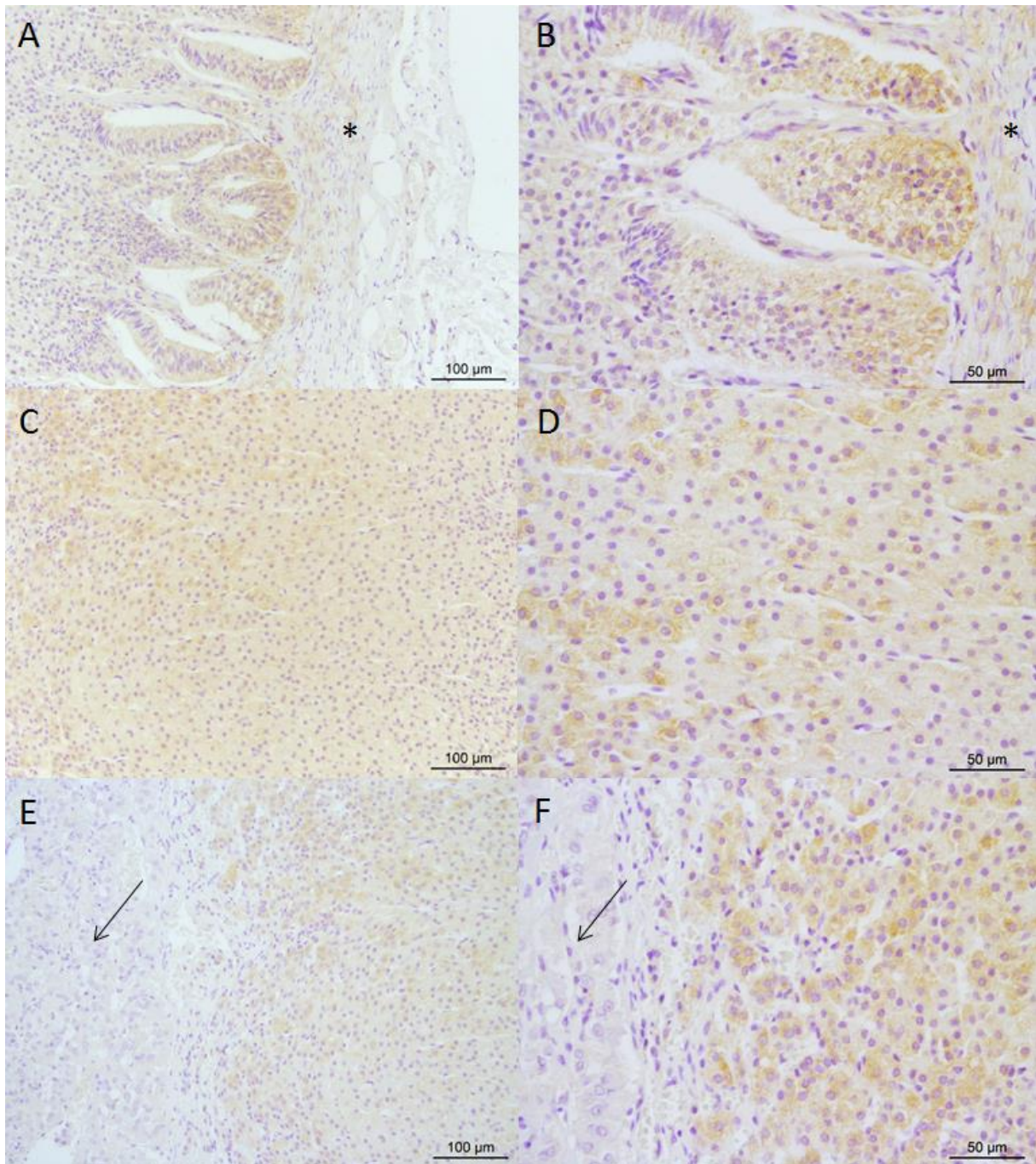


Figure 11: Sterol-O-acyl transferase 1 (SOAT1) protein expression in the different zones of a normal adrenal (NA). A NA with an H-score of 6.4. SOAT1 protein expression in the zona glomerulosa (zG), zona fasciculata (zF) and zona reticularis (zR) was comparable. A = zG and capsule (asterisk), B = zG and capsule, C = zF, D = zF, E = zR and medulla (arrow), F = zR and medulla. Scale bar represents 100 μ M (A, C and E) or 50 μ M (B, D and F).

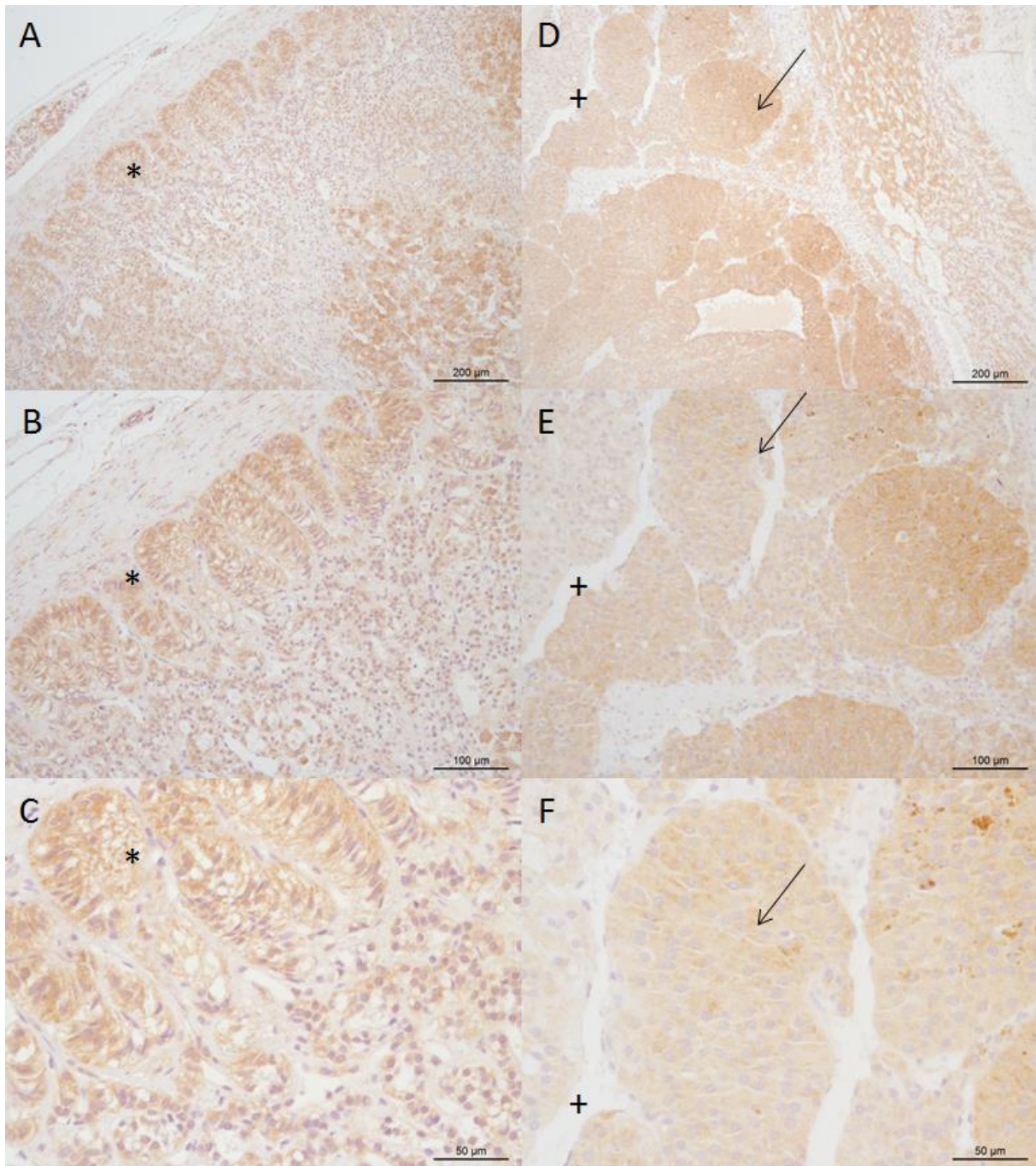


Figure 12: Sterol-O-acyl transferase 1 (SOAT1) protein expression in an adrenocortical adenoma (ACA). An ACA with an H-score of 7.4. In A, B and C normal zona glomerulosa is represented (asterisk). In D, E and F a lobulated pattern (arrow) with vascularization (plus) is represented. Scale bar represents 200 μM (A and D), 100 μM (B and E) and 50 μM (C and F).

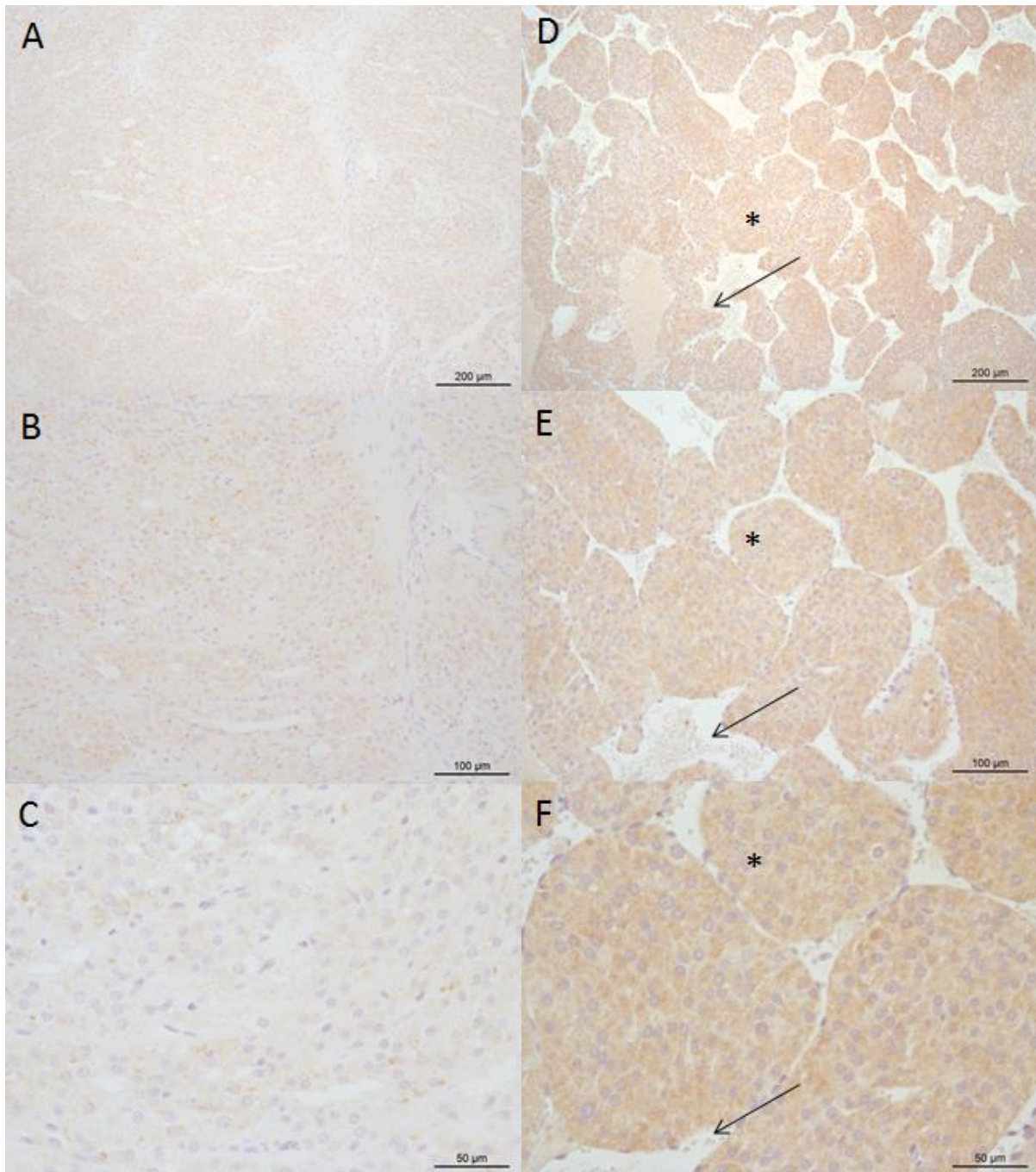


Figure 13: Sterol-O-acyl transferase 1 (SOAT1) protein expression in two adrenocortical carcinomas (ACCs). Pictures on the left (A, B and C) represent SOAT1 protein expression of an ACC with an H-score of 0.2. Pictures on the right (D, E and F) represent SOAT1 protein expression of an ACC with an H-score of 9.4. This ACC showed a lobulated pattern (asterisk) with intense vascularization (arrow). Scale bar represents 200 μ M (A and D), 100 μ M (B and E) and 50 μ M (C and F).

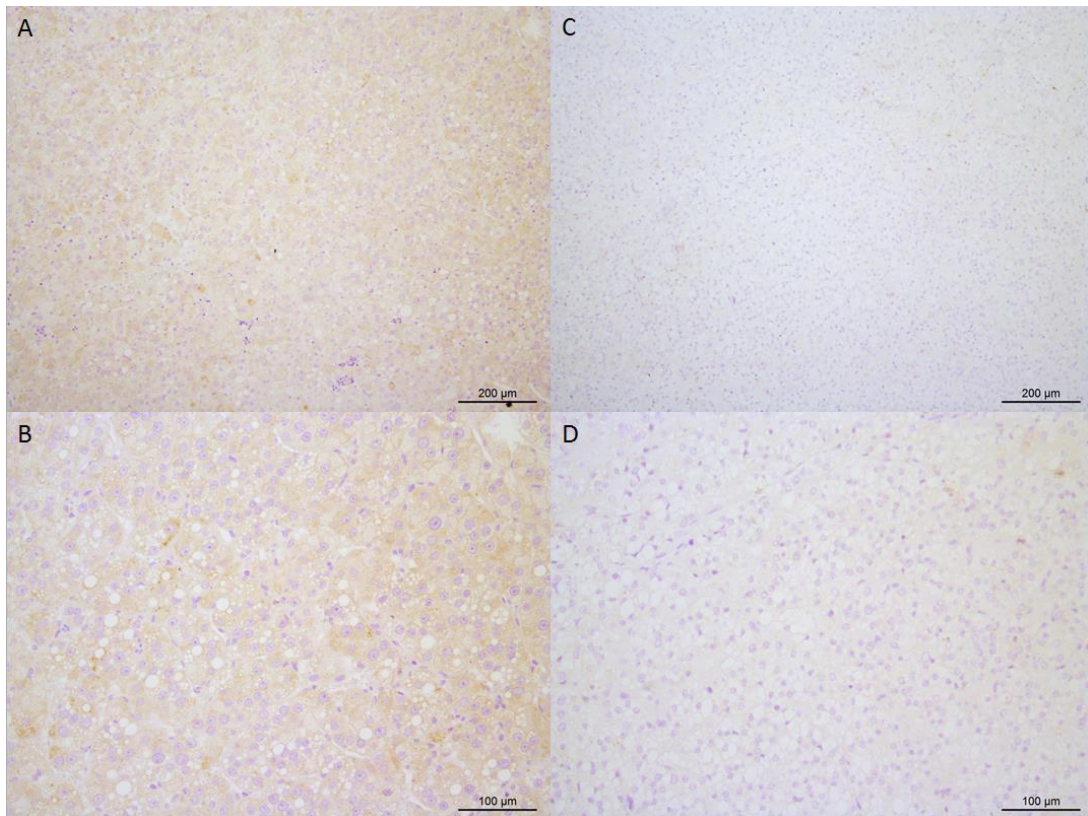


Figure 14: Sterol-O-acyl transferase 1 (SOAT1) protein expression in a liver metastasis. The H-score of SOAT1 protein expression in the liver metastasis was 5.0. Part of the liver metastasis stained stronger (A and B) compared to the other part (C and D). Scale bar represents 200 μ M (A and C) or 100 μ M (B and D).

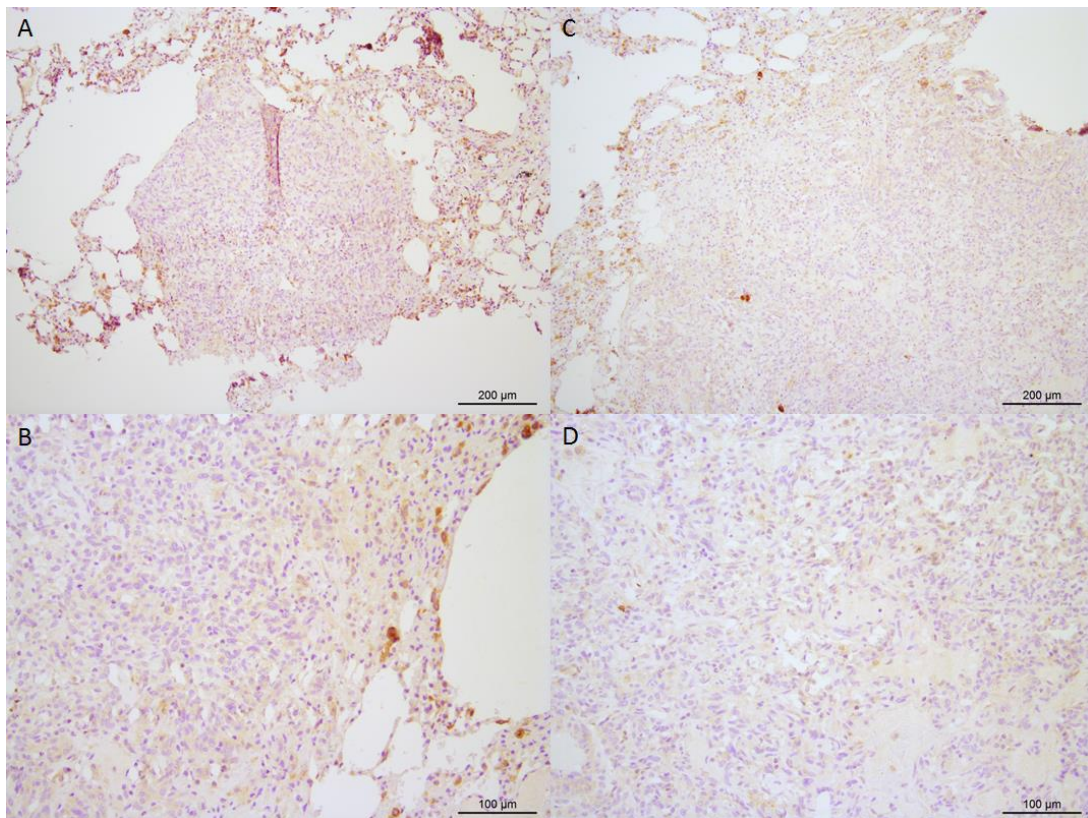


Figure 15: Sterol-O-acyl transferase 1 (SOAT1) protein expression in lung metastases. The H-score of SOAT1 protein expression in the lung metastases was 3.6. Scale bar represents 200 μ M (A and C) or 100 μ M (B and D).

Expression of SOAT1 protein in pituitaries was variable. One pituitary showed more staining for SOAT1 in comparison to the other pituitary. The pars distalis, pars intermedia and pars nervosa stained in both pituitaries, suggesting SOAT1 protein expression in all three zones, although differing between individuals (figure 16).

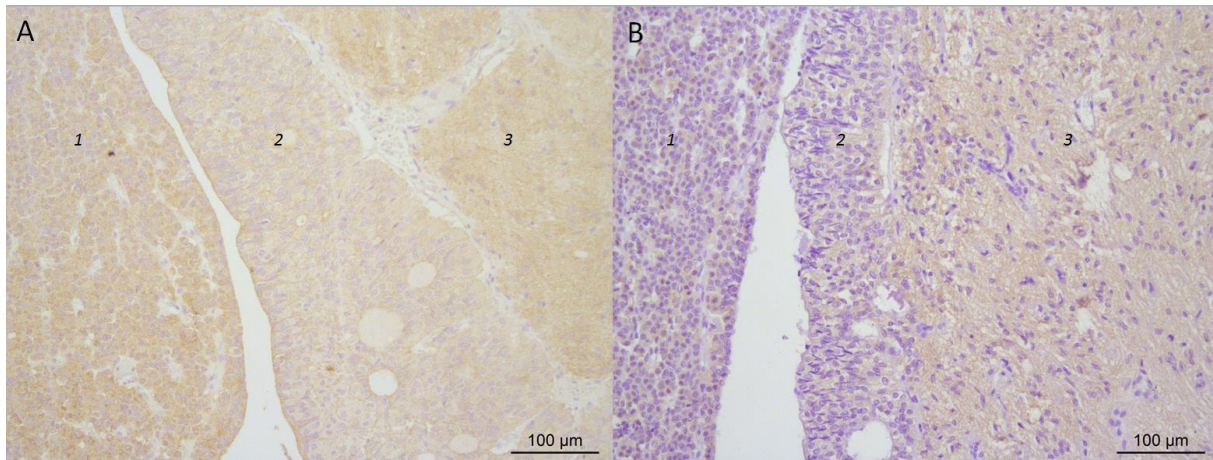


Figure 16: Different sterol-O-acyl transferase 1 (SOAT1) protein expression in the pituitary. One pituitary (A) showed stronger SOAT1 protein expression in comparison to the other pituitary (B). 1 = pars distalis, 2 = pars intermedia, 3 = pars nervosa. Scale bar represents 100 µM.

Paragraph 4.2: *In vitro* studies

Paragraph 4.2.1: Cortisol concentration

Paragraph 4.2.1.1: Pilot studies

Pilot study 1

Mitotane (100 µM) increased the cortisol concentration of non-stimulated normal adrenocortical cells after 6 hours (159.7%) and 24 hours (160.2%). S035 (100 µM) decreased the cortisol concentration of non-stimulated normal adrenocortical cells after 6 hours (79.7%). After 24 hours, S035 increased the cortisol concentration of non-stimulated normal adrenocortical cells (243.0%) (figure 17A and 18A).

Mitotane decreased the cortisol concentration of ACTH-stimulated normal adrenocortical cells after 6 and 24 hours (45.9% and 13.6%, respectively). S035 did not affect the cortisol concentration of ACTH-stimulated normal adrenocortical cells after 6 hours (99.1%). S035 decreased the cortisol concentration of ACTH-stimulated normal adrenocortical cells after 24 hours (72.3%) (figure 17B and 18B).

These results suggested that both compounds can decrease cortisol concentration when hypercortisolism was induced. Mitotane induced a stronger cortisol-decreasing effect.

Absolute data of the cortisol concentration and the number of proteins is presented in appendix 4.1.

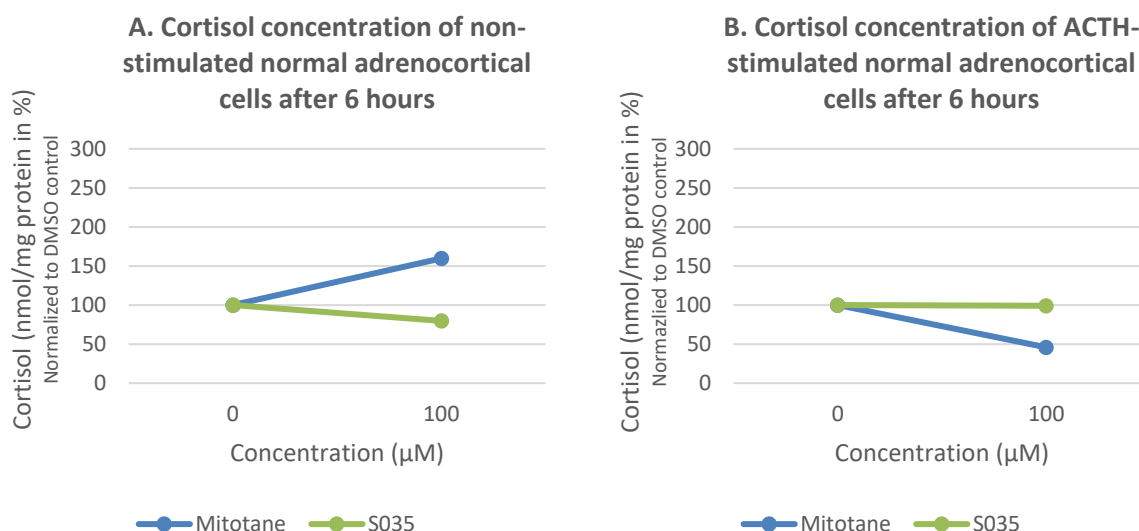


Figure 17: Effects of mitotane and Sandoz 58-035 (S035) on the cortisol concentration of non-stimulated (A) and ACTH-stimulated (B) normal adrenocortical cells (n=1) after 6 hours.

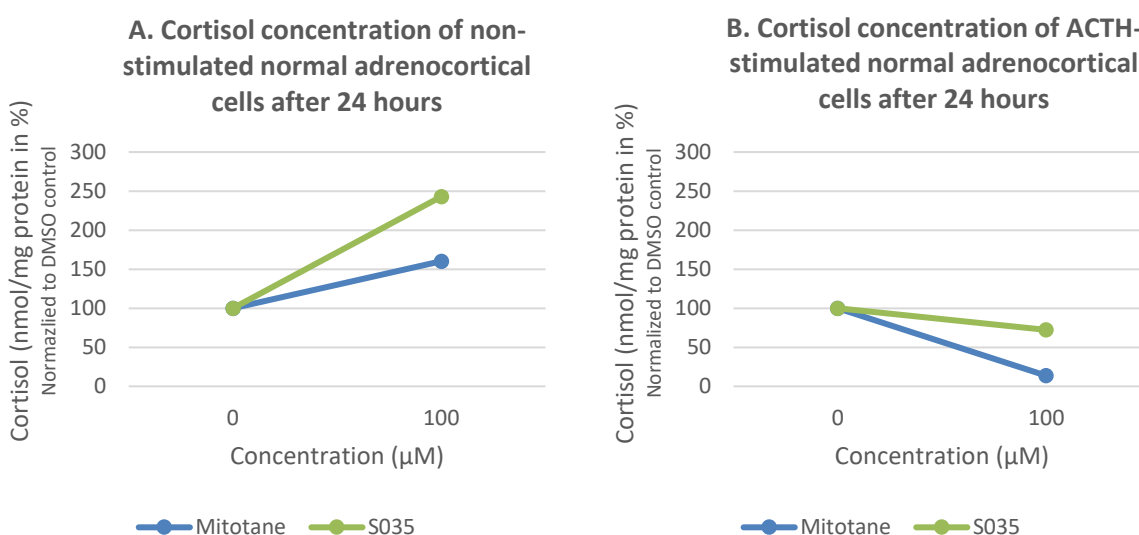


Figure 18: Effects of mitotane and Sandoz 58-035 (S035) on the cortisol concentration of non-stimulated (A) and ACTH-stimulated (B) normal adrenocortical cells (n=1) after 24 hours.

Pilot study 2

After 6 hours, the cortisol concentration of non-stimulated normal adrenocortical cells incubated with mitotane fluctuated around the control level (100%) (figure 19A). At some compound concentrations, the cortisol concentration was decreased, for example at the 20 μM concentration (70.6% ± 37.9) the lowest cortisol concentration was observed. At the highest compound concentration, the cortisol concentration was increased the most (133.9% ± 73.7). Mitotane decreased the number of proteins at higher compound concentrations (appendix 4.2 figure 47A). The cortisol concentration of non-stimulated normal adrenocortical cells incubated with S035 always remained beneath the control level, with the lowest cortisol concentration at the 10 μM concentration (61.9% ± 2.1), after which an increase to 94.7% ± 28.0 at the highest compound concentration was observed (figure 19A). No obvious effect on the number of proteins was observed (appendix 4.2 figure 47A). ATR-101 increased the cortisol concentration with a maximal production of 402.6% ± 194.2 at the 100 nM concentration (figure 19A). ATR-101 did not obviously affect the number of proteins (appendix 4.2 figure 47A).

The cortisol concentration of the ACTH-stimulated normal adrenocortical cells incubated with mitotane initially increased, after which a decrease to $64.1\% \pm 23.6$ at the $50 \mu\text{M}$ concentration was observed (figure 19B). At the highest concentration, the cortisol concentration increased ($82.7\% \pm 23.0$). Mitotane decreased the number of proteins at higher compound concentrations (appendix 4.2 figure 47B). The cortisol concentration of cells incubated with S035 increased to $205.8\% \pm 6.4$ at the $100 \mu\text{M}$ concentration (figure 19B). ATR-101 decreased the cortisol concentration with a minimal production of $38.8\% \pm 21.8$ at the highest concentration (figure 19B). S035 and ATR-101 had little effect on the number of proteins (appendix 4.2 figure 47B).

Absolute data of the cortisol concentration and the number of proteins is presented in appendix 4.2.

Absolute cortisol concentrations in our pilot studies at 6 hours were generally low (appendix 4.1 figure 40). In addition, the cortisol inhibiting effects of mitotane and S035 in ACTH-stimulated normal adrenocortical cells were more obvious after 24 hours of incubation (figure 18). Therefore, we decided to incubate normal adrenocortical cells and ACC cells for 24 hours in our follow-up cortisol experiments. In addition, a serial dilution gave better insight into the concentration dependent effects of our compounds on the cortisol concentration.

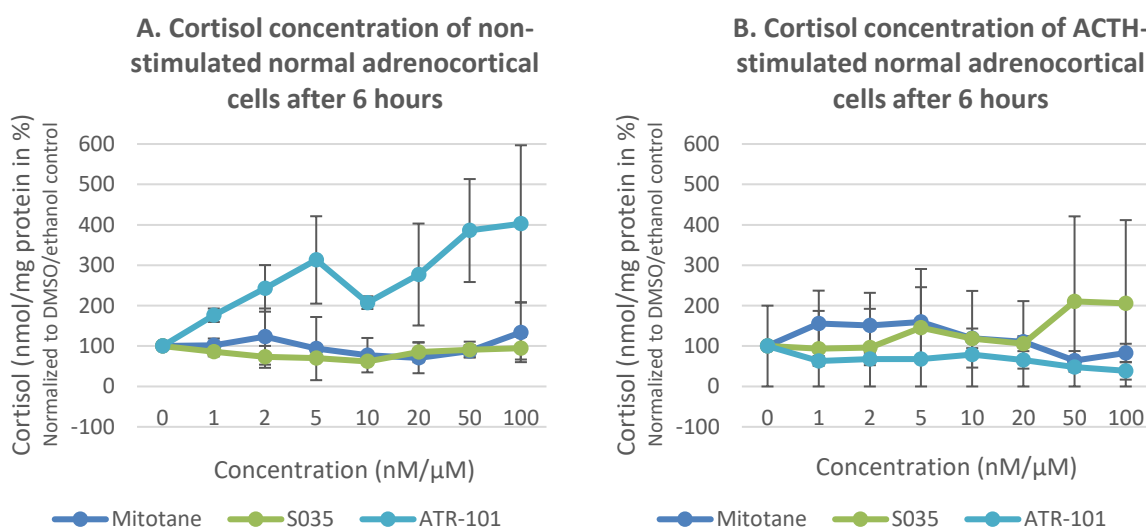


Figure 19: Effects of mitotane, Sandoz 58-035 (S035) and ATR-101 on the cortisol concentration of non-stimulated (A) and ACTH-stimulated (B) normal adrenocortical cells (n=2) after 6 hours.

Paragraph 4.2.1.2: Follow-up experiments

After 24 hours, the cortisol concentration of mitotane incubated non-stimulated normal adrenocortical cells fluctuated around the 200%. The cortisol concentration was maximal at the highest compound concentration ($282.0\% \pm 149.3$) (figure 20A). Mitotane decreased the number of proteins at higher compound concentrations (appendix 4.3 figure 50A). S035 increased the cortisol concentration with increasing compound concentrations. The cortisol concentration was maximal at the highest compound concentration ($210.8\% \pm 59.7$) (figure 20A). S035 did not affect the number of proteins (appendix 4.3 figure 50A). ATR-101 increased the cortisol concentration to $593.1\% \pm 226.7$ at the maximal compound concentration (figure 20A). ATR-101 decreased the number of proteins at higher compound concentrations (appendix 4.3 figure 50A). Statistics revealed no significant differences in cortisol concentrations at different compound concentrations (table 3).

Mitotane initially concentration dependently decreased the cortisol concentration of ACTH-stimulated normal adrenocortical cells to $10.3\% \pm 12.4$ at the $50 \mu\text{M}$ concentration, after which an

increase to $32.9\% \pm 54.2$ at the maximum compound concentration was observed (figure 20B). Mitotane decreased the number of proteins at higher compound concentrations (appendix 4.3 figure 50B). The cortisol production of S035 incubated ACTH-stimulated normal adrenocortical cells fluctuated between the 100 and 150%. The highest cortisol concentration was reached at the $5\ \mu\text{M}$ concentration ($142.2\% \pm 81.9$) (figure 20B). S035 had no obvious effect on the number of proteins (appendix 4.3 figure 50B). The cortisol concentration of ATR-101 incubated cells initially fluctuated around control level (100%), after which a decrease to $21.6\% \pm 20.6$ at the $50\ \text{nM}$ concentration was observed (figure 20B). At the maximal compound concentration, the cortisol concentration slightly increased ($28.8\% \pm 31.2$). ATR-101 decreased the number of proteins at higher compound concentrations (appendix 4.3 figure 50B). Statistics revealed no significant differences in cortisol concentrations at different compound concentrations (table 3).

Absolute data of the cortisol concentration and the number of proteins is presented in appendix 4.3.

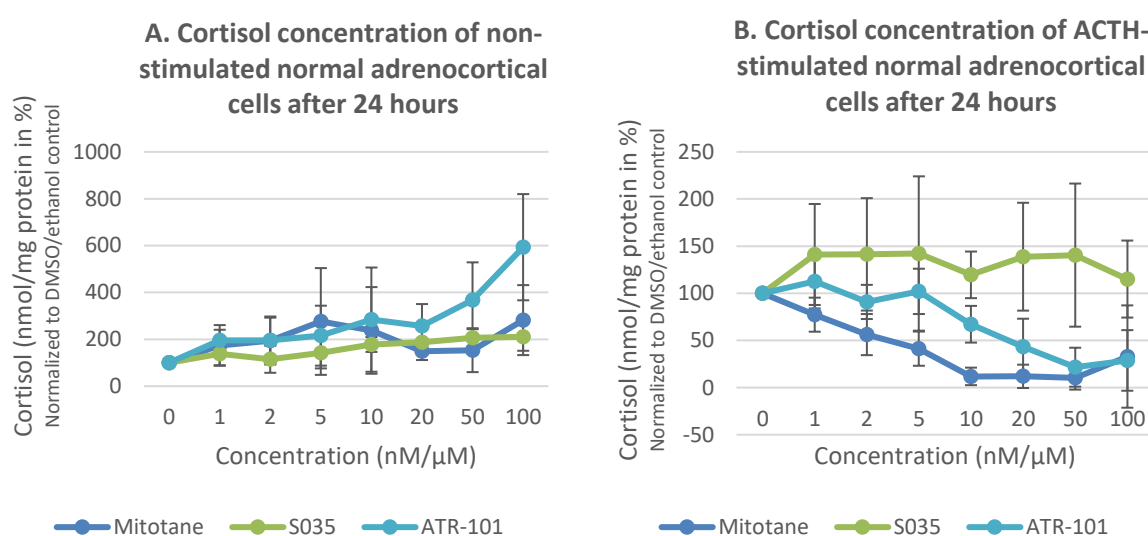


Figure 20: Effects of mitotane, Sandoz 58-035 (S035) and ATR-101 on the cortisol concentration of non-stimulated (A) and ACTH-stimulated (B) normal adrenocortical cells (n=4) after 24 hours.

Table 3: Statistics of cortisol concentrations. No significant differences were observed between the cortisol concentrations of non-stimulated and ACTH-stimulated normal adrenocortical cells (n=4) at different compound concentrations.

	Friedman test p-value	Wilcoxon Signed Rank Test p-values (before and after applying Bonferroni correction)						
		Control – 1 nM/μM	Control – 2 nM/μM	Control – 5 nM/μM	Control – 10 nM/μM	Control – 20 nM/μM	Control – 50 nM/μM	Control – 100 nM/μM
Non-stimulated	Mitotane: p=0.139	N/a	N/a	N/a	N/a	N/a	N/a	N/a
	S035: p=0.070	N/a	N/a	N/a	N/a	N/a	N/a	N/a
	ATR-101: p=0.006	p = 0.068 → p = 0.476	p = 0.465 → p = 3.255	p = 0.465 → p = 3.255	p = 0.068 → p = 0.476			
ACTH-stimulated	Mitotane: p=0.005	p = 0.144 → p = 1.008	p = 0.068 → p = 0.476	p = 0.144 → p = 1.008				
	S035: p=0.921	N/a	N/a	N/a	N/a	N/a	N/a	N/a
	ATR-101: p=0.001	p = 0.465 → p = 3.255	p = 0.273 → p = 1.911	p = 0.715 → p = 5.005	p = 0.068 → p = 0.476			

Mitotane increased the cortisol concentration of the non-stimulated ACC cells to 698.1% at the $5\ \mu\text{M}$ concentration, after which the cortisol concentration fluctuated around the 500%. The cortisol

concentration was the lowest at the highest compound concentration (357.4%) (figure 21A). S035 increased the cortisol concentration to 1056.7% at the 50 μ M concentration, after which a decrease to 709.1% at the 100 μ M concentration was observed (figure 21A). ATR-101 increased the cortisol concentration to 3247.8% at the 10 nM concentration, after which a decrease to 1640.1% at the 100 nM concentration was observed (figure 21A).

In ACTH-stimulated ACC cells, mitotane decreased the cortisol concentration to 8.5% at the maximal compound concentration (figure 21B). The cortisol concentration of S035 incubated ACC cells fluctuated around control level (100%) (figure 21B). ATR-101 initially increased the cortisol concentration to 138.1% at the 10 nM concentration, after which the cortisol concentration decreased to 7.1% at the 50 nM concentration. At the maximal compound concentration, the cortisol concentration increased (65.5%) (figure 21B).

No effect of mitotane, S035 and ATR-101 on the number of proteins was observed (appendix 4.3 figure 53). Absolute data of the cortisol concentration is presented in appendix 4.3.

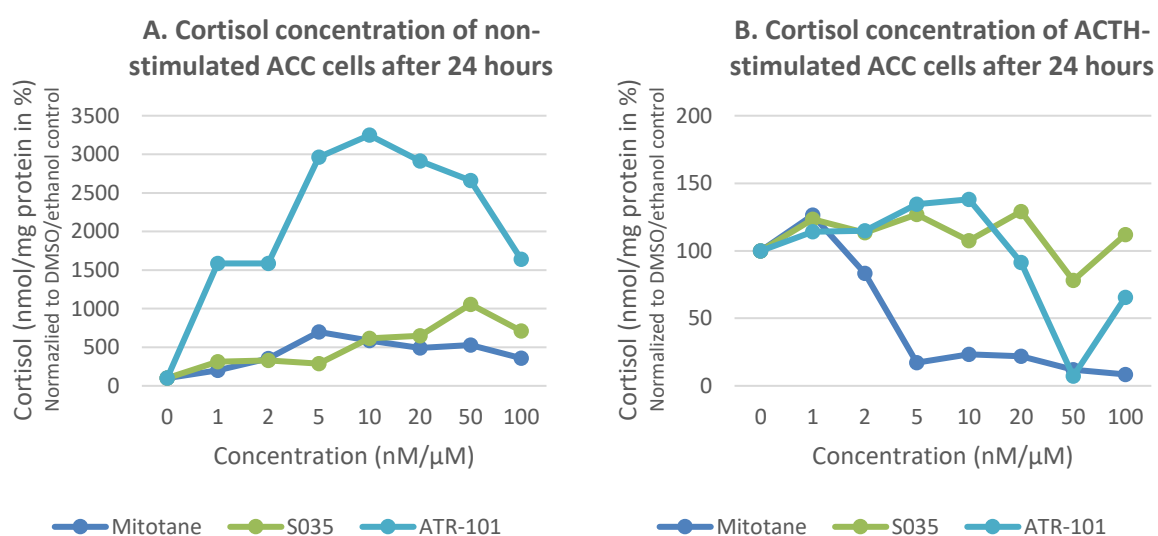


Figure 21: Effects of mitotane, Sandoz 58-035 (S035) and ATR-101 on the cortisol concentration of non-stimulated (A) and ACTH-stimulated (B) adrenocortical carcinoma (ACC) cells (n=1) after 24 hours.

Paragraph 4.2.2: Viability, cytotoxicity and apoptosis

Paragraph 4.4.2.1: ApoTox-Glo™ Triplex Assay

After an initial slight increase, viability of the non-stimulated and ACTH-stimulated normal adrenocortical cells incubated with increasing mitotane concentrations decreased to 13.5% and 14.2% at the 100 μ M concentration, respectively. Surprisingly, cytotoxicity of the non-stimulated and ACTH-stimulated normal adrenocortical cells ultimately decreased to 37.9% and 56.1% at the 100 μ M concentration, respectively. Apoptosis of the non-stimulated and ACTH-stimulated normal adrenocortical cells increased to 413% and 352.9% at the 100 μ M concentration, respectively (figure 22A and B). Because apoptosis increased, we expected viability to decrease and cytotoxicity to increase or stay constant. However, this was not the case. An explanation could be that the cytotoxic effect of mitotane occurs early after incubation. The dead cell proteases (e.g. Tripeptidyl peptidase II), which are released from cells losing membrane integrity, could have a short half life time. Since the assay relies on the measurement of these proteases, the possible early cytotoxic effect could lead to underestimation of cytotoxicity.^{57,58} This made the ApoTox-Glo™ Triplex Assay unsuitable for measuring effects of our compounds on cytotoxicity after 24 hours. Absolute data are presented in appendix 4.4 figure 55.

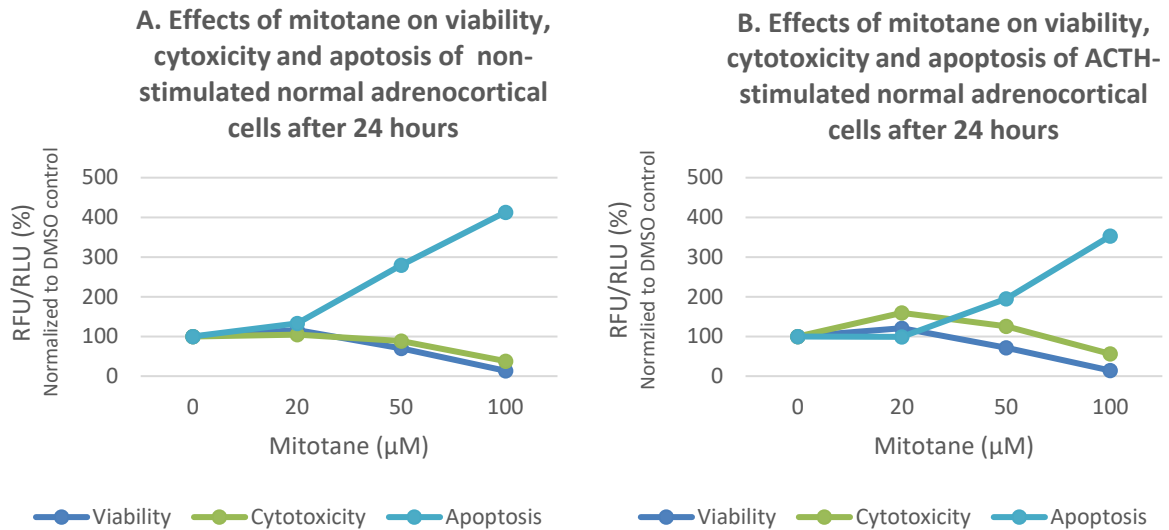


Figure 22: Effects of mitotane on viability, cytotoxicity and apoptosis of non-stimulated (A) and ACTH-stimulated (B) normal adrenocortical cells (n=1) after 24 hours measured by the ApoTox-Glo™ Triplex Assay. RFU = relative fluorescence units, RLU = relative luminescence units.

As depicted in figure 23, increasing ethanol concentrations seemed to have little effect on cell viability, cytotoxicity or apoptosis. Based on this result, we concluded that 0.96% ethanol was not harmful to our cells, and we could thus use a maximal ATR-101 concentration of 100 nM. Absolute data are presented in appendix 4.4 figure 56.

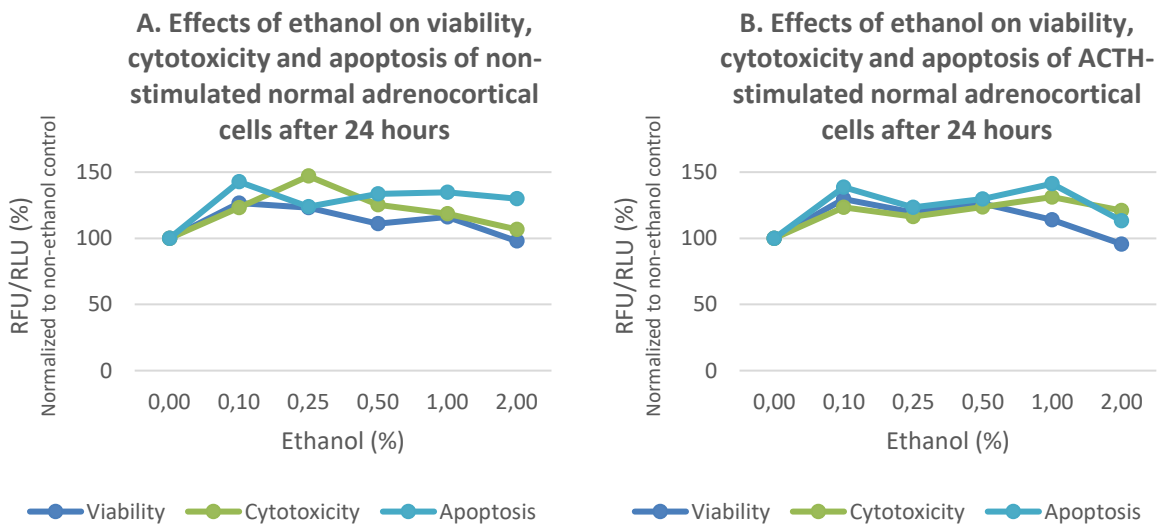


Figure 23: Effects of ethanol on viability, cytotoxicity and apoptosis of non-stimulated (A) and ACTH-stimulated (B) normal adrenocortical cells (n=1) after 24 hours measured by the ApoTox-Glo™ Triplex Assay. RFU = relative fluorescence units, RLU = relative luminescence units.

Paragraph 4.4.2.2: Follow-up experiments

Although the ApoTox-Glo™ Triplex Assay was unsuitable to determine effects on cytotoxicity, it was capable to determine effects of mitotane on apoptosis. We decided to measure apoptosis using the Caspase-Glo® 3/7 assay, which was the component of the ApoTox-Glo™ Triplex Assay that was used for measurements of apoptosis, and to measure the cell viability using the alamarBlue® Assay.

Apoptosis

Apoptosis was measured using the Caspase-Glo® 3/7 assay. Mitotane increased apoptosis of non-stimulated normal adrenocortical cells to a maximum of $476.0\% \pm 132.5$. S035 had little effect on apoptosis. Similar to mitotane, ATR-101 increased apoptosis to $433.5\% \pm 19.7$ (figure 24A).

In the non-stimulated ACC cells, mitotane increased apoptosis with $842.7\% \pm 265.2$, ATR-101 with $571.0\% \pm 1.0$ and S035 with $372.8\% \pm 188.9$ (figure 24B).

Absolute data are presented in appendix 4.5.

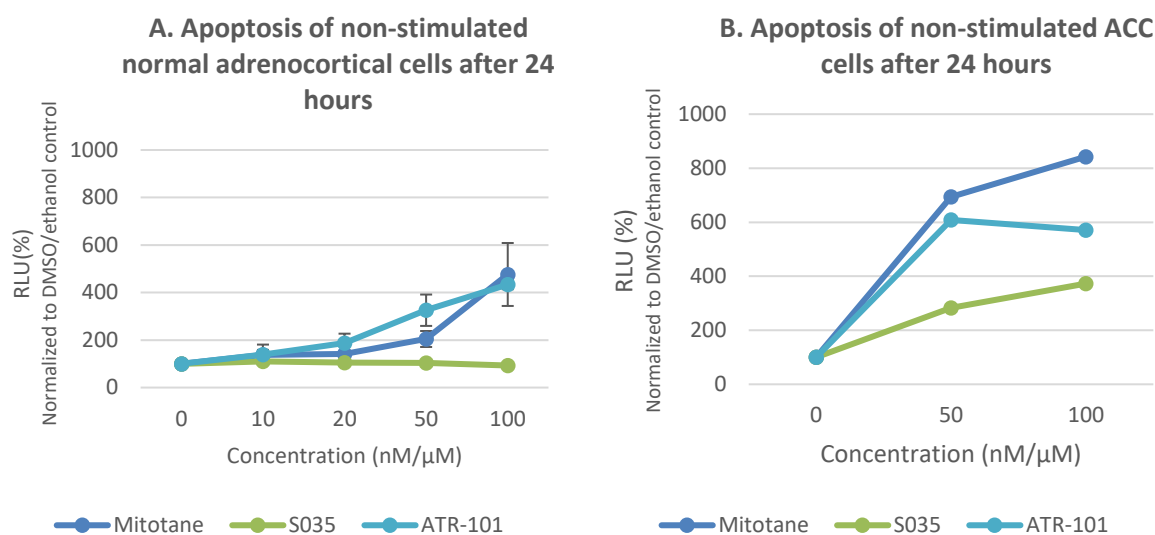


Figure 24: Effects of mitotane, Sandoz 58-035 (S035) and ATR-101 on apoptosis of non-stimulated normal adrenocortical cells (n=2) (A) and non-stimulated adrenocortical carcinoma (ACC) cells (n=1) (B) after 24 hours. RLU = relative luminescence units.

Viability

Viability was measured using the alamarBlue® Assay. Viability of non-stimulated normal adrenocortical cells incubated with mitotane decreased with higher compound concentrations. Minimal viability was observed at the 100 μM concentration ($51.2\% \pm 22.0$) (figure 25A). Increasing apoptosis was thus accompanied by decreasing viability. S035 dose-dependently increased viability of non-stimulated normal adrenocortical cells with a maximal viability at the 100 μM concentration ($131.4\% \pm 2.4$) (figure 25A). ATR-101 initially increased viability to $194.2\% \pm 23.6$ at the 50 nM concentration. At the highest compound concentration (100 nM), viability decreased ($148.4\% \pm 56.2$) (figure 25A). The increased viability is in contradiction with increased apoptosis (figure 24A).

Viability of ACTH-stimulated normal adrenocortical cells incubated with mitotane decreased with increasing compound concentrations. Minimal viability of $50.4\% \pm 27.5$ was reached at the highest compound concentration (100 μM) (figure 25B). S035 increased viability with increasing compound concentrations. Maximal viability of $126.0\% \pm 19.5$ was reached at 100 μM concentration (figure 25B). ATR-101 increased viability to $157.4\% \pm 42.0$ at the 50 nM concentration. Thereafter, viability decreased to $126.2\% \pm 28.2$ at the 100 nM concentration (figure 25B).

Statistics revealed no significant difference in viability at different compound concentrations (table 4).

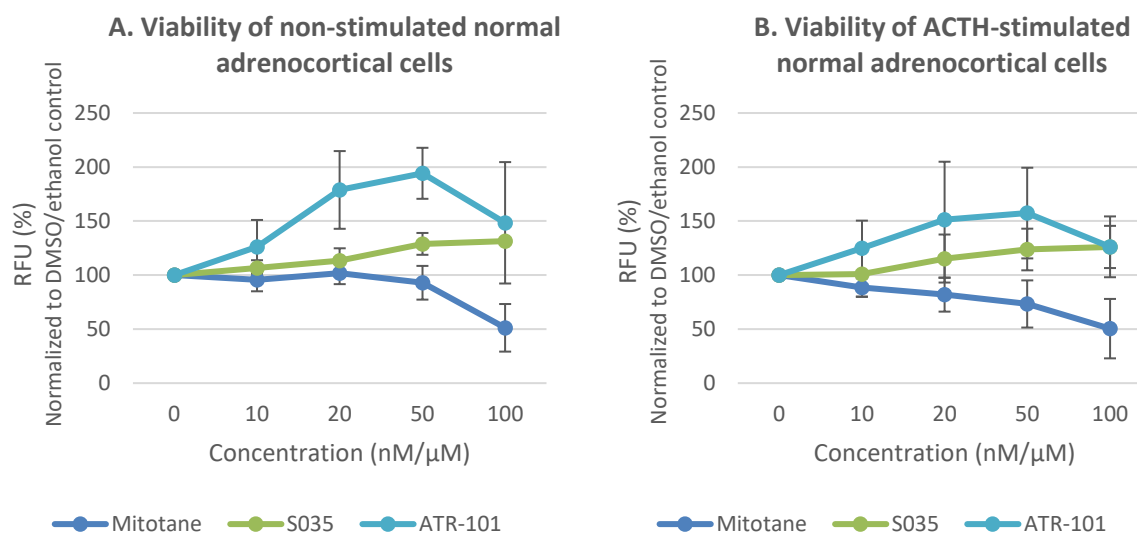


Figure 25: Effects of mitotane, Sandoz 58-035 (S035) and ATR-101 on the viability of non-stimulated (A) and ACTH-stimulated (B) normal adrenocortical cells (n=4) after 24 hours. RFU = relative fluorescence units.

Table 4: Statistics of viability. Statistics revealed no significant difference in viability of non-stimulated and ACTH-stimulated normal adrenocortical cells (n=4) at different compound concentrations.

	One-Way ANOVA p-value
Non-stimulated	Mitotane: p = 0.843 S035: p = 0.974 ATR-101: p = 0.657
ACTH-stimulated	Mitotane: p = 0.894 S035: p = 0.973 ATR-101: p = 0.925

In the ACC cells, mitotane decreased viability with increasing compound concentrations to 11.7% (non-stimulated) and 13.6% (ACTH-stimulated) (figure 26). Increasing apoptosis was thus accompanied by decreasing viability (figure 24B). S035 increased viability of the ACC cells to 202.7% (non-stimulated) and 193.5% (ACTH-stimulated) at the 50 μM concentration. At the 100 μM concentration, a slight decrease was observed in the ACTH-stimulated ACC cells (166.9%), but not in the non-stimulated ACC cells (189.6%) (figure 26). Despite increasing apoptosis (figure 24B), viability did increase. In non-stimulated ACC cells, ATR-101 initially increased viability (20 nM: 163.2%), after which a decrease to 28.9% at the highest compound concentration was observed (figure 26A). In ACTH-stimulated ACC cells, viability decreased to 16.4% at the maximal compound concentration (100 nM), although an increase was observed at the 20 nM concentration (88.1%) (figure 26B). The increase in apoptosis was thus accompanied by a decrease in viability.

Absolute data are presented in appendix 4.5.

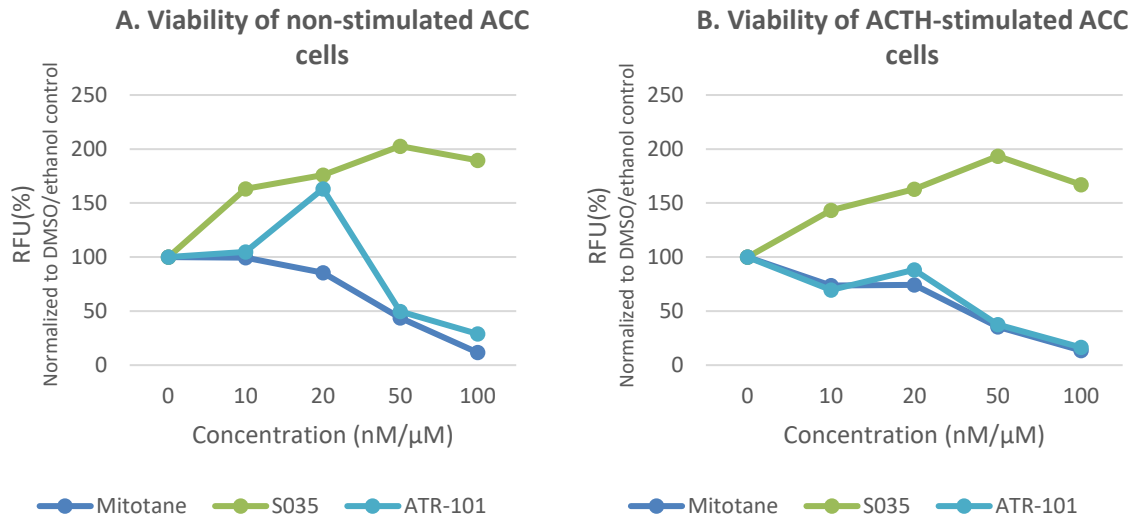


Figure 26: Effects of mitotane, Sandoz 58-035 (S035) and ATR-101 on the viability of non-stimulated (A) and ACTH-stimulated (B) adrenocortical carcinoma (ACC) cells (n=1) after 24 hours. RFU = relative fluorescence units.

Paragraph 4.2.3: Lipidomics

The lipid profile of the normal adrenocortical cells incorporated in our first pilot study was determined. In figure 27 the number of cholesteryl esters in every sample is expressed as a percentage of total cholesterol (free cholesterol and cholesteryl esters) and lipids. The total number of cholesteryl esters differed between the samples. In mitotane incubated non-stimulated normal adrenocortical cells, cholesteryl esters increased after 6 hours, but decreased after 24 hours. In ACTH-stimulated normal adrenocortical cells, cholesteryl esters decreased after 6 hours. After 24 hours, the number of cholesteryl esters was at the control level. S035 did not affect the number cholesteryl esters in non-stimulated normal adrenocortical cells. In ACTH-stimulated normal adrenocortical cells, cholesteryl esters were decreased after 6 hours and increased after 24 hours. Based on these results, it could thus be possible that mitotane and S035 both cause an early decrease and a late increase in cholesteryl esters in a hypercortisolic environment, suggesting early SOAT1 inhibition. However, we have to take into consideration that only one NA was incorporated in this study. Output of the principal component analysis is presented in appendix 5.

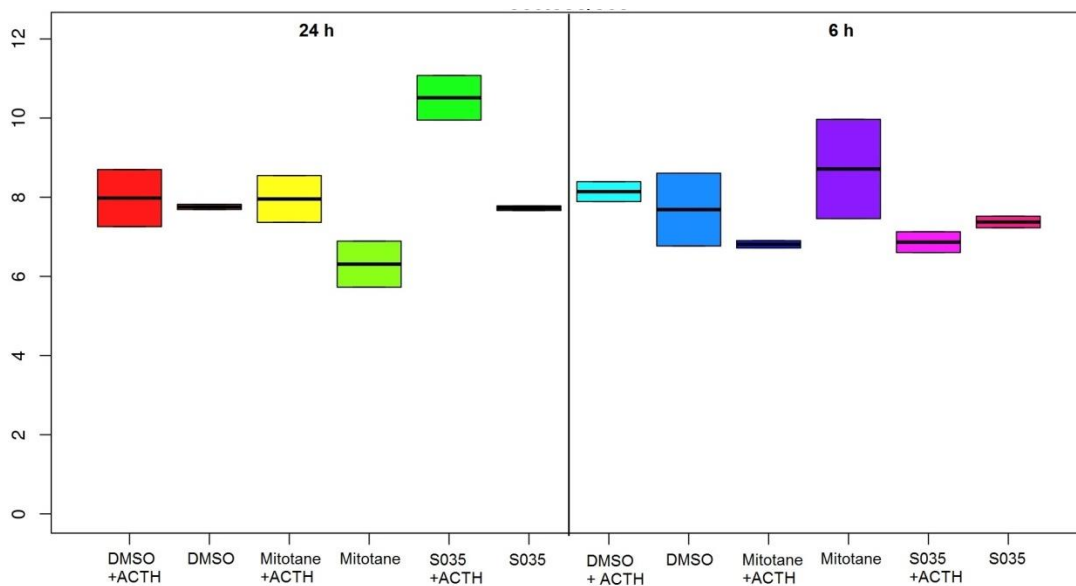


Figure 27: Effects of mitotane and Sandoz 58-035 (S035) on lipid metabolism of non-stimulated and ACTH-stimulated normal adrenocortical cells (n=1) after 6 and 24 hours.

Paragraph 4.2.4: Lipid droplets

We aimed to visualize the SOAT1 inhibiting effects by evaluating the number and size of lipid droplets in normal adrenocortical cells. Therefore, we stained normal adrenocortical cells using an immunofluorescent dye for lipid droplets. Lipid droplets were successfully visualized in non-stimulated normal adrenocortical cells, although no obvious increase in number or size of lipid droplets was observed in non-stimulated normal adrenocortical cells incubated with mitotane or S035 (figure 28). Lipid droplets of fibroblasts stained also. Therefore, it was difficult to distinguish normal adrenocortical cells from fibroblasts.

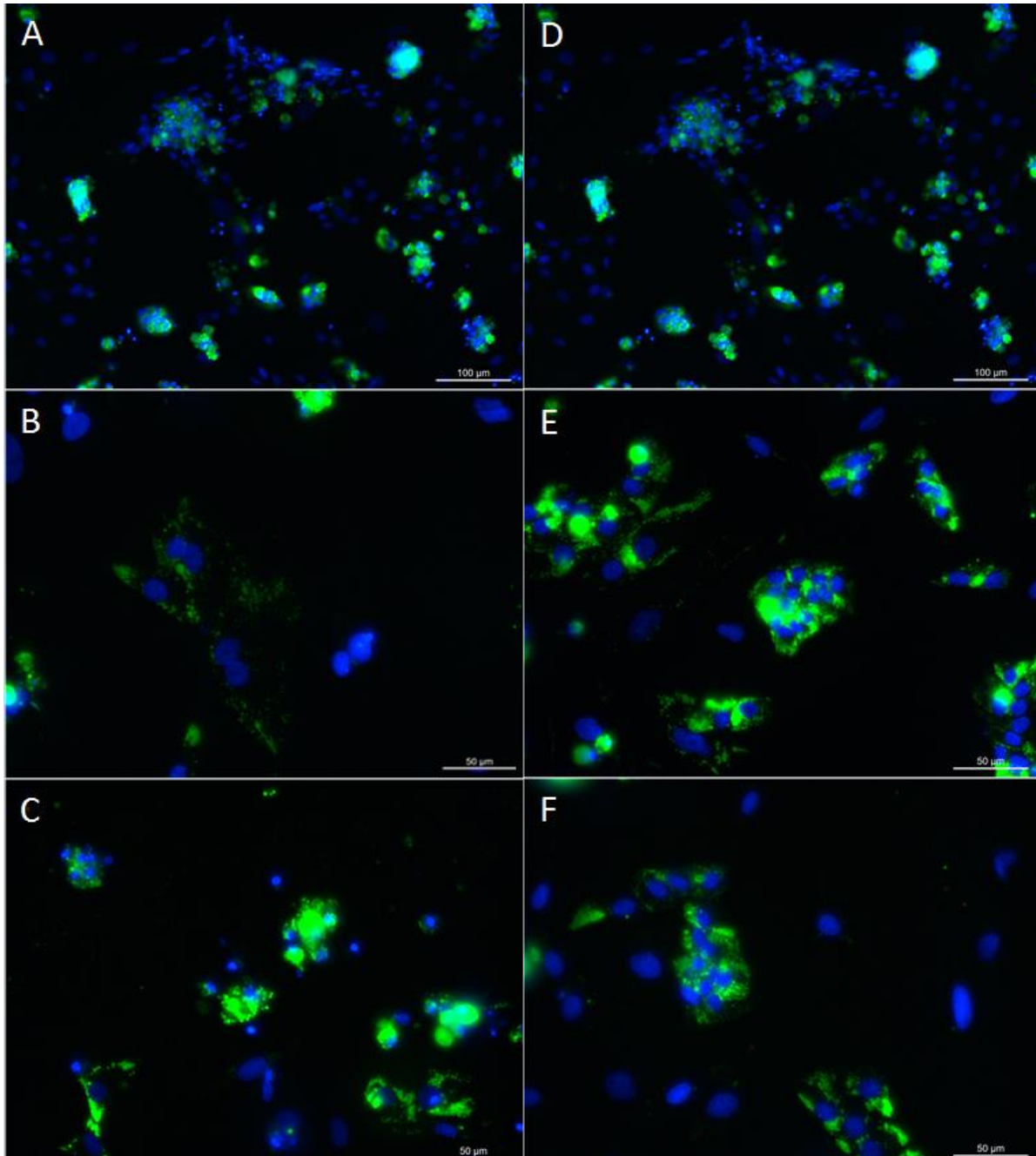


Figure 28: Immunofluorescent imaging of lipid droplets. Blue colour is nuclear DAPI staining. Green colour is LD540 staining for lipid droplets. A and D = DMSO control, B = 50 μM mitotane, C = 100 μM mitotane, E = 50 μM S035, F = 100 μM S035. Scale bar represents 100 μm (A and D) or 50 μm (B, C, E and F).

Paragraph 4.2.5: ER-stress and the UPR

Paragraph 4.2.5.1: RT-qPCR

Originally, we wanted to evaluate the relative mRNA expression after 6 and 24 hours of incubation. However, little mRNA was left in our 24-hour samples incubated with mitotane and ATR-101. An explanation could be that we removed detached apoptotic cells when we gathered medium, thereby losing valuable mRNA. Therefore, we only report relative mRNA expression after 6 hours.

The relative mRNA expression of ATF4 was used as a marker of PERK-pathway activity. The relative mRNA expression of ATF4 in non-stimulated ACC cells was increased when the cells were incubated with mitotane (fold change: 2.7). The relative mRNA expression further increased in ACTH-stimulated cells (fold change: 4.5), suggesting PERK-pathway activity in ACC cells incubated with mitotane. S035 did not increase PERK-pathway in the non-stimulated as well as in the ACTH-stimulated ACC cells. PERK-pathway activity in ACC cells incubated with ATR-101 was slightly increased in non-stimulated ACC cells (fold change: 1.8), but not in ACTH-stimulated ACC cells (table 5).

Table 5: Effects of mitotane, Sandoz 58-035 (S035) and ATR-101 on protein kinase RNA (PKR)-like ER kinase (PERK) pathway activity in non-stimulated and ACTH-stimulated adrenocortical carcinoma cells (n=1). PERK-pathway activity was evaluated based on the relative mRNA expression of activating transcription factor 4 (ATF4).

Pathway	Factor	Non-stimulated (fold change)	ACTH-stimulated (fold change)
PERK	ATF4	Mitotane: 2.7	Mitotane: 4.5
		S035: 1.1	S035: 1.4
		ATR-101: 1.8	ATR-101: 1.2

Splicing of uXBP1 was used as a marker for IRE1-pathway activity. Incubating non-stimulated ACC cells with mitotane increased uXBP1 splicing, because the relative mRNA expression of uXBP1 decreased (fold change: 0.3) and the relative mRNA expression of sXBP1 increased (fold change: 2.2). In ACTH-stimulated cells, the relative mRNA expression of uXBP1 was also decreased (fold change: 0.4), accompanied with a slightly increased relative mRNA expression of sXBP1 (fold change: 1.8). These results indicated IRE1-pathway activity in non-stimulated and ACTH-stimulated ACC cells incubated with mitotane. ATR-101 decreased relative mRNA expression of uXBP1 in non-stimulated and ACTH-stimulated ACC cells (fold changes: 0.5), but expression of sXBP1 was not increased. S035 did not affect the IRE1-pathway (table 6).

Table 6: Effects of mitotane, Sandoz 58-035 (S035) and ATR-101 on inositol-requiring protein 1 (IRE1) pathway activity in non-stimulated and ACTH-stimulated adrenocortical carcinoma cells (n=1). IRE1-pathway activity was evaluated based on the relative mRNA expressions of unspliced X-box binding protein 1 (uXBP1) and spliced X-box binding protein 1 (sXBP1).

Pathway	Factor	Non-stimulated (fold change)	ACTH-stimulated (fold change)
IRE1	uXBP1	Mitotane: 0.3	Mitotane: 0.4
		S035: 0.9	S035: 1.2
		ATR-101: 0.5	ATR-101: 0.5
	sXBP1	Mitotane: 2.2	Mitotane: 1.8
		S035: 1.0	S035: 0.7
		ATR-101: 1.4	ATR-101: 1.1

ERAD activity was determined by evaluating the relative mRNA expressions of EDEM1 and HERPUD1, two components of ERAD. Mitotane increased the relative mRNA expression of HERPUD1 in non-stimulated (fold change: 11.8) and ACTH-stimulated ACC cells (fold change: 21.2). S035 only increased the relative mRNA expression of HERPUD1 in the ACTH-stimulated ACC cells (fold change: 1.9), however to a much lesser extent in comparison to mitotane. ATR-101 increased the relative mRNA

expression of HERPUD1 in non-stimulated (fold change: 3.9) and ACTH-stimulated (fold change: 4.4) ACC cells, but again to a lesser extent in comparison to mitotane. None of the compounds affected the relative mRNA expression of EDEM1. These results thus suggested that ERAD was activated in non-stimulated and ACTH-stimulated ACC cells incubated with mitotane and ATR-101 and in ACTH-stimulated ACC cells incubated with S035 (table 7).

Table 7: Effects of mitotane, Sandoz 58-035 (S035) and ATR-101 on ER-associated protein degradation (ERAD) activity in non-stimulated and ACTH-stimulated adrenocortical carcinoma cells (n=1). ERAD activity was evaluated based on the relative mRNA expressions of ER degradation enhancing α -mannosidase like protein 1 (EDEM1) and homocysteine inducible endoplasmic reticulum protein with ubiquitin like domain 1 (HERPUD1).

Pathway	Factor	Non-stimulated (fold change)	ACTH-stimulated (fold change)
ERAD	EDEM1	Mitotane: 0.9	Mitotane: 1.0
		S035: 1.2	S035: 1.0
		ATR-101: 1.4	ATR-101: 1.0
	HERPUD	Mitotane: 11.8	Mitotane: 21.2
		S035: 1.5	S035: 1.9
		ATR-101: 3.9	ATR-101: 4.4

The relative mRNA expressions of ERP72, GRP78 and p58^{ipk} were determined as the effectors of the UPR. The relative ERP72 mRNA expression was the highest in non-stimulated (fold change: 16.1) and ACTH-stimulated (fold change: 18.2) ACC cells incubated with mitotane. Also, the relative mRNA expression of GRP78 in the ACTH-stimulated ACC cells was stronger increased (fold change: 23.1) compared to the non-stimulated ACC cells (fold change: 7.6). Interestingly, the relative mRNA expression of p58^{ipk} was stronger increased in non-stimulated ACC cells (fold change: 5.5) compared to ACTH-stimulated ACC cells (fold change: 2.5). S035 only slightly increased the relative ERP72 mRNA expression in non-stimulated cells (fold change 1.7) and the relative GRP78 mRNA expression in ACTH-stimulated cells (fold change: 3.8). In non-stimulated cells, ATR-101 increased the relative mRNA expression of all three effectors (fold changes: 4.3, 2.0 and 1.6, respectively), although to a lesser extent compared to mitotane. Only the relative mRNA expression of ERP72 was increased in ACTH-stimulated ACC cells (fold change: 4.0) (table 8).

Table 8: Effects of mitotane, Sandoz 58-035 (S035) and ATR-101 on effectors of the unfolded protein response (UPR) in non-stimulated and ACTH-stimulated adrenocortical carcinoma cells (n=1). The relative mRNA expressions of the following effectors were evaluated: ER protein 72 (ERP72), glucose-regulated protein 78 (GRP78) and DnaJ heat shock protein family member C3 (p58^{ipk}).

Pathway	Factor	Non-stimulated (fold change)	ACTH-stimulated (fold change)
Effectors	ERP72	Mitotane: 16.1	Mitotane: 18.2
		S035: 1.7	S035: 1.5
		ATR-101: 4.3	ATR-101: 4.0
	GRP78	Mitotane: 7.6	Mitotane: 23.1
		S035: 1.2	S035: 3.8
		ATR-101: 2.0	ATR-101: 1.4
	p58 ^{ipk}	Mitotane: 5.5	Mitotane: 2.5
		S035: 1.2	S035: 0.9
		ATR-101: 1.6	ATR-101: 1.3

The relative mRNA expression of CHOP, an important ER-stress marker of the apoptotic phase of the UPR, was strongly increased in non-stimulated (fold change: 57.7) and ACTH-stimulated (fold change: 98.3) ACC cells incubated with mitotane. The relative mRNA expression of CHOP was also increased in non-stimulated (fold change: 16.2) and ACTH-stimulated (fold change: 16.4) cells incubated with ATR-101, however, to a lesser extent. S035 minimally increased the relative mRNA

expression of CHOP in ACTH-stimulated cells (fold change: 3.4) compared to ACTH-stimulated cells incubated with mitotane or ATR-101 (table 9).

Table 9: Effects of mitotane, Sandoz 58-035 (S035) and ATR-101 on the relative CCAAT/enhancer-binding protein homologous protein (CHOP) mRNA expression in non-stimulated and ACTH-stimulated adrenocortical carcinoma cells (n=1).

Pathway	Factor	Non-stimulated (fold change)	ACTH-stimulated (fold change)
Apoptosis	CHOP	<i>Mitotane</i> : 57.7	<i>Mitotane</i> : 98.3
		<i>S035</i> : 1.3	<i>S035</i> : 3.4
		<i>ATR-101</i> : 16.2	<i>ATR-101</i> : 16.4

As described previously, CHOP initiates the apoptotic phase of the UPR by decreasing BCL-2 expression, thereby releasing pro-apoptotic factors for the initiation of BAX/BAK mediated permeabilization of the mitochondrial membrane. Upon permeabilization, cytochrome c is released, which triggers caspase activation. Surprisingly, mitotane decreased the relative mRNA expression of BAX in non-stimulated (fold change: 0.6) and ACTH-stimulated (fold change: 0.5) ACC cells while decreasing the relative mRNA expression of BCL-2 in ACTH-stimulated cells (fold change: 0.5) as well. Mitotane increased the relative mRNA expression of Casp3 in non-stimulated (fold change: 3.9) and ACTH-stimulated (fold change: 3.9) cells. S035 did not affect the relative mRNA expressions of BAX, BCL-2 and Casp3. ATR-101 did not affect the relative mRNA expression of BAX, but did increase the relative mRNA expressions of BCL-2 in ACTH-stimulated cells (fold change: 1.6) and of Casp3 in non-stimulated cells (fold change: 1.8) (table 10).

Table 10: Effects of mitotane, Sandoz 58-035 (S035) and ATR-101 on CHOP-mediated apoptosis in non-stimulated and ACTH-stimulated adrenocortical carcinoma cells (n=1). BCL-2 associated X (BAX), B-cell lymphoma 2 (BCL-2), caspase 3 (Casp3).

Pathway	Factor	Non-stimulated (fold change)	ACTH-stimulated (fold change)
Apoptosis	BAX	<i>Mitotane</i> : 0.6	<i>Mitotane</i> : 0.5
		<i>S035</i> : 0.8	<i>S035</i> : 1.1
		<i>ATR-101</i> : 1.1	<i>ATR-101</i> : 1.2
	BCL-2	<i>Mitotane</i> : 0.7	<i>Mitotane</i> : 0.5
		<i>S035</i> : 1.2	<i>S035</i> : 0.7
		<i>ATR-101</i> : 1.4	<i>ATR-101</i> : 1.6
	Casp3	<i>Mitotane</i> : 3.9	<i>Mitotane</i> : 3.9
		<i>S035</i> : 1.5	<i>S035</i> : 1.2
		<i>ATR-101</i> : 1.8	<i>ATR-101</i> : 1.2

To evaluate the effects of the UPR on steroidogenesis, we determined the expression of CYP17, SOAT1 and SREBF2. In non-stimulated ACC cells incubated with mitotane, the relative mRNA expressions of CYP17 (fold change: 0.3) and SOAT1 (fold change: 0.3) were decreased. The relative mRNA expression of SREBF2 was not affected. S035 did not affect the relative mRNA expressions of CYP17, SOAT1 and SREBF2 in non-stimulated cells. ATR-101 decreased the relative mRNA expression of CYP17 (fold change: 0.5). In ACTH-stimulated ACC cells, mitotane increased the relative mRNA expression of SOAT1 (fold change: 2.3), but did not affect the relative mRNA expressions of CYP17 and SREBF2. S035 increased the relative mRNA expressions of CYP17 (fold change: 1.8) and SOAT1 (fold change: 3.8), but did not affect the relative mRNA expression of SREBF2. ATR-101 did not affect the relative mRNA expressions of SOAT1 or SREBF2, but decreased the relative mRNA expression of CYP17 (fold change: 0.5) (table 11).

Table 11: Effects of mitotane, Sandoz 58-035 (S035) and ATR-101 on steroidogenesis of non-stimulated and ACTH-stimulated adrenocortical carcinoma cells (n=1). The effects on steroidogenesis were evaluated based on the relative mRNA expressions of 17 α -hydroxylase (CYP17), sterol-O-acyl transferase 1 (SOAT1) and sterol regulatory element-binding transcription factor 2 (SREBF2).

Pathway	Factor	Non-stimulated (fold change)	ACTH-stimulated (fold change)
Steroidogenesis	CYP17	Mitotane: 0.3	Mitotane: 0.9
		S035: 1.0	S035: 1.8
		ATR-101: 0.5	ATR-101: 0.5
	SOAT1	Mitotane: 0.3	Mitotane: 2.3
		S035: 1.0	S035: 3.8
		ATR-101: 0.9	ATR-101: 0.8
	SREBF2	Mitotane: 1.1	Mitotane: 1.1
		S035: 0.8	S035: 0.7
		ATR-101: 1.0	ATR-101: 0.9

Out of curiosity, we wanted to determine the effects of our compounds on the relative mRNA expression of SF1. SF1 is nuclear receptor that is important in adrenal development and steroidogenesis. The relative mRNA expression of SF1 was decreased in non-stimulated ACC cells incubated with mitotane (fold change: 0.1) and S035 (fold change: 0.4), but increased in ATR-101 incubated cells (fold change: 1.7). The relative mRNA expression of SF1 in ACTH-stimulated cells incubated with mitotane (fold change: 2.2) and S035 (fold change: 2.4) increased, while ATR-101 decreased relative mRNA expression of SF1 (fold change: 0.6) (table 12). ACTH-stimulation thus had contrasting effects on the relative SF1 mRNA expression in incubated ACC cells.

Table 12: Effects of mitotane, Sandoz 58-035 (S035) and ATR-101 on the relative steroidogenic factor 1 (SF1) mRNA expression of in non-stimulated and ACTH-stimulated adrenocortical carcinoma cells (n=1).

Pathway	Factor	Non-stimulated (fold change)	ACTH-stimulated (fold change)
Adrenal development and steroidogenesis	SF1	Mitotane: 0.1	Mitotane: 2.2
		S035: 0.4	S035: 2.4
		ATR-101: 1.7	ATR-101: 0.6

Paragraph 4.2.5.2: Western Blot

To evaluate the effects of ER-stress on the protein level, we needed antibodies that could recognize canine proteins of ER-stress factors. Therefore, we tested antibodies against (p)-eIF2 α , CHOP and ATF6.

The anti-ATF6-antibody detected a protein with a molecular weight of 34 kDa in normal adrenocortical cells incubated with mitotane (figure 29). ATF6 is a 90 kDa protein, which let us to conclude that our anti-ATF6-antibody was not suitable for canine adrenocortical cells.

Our anti-CHOP-antibody detected several proteins with a molecular weight higher than 27 kDa, which is the molecular weight of CHOP. Therefore, our anti-CHOP-antibody was not suitable for canine adrenocortical cells either (figure 29).

Anti-eIF2 α -antibody detected a 36.1 kDa protein (figure 29). Because the molecular weight of eIF2 α is 38 kDa, this antibody succeeded in recognizing eIF2 α protein.

The anti-p-eIF2 α -antibody detected a 37 kDa protein. Because the molecular weight of eIF2 α is 38 kDa, this antibody also succeeded in recognizing the correct protein. However, a 58 kDa protein was also detected (figure 29).

The anti-eIF2 α -antibody and the anti-p-eIF2 α -antibody could thus be useful in evaluating the effects of our compounds on the UPR. ER-stress was successfully initiated in normal adrenocortical cells incubated with several mitotane concentrations, because the anti-eIF2 α -antibody and the anti-p-eIF2 α -antibody detected (p)-eIF2 α : components of the PERK-pathway of the UPR.

The expression of eIF2 α was not determined on the mRNA level, because phosphorylation of eIF2 α is a marker of UPR activity. The expression of ATF6 was not determined at the mRNA level as well, because ATF6 is cleaved and no mRNA sequence of cleaved ATF6 was available.

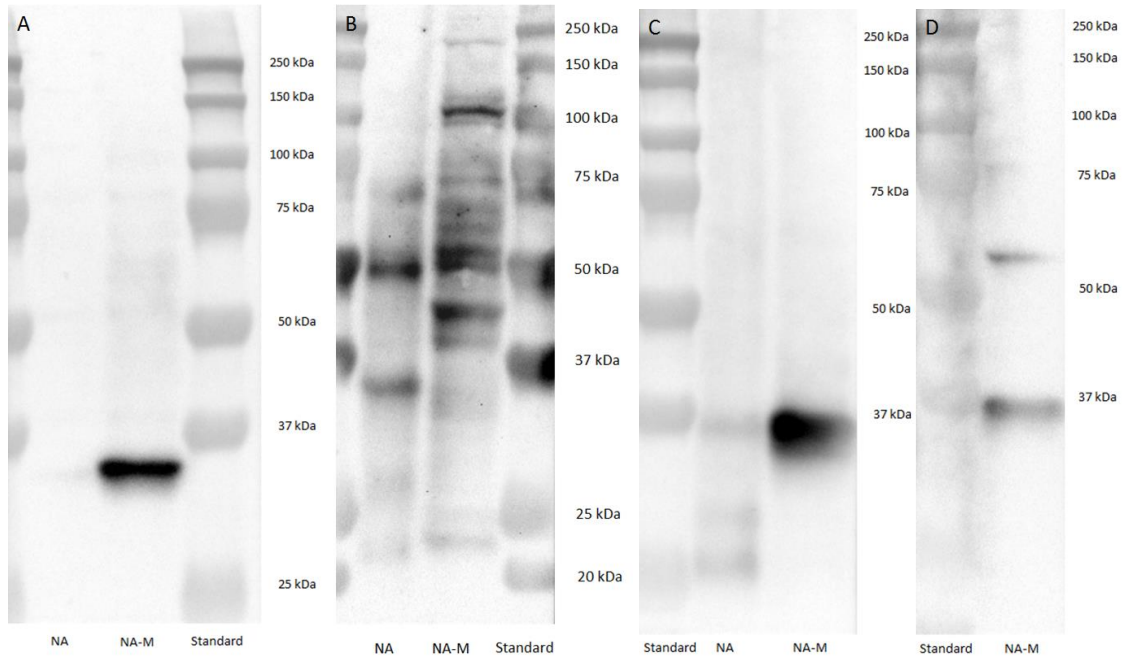


Figure 29: Western Blot of UPR antibodies activating transcription factor 6 (ATF6) (A), CCAAT/enhancer-binding protein homologous protein (CHOP) (B), eukaryotic initiation factor 2 alpha (eIF2 α) (C) and phosphorylated eIF2 α (p-eIF2 α) (D). NA = normal adrenocortical cells, NA-M = normal adrenocortical cells incubated with mitotane.

Chapter 5: Discussion and Conclusion

Paragraph 5.1: SOAT1 expression

SOAT1 was expressed in all ACAs and ACCs on the mRNA as well as on the protein level, providing a solid base that a selective SOAT1 inhibitor could have potential as a future treatment in canine ATs. SOAT1 expression at the mRNA and protein level was more variable in ACCs, similar has been observed in humans as well.¹¹

Some ACAs and ACCs showed low SOAT1 mRNA expression and high SOAT1 protein expression (or clockwise), something which probably relates to tumors being very heterogeneous tissues.⁵⁹ It could thus be possible that RT-qPCR was performed at AT tissue with low SOAT1 mRNA expression, while AT tissue with high SOAT1 protein expression was used for H-scoring. A factor hampering determining SOAT1 protein expression was differing staining intensity between the batches. To solve this problem, the same control tissue should be incorporated in every batch. However, this was not the case and thus the differing staining intensity could be an explanation for the discrepancy between SOAT1 mRNA and protein expression as well. In future experiments, in every batch the same control tissue should be included and intensity grading should be related to the intensity of control tissue.

Due to variation in SOAT1 expression, variation in response to SOAT1 inhibitor treatment is expected, something which was shown in the study of Sbera *et al.* 2015: responders to mitotane therapy showed higher SOAT1 protein expression in comparison to non-responders.¹¹ In dogs, no studies, including a large sample size, into the relationship between SOAT1 protein expression and response to mitotane therapy have been performed so far. The variation in SOAT1 protein expression in canine ATs implies, that also in dogs, a failure to respond to mitotane therapy could be possible.

In terms of using SOAT1 inhibitor as an adjuvant treatment after adrenalectomy, SOAT1 expression of the AT should be determined by IHC. It is important to use several tissue samples to obtain insight in SOAT1 expression throughout the whole AT, because SOAT1 expression varies within the AT. Few samples with low SOAT1 expression might incorrectly reject SOAT1 inhibitor therapy as adjuvant therapy post-adrenalectomy. Determining SOAT1 expression in case of SOAT1 inhibitors as a primary treatment is currently impossible. Therefore, no or little response to mitotane treatment might indicate low SOAT1 expression. Studies into methods for determining SOAT1 expression in patients in which SOAT1 inhibitor therapy as a primary treatment is desired, are warranted.

We succeeded in IHC staining of ACA and ACC slides. However, our negative control tissues (colon, liver and muscle) stained as well (appendix 2.3). This is not surprising, because SOAT1 protein is present in these tissues, although the expression of SOAT1 protein is reported to be the highest in adrenals.^{22,60,61} It is difficult to find suitable negative control tissue, because SOAT1 is ubiquitously expressed.²²

The manufacturer of our anti-SOAT1 antibody reported that our anti-SOAT1-antibody should be functional in canine tissues. Western Blot showed that the anti-SOAT1 antibody did cross react with additional proteins. It is reported that Western Blot of SOAT1 yields a band around 50 kDa, which was the case in this study, but also around 30 and 120 kDa, because of cleavage and binding of hydrophobic SOAT1 to other proteins, respectively.⁶² It could be possible that our anti-SOAT1 antibody detected SOAT2 as well. Blasting protein sequences of SOAT1 and SOAT2 revealed an identity of 47%-53%. However, SOAT2 expression in adrenals is low to absent.²² Summarized, our anti-SOAT1 antibody was possibly not the best antibody to use for IHC and new anti-SOAT1 antibodies, especially for canine tissues, should be tested and/or developed.

In the current study, slides were judged by two researches, although not independently. In the future, slides should thus be judged by several researchers independently.

Paragraph 5.2: *In vitro* studies

Paragraph 5.2.1: Steroidogenesis

Mitotane and ATR-101 strongly decreased the cortisol concentration of ACTH-stimulated normal adrenocortical cells and ACC cells after 24 hours, while S035 was not effective. The reduction in the cortisol concentration could be due to a decreasing number of viable cortisol-producing cells, because mitotane and ATR-101 increased apoptosis of normal adrenocortical cells and ACC cells in a dose-dependent way. S035 increased apoptosis in ACC cells, while the cortisol concentration increased. Another explanation for the decreased cortisol concentration could be that mitotane and ATR-101 disturb cholesterol metabolism, in which SREBP2 plays an important role. Elevated levels of free cholesterol inhibit the release of SREBP2, thereby inhibiting the transcription of genes involved in cholesterol metabolism.⁴⁷ With SREBP2 not being released, no new SREBP2, and thus no transcription of SREBF2, is needed. After 6 hours, SREBF2 mRNA expression of ACTH-stimulated ACC cells was not affected by our compounds. Perhaps, the expression of SREBF2 will decrease after 24 hours of incubation, but in these samples, little mRNA was left and we thus could not determine SREBF2 expression. In the future, we could overcome this problem by centrifuging medium, which possibly contains cells. After centrifuging, one can easily use the supernatant for cortisol measurements. The pellet, containing cells and thus hopefully mRNA, could be suspended in RLT and β -ME and used for RNA isolation. However, it is possible that RNA of apoptotic cells is degraded and thus not useful. Therefore, we can incubate cells with lower compound concentrations in order to observe effects of mitotane, S035 and ATR-101 after longer incubation times.

Originally, we wanted to evaluate the mRNA expression of SREBF1 as well, however, primers of SREBF1 turned out not to be working. Therefore, SREBF1 was excluded from our analysis. For future experiments, new primers for SREBF1 need to be designed and tested.

Several *in vitro* studies into the effects and mechanism of action of mitotane in the NCI-H295R cell line reported inhibitory effects of mitotane on the cortisol concentration in a dose-dependent way.^{11,63-65} Recently, Sbiera *et al.* 2015 reported that S035 also decreased the cortisol concentration, but the decrease was less compared to the cortisol concentration of NCI-H295R cells incubated with mitotane.¹¹ A study by Jamal *et al.* 1985 into the effects of S035 on bovine adrenocortical cell culture reported that S035 was capable of inhibiting SOAT1, however, this was not accompanied with a decrease in the cortisol concentration.⁶⁶ *In vitro* studies into the effects of ATR-101 in the NCI-H295R cell line and in guinea pig, canine and monkey primary adrenocortical cell cultures showed cortisol decreasing effects. In these studies, 100 μ M and 10 μ M ATR-101 were used and in our study a maximum concentration of 100 nM ATR-101 was used.^{67,68} It thus remains uncertain at what concentration ATR-101 exerts its effects the best. *In vivo*, ATR-101 decreased the cortisol concentration in guinea pigs and canines.^{26,69,70}

The relative CYP17 mRNA expression was used as an indicator of steroidogenesis activity at the mRNA level. Because RT-qPCR of our 24-hour mRNA samples was not possible, no conclusions regarding the relationship between the cortisol concentration and the relative CYP17 mRNA expression can be drawn. It remains interesting to study the effects of our compounds on the steroidogenesis enzymes, especially for mitotane, because it is reported that mitotane interferes with steroidogenesis enzymes.⁶⁵

Surprisingly, all three compounds increased the cortisol concentration of non-stimulated normal adrenocortical cells. The degree of increase was influenced by correcting cortisol concentrations using protein concentrations. Due to the strong apoptotic effects of mitotane and ATR-101 at higher compound concentrations, cells were detached. Correcting the cortisol concentration by the attached cells, thus most likely led to an overestimation of cortisol concentration per protein. Therefore, one must carefully interpret corrected cortisol concentrations. S035 did not increase apoptosis and seemed to have little effect on protein concentrations. Therefore, the cortisol

concentration of normal adrenocortical cells incubated by S035 was not overestimated. In contrast to normal adrenocortical cells, all three compounds had little effect on protein concentrations of non-stimulated ACC cells, while apoptosis increased.

Mitotane and ATR-101 decreased cortisol concentration of ACTH-stimulated normal adrenocortical cells, but this decrease was not significant. Further testing in a larger sample size is needed to judge the value of this result.

According to the first requirement of treatment of cortisol-secreting ATs, i.e. suppression of cortisol production, it seemed that ATR-101 and not S035 is preferred, however no strong conclusions can be drawn due to the low sample size. In future studies, it is warranted to determine the cortisol concentration and the relative CYP17, SREBF1 and SREBF2 mRNA expression of more NAs and ATs after the same incubation time.

Paragraph 5.2.2: Viability and apoptosis

The second and most important requirement of treatment of cortisol-secreting ATs is reduction of tumor size. In order to determine the effects of our compounds on cell viability, cytotoxicity and apoptosis, we tested the ApoTox-Glo™ assay. The assay was not suitable for determining the effects on cytotoxicity, because cytotoxicity decreased, while viability also decreased and apoptosis increased. As described previously, this could be due to early cytotoxic effects of mitotane. In a study by Wolfgang *et al.* 1994 it was shown that the cytotoxic effects of mitotane indeed started early after incubation.⁶⁸ To confirm whether this is indeed the case in our cells, repeat experiments could include cytotoxicity assays with short incubation intervals to determine when the cytotoxic effect of mitotane exactly occurs. When it is known at what time the cytotoxic effect occurs, incubation times of future experiments can be adapted.

In the current experiment, we decided to measure apoptosis using the Caspase-Glo® 3/7 Assay, which was the part of the ApoTox-Glo™ assay that determined apoptosis, and the alamarBlue® Assay to measure viability. No obvious differences in apoptosis were observed between non-stimulated and stimulated normal adrenocortical cells (figure 22). Therefore, we decided to perform the Caspase-Glo™ 3/7 Assay only on non-stimulated normal adrenocortical cells and ACC cells. The alamarBlue® Assay was performed in non-stimulated and ACTH-stimulated normal adrenocortical cells and ACC cells. The effects of our compounds on viability of non-stimulated normal adrenocortical cells and ACC cells were similar to the effects of our compounds observed in ACTH-stimulated normal adrenocortical cells and ACC cells (figures 25 and 26).

We expected that our compounds would decrease viability and increase apoptosis of normal adrenocortical and ACC cells. The viability of non-stimulated and ACTH-stimulated normal adrenocortical cells and ACC cells incubated with mitotane decreased. This was accompanied by an increase in apoptosis. A dose-dependent increase of apoptosis and decrease of viability in NCI-H295R cells was already observed before.^{11,71,72} Surprisingly, sometimes it was reported that mitotane did not alter viability, although lower concentrations were used.^{64,65}

The viability of non-stimulated and ACTH-stimulated normal adrenocortical cells incubated with S035 increased, while no effect on apoptosis was observed. The viability of non-stimulated and ACTH-stimulated ACC cells incubated with S035 increased, while an increase of apoptosis was observed. An increase in apoptosis was observed previously.¹¹ Sbiera *et al.* 2015 did observe decreasing viability in the NCI-H295R cell line, although the decrease of viability in these cells was of lesser magnitude in comparison to NCI-H295R cells incubated with mitotane.¹¹

The viability of non-stimulated and ACTH-stimulated normal adrenocortical cells incubated with ATR-101 did increase, while apoptosis increased. The viability of non-stimulated and ACTH-stimulated ACC cells decreased, accompanied with an increase in apoptosis. An increase in apoptosis

and a decrease of viability were observed in previous studies.^{26,67,68,73-75} An explanation for increasing viability, while apoptosis increased at the same time, could be related to the mechanism on which the alamarBlue® Assay relies. The alamarBlue® Assay relies on transforming resazurin into resofurin. This reaction is a reduction reaction for which NADH could be used. Normally, NADH is oxidized to NAD + H⁺ in the mitochondria of the cell. ATR-101 is reported to interfere with the mitochondrial oxidative phosphorylation⁷⁴, thereby creating more NADH, which can be used for reduction of resazurin.

As indicators for apoptosis at the mRNA level, we determined the relative mRNA expression of BAX, BCL-2 and Casp3. Mitotane increased the relative mRNA expression of Casp3 in non-stimulated and ACTH-stimulated ACC cells. This corresponds to increasing apoptosis, measured by the Caspase-Glo® 3/7 Assay. Amongst apoptotic conditions, BAX expression is increased and BCL-2 expression decreased.^{27,46} Surprisingly, the relative mRNA expression of BAX was decreased in non-stimulated and ACTH-stimulated ACC cells and the expression of BCL-2 was increased in ACTH-stimulated ACC cells, pointing to survival. Increased expression of BAX was observed in the NCI-H295R studies of Sbiera *et al.* 2015.¹¹ Because increased BAX expression was observed after 24 hours in this study, this might be an explanation for why we did not observe increased BAX (and decreased BCL-2) expression. S035 did not affect the relative mRNA expressions of BAX, BCL-2 and Casp3. ATR-101 increased the relative mRNA expression of Casp3 in the non-stimulated ACC cells, although expression of BAX and BCL-2 was not affected. In ACTH-stimulated ACC cells the relative mRNA expression of BCL-2 was increased, pointing to survival instead of apoptosis. No strong conclusions based on the relative mRNA expressions can be elicited, because the sample size was only one.

Paragraph 5.2.3: SOAT1 and cholesterol esterification

We performed lipidomics of mitotane and S035 incubated non-stimulated and ACTH-stimulated normal adrenocortical cells. The results suggested that mitotane and S035 inhibit SOAT1 of ACTH-stimulated normal adrenocortical cells early after incubation. The early decrease and late increase in cholesteryl esters was observed by Sbiera *et al.* 2015 as well, although in a shorter time span (0.5-6 hours instead of 6-24 hours).¹¹ Because only one NA was incorporated in this study and we did not test the effects of ATR-101 on lipid profile, we wanted to determine additional lipid profiles to draw any conclusions. Unfortunately, the results of these additional lipid profiles were unsatisfactory due technical errors. No internal standard was incorporated and we did not receive absolute data regarding the total amounts of free cholesterol, cholesteryl esters and fatty acids. In the future, we still need lipid profiles to evaluate the SOAT1 inhibiting effects. The future lipid profiles should contain an internal standard. In addition, the sample size should be larger, involving NAs and ATs.

To determine whether SOAT1 inhibition affected the number and size of lipid droplets, we stained lipid droplets using LD450 staining. We succeeded in staining lipid droplets, however, fibroblasts stained positive as well. In future experiments, we therefore need to include an additional staining typical for adrenocortical cells: an ongoing research project. In addition, it may be interesting to analyse the incorporation of fluorescent labelled cholesterol in lipid droplets. Decreased fluorescence means decreased incorporation of cholesterol in lipid droplets and thus inhibition of SOAT1. Sbiera *et al.* 2015 showed decreased incorporating of fluorescent labelled cholesterol in lipid droplets with increasing mitotane and S035 concentrations.¹¹ Reindel *et al.* 1994 electron microscopy showed decreased lipid droplet formation in monkey adrenal cells incubated with ATR-101.⁷⁶

We determined the relative mRNA expression of SOAT1 to gain insight in the effects of our compounds at the mRNA expression of SOAT1. In non-stimulated ACC cells, SOAT1 expression was decreased in mitotane incubated cells and not affected in ATR-101 or S035 incubated cells. In ACTH-stimulated ACC cells, the relative mRNA expression of SOAT1 was increased in mitotane and S035 incubated cells. Looking back at the results of the lipid profile, cholesteryl esters were decreased after 6 hours of incubation and increased after 24 hours of incubation. Maybe, SOAT1 mRNA expression is increased after 6 hours of incubation to create more SOAT1 proteins in order to esterify cholesterol to

cholesteryl esters at 24 hours of incubation. ATR-101 did not affect SOAT1 expression of ACTH-stimulated ACC cells. Because of the small sample size, no strong conclusions can be drawn.

Paragraph 5.2.4: ER-stress and the UPR

The effects of our compounds on ER-stress and the UPR were researched into using Western Blot and RT-qPCR. To evaluate the protein expression of the UPR components, we determined the specificity of antibodies against eIF2 α , p-eIF2 α , CHOP and ATF6. The antibodies against (p-)eIF2 α are suitable to determine canine PERK-pathway activity. The normal adrenocortical cells incorporated in this study were incubated with several concentrations mitotane. Because p-eIF2 α and eIF2 α were recognized, this suggested PERK-pathway activity and ER-stress in mitotane incubated normal adrenocortical cells. Corresponding to our findings, Sbiera *et al.* 2015 showed increased phosphorylation of eIF2 α in NCI-H295R cells incubated with mitotane.¹¹ The antibodies against ATF6 and CHOP might not be working in canine adrenocortical cells or the expression of ATF6 and CHOP proteins was too low to be detected. Because we want to know the effects of our compounds on the ATF6-pathway, the anti-ATF6-antibody should be tested again and/or new antibodies against ATF6 should be tested. Because CHOP is an important ER-stress marker, anti-CHOP-antibodies also need to be (re)tested.

The relative mRNA expression of ATF4, a marker of PERK-pathway activity, was increased in mitotane incubated non-stimulated and ACTH-stimulated ACC cells, suggesting PERK-pathway activity. As an indicator of IRE1-pathway activity, we determined the relative mRNA expressions of uXBP1 and sXBP1. The relative mRNA expression of sXBP1 was increased in non-stimulated and ACTH-stimulated ACC cells incubated with mitotane, while the relative mRNA expression of uXBP1 was decreased. Mitotane thus induced IRE1-pathway activity, something which was also observed by Sbiera *et al.* 2015.¹¹ The relative mRNA expressions of additional components of the UPR like ERP72, GRP78, p58^{ipk} and CHOP were increased as well. Sbiera *et al.* 2015 studied CHOP expression in mitotane incubated NCI-H295R cells as well, which was increased.¹¹ The relative mRNA expression of HERPUD1, a compound of ERAD, was increased, although the relative mRNA expression of EDEM1, another component of ERAD, was not increased. These results suggested that ER-stress is initiated in mitotane incubated ACC cells. However, because only one ACC was incorporated in this study, no strong conclusions can be elicited.

We observed no XBP1 splicing in non-stimulated and ACTH-stimulated ACC cells incubated with S035. The transcription factor sXBP1 induces transcription of EDEM1. The relative mRNA expression of EDEM1 was not affected. This corresponds to observing no XBP1 splicing, suggesting no IRE1-pathway activity in S035 incubated ACC cells. In contrast, Sbiera *et al.* 2015 did find XBP1 splicing in NCI-H295R cells incubated with S035.¹¹ The relative mRNA expression of ATF4 was not increased in ACTH-stimulated and non-stimulated ACC cells. However, the relative mRNA expression of CHOP was increased in ACTH-stimulated ACC cells. Because the expression of CHOP is regulated by ATF4, increased relative CHOP mRNA expression could thus point to PERK-pathway activity. CHOP expression is regulated by ATF6 as well. The relative mRNA expression of p58^{ipk}, a ATF6-dependent factor, was not increased. These results suggested that CHOP expression was solely due to ATF4 and that the PERK-pathway may be active in ACTH-stimulated ACC cells incubated with S035. Because we expected increased relative mRNA expressions of ATF4 and CHOP, we tried to explain why only the relative mRNA expression of CHOP was increased. An explanation could be that little ATF4 mRNA and thus protein (transcription factor) is sufficient to initiate strong CHOP expression, a relationship which was observed between the fold changes of ATF4 versus CHOP in ACC cells incubated with mitotane. Lastly, some additional UPR components were increased expressed: ERP72 in non-stimulated ACC cells and HERPUD1 and GRP78 in ACTH-stimulated ACC cells. These results suggested that ER-stress was initiated to some point, however, no strong conclusions can be drawn.

ATR-101 did, based on the relative mRNA expression of ATF4, activate the PERK-pathway in non-stimulated ACC cells. Corresponding to this finding, the relative mRNA expression of CHOP was

increased in non-stimulated ACC cells. The relative CHOP mRNA expression was also increased because of ATF6-pathway activity, because the relative mRNA expression of p58^{ipk}, an ATF6-specific factor, was increased in non-stimulated ACC cells. The relative mRNA expression of uXBP1 was decreased, indicating IRE1-pathway activity, although the relative mRNA expression of EDEM1 was not increased. The relative mRNA expression of HERPUD1 was increased in non-stimulated ACC cells, suggesting ERAD activity. In addition, ATR-101 increased the relative mRNA expressions of ERP72 and GRP78. In ACTH-stimulated ACC cells, the relative mRNA expression of ATF4 was not affected, although the relative CHOP mRNA expression was increased. Again, this could be due to ATF4 and ATF6. The relative expression of p58^{ipk} mRNA was not increased, suggesting that ATF4, but not ATF6 was responsible for the increased relative mRNA expression of CHOP. The relative mRNA expression of uXBP1 was decreased, pointing to IRE1-pathway activity, although expression of EDEM1 was not affected. In ACTH-stimulated cells, the relative mRNA expression of ERP72 was increased. The relative mRNA expression of HERPUD1 was increased, suggesting ERAD activity. LaPensee *et al.* 2016 did observe PERK-pathway and IRE1-pathway activity based on CHOP mRNA expression, immunoblots of (p-)eIF2 α and XBP1 splicing when incubating NCI-H295R cells with 30 nM ATR-101 and 45 μ g/mL cholesterol during 4 or 5 hours. Cholesterol was added, because ATR-101 did not cause cytotoxicity in the absence of cholesterol. We did not use cholesterol, although we did observe apoptotic effects of ATR-101. The role of cholesterol in ATR-101's cytotoxicity remains thus unclear and needs to be clarified.

The relative SF1 mRNA expression was decreased by mitotane in non-stimulated ACC cells. Low relative SF1 mRNA expression was accompanied by low relative SOAT1 mRNA expression. In ACTH-stimulated ACC cells, the relative mRNA expressions of SF1 and SOAT1 were increased. These results pointed to SF1 regulated SOAT1 expression, which was previously shown.⁷⁷ A similar connection between those two factors was observed for ACTH-stimulated ACC cells incubated with S035. Such a relation was not observed in non-stimulated ACC cells incubated with S035 and ATR-101 and not in ACTH-stimulated ACC cells incubated with ATR-101. No strong conclusions can be drawn, because of the low sample size.

Medical therapies of canine ACTH-independent hypercortisolism are limited. Therefore, new medical therapies are warranted. According to the current study, it seems that ATR-101 has the potency to become a suitable therapy of cortisol-producing ATs because of its anti-steroidogenic and anti-tumor effects. S035 is not recommended, because no desired effects were observed. Just like mitotane, ATR-101 had anti-steroidogenic and anti-tumor effects. Whether SOAT1 inhibition is part of the mechanism of action, remains unclear. SOAT1 inhibitor S035 had no cortisol decreasing and apoptosis increasing effects, suggesting that the effects of mitotane and ATR-101 were not due to SOAT1 inhibition. Maybe the effects of mitotane and ATR-101 are due to interference with mitochondrial respiration.^{63,73,74} Based on the current study, SOAT1 inhibition cannot be excluded due to the low sample size. In the future, a similar study needs to be performed. To determine whether SOAT1 inhibition is the cause of the cortisol decreasing and apoptosis increasing effects of mitotane and ATR-101, the IC₅₀ of the esterase activity of SOAT1, of cortisol production and of apoptosis need to be determined. When the IC₅₀ of apoptosis and cortisol production are not similar to the IC₅₀ of the esterase activity of SOAT1, SOAT1 inhibition is not and the effects on mitochondrial respiration might be responsible for the effects. Therefore, assays regarding the mitochondrial membrane potential, the activities of the complexes of the oxidative phosphorylation and the ATP level of the cell need to be performed. When the IC₅₀ of SOAT1 esterase activity, apoptosis and cortisol production are similar, SOAT1 inhibition is part of the mechanism of action. In that case, the relationship between SOAT1 inhibition and the development of ER-stress needs to be clarified. Recently, it is demonstrated that mitotane directly interacts with lipid bilayers containing phosphatidylethanolamine.⁷⁸ The ER membranes are rich in phosphatidylethanolamine, making it likely that mitotane could decrease membrane stability of the ER. Decreased membrane stability could result in improper functioning of enzymes localized in the ER membranes, for example SOAT1, but also sarcoplasmic/endoplasmic reticulum calcium ATPase (SERCA). SERCA is responsible for maintaining high calcium concentration within the ER.

Malfunctioning of SERCA could result in decreased calcium and thus disturbance of ER-chaperons.⁷⁹ This, in turn, could lead to an imbalance between protein folding and loading: ER-stress. Via the UPR, this could result in apoptosis.

Before starting additional research projects, it needs to be clarified at what concentration ATR-101 exerts its effects the best and if co incubation with cholesterol is required. Currently, ATR-101 is tested in a clinical phase II study.⁸⁰ Perhaps, this study could yield information regarding effective compound concentrations.

Current study has brought important preliminary data on SOAT1 inhibitors in dogs. It will serve as a solid base for further studies about SOAT1 inhibitors in humans and dogs, which we are setting up in cooperation with the Endocrine research group from the Medical Center from Würzburg, Germany.

Acknowledgements

During the past 8 months, I was blessed with a super @drenal team. Without this team, my research project was not possible. A few people deserve special thanks, especially Karin Sanders and Sara Galac who supported me during the whole process, starting with writing a research proposal, from labwork to processing the results and writing the report. I also would like to thank Adri Slob for preparing cell suspensions, performing RIA, staining slides, making IHC pictures and teaching me sequencing. In addition, I would like to thank Wesley de Wit for preparing cell suspensions and teaching me this. I thank Denah Peterson for scoring IHC slides. My research project strengthened my interest in research. Hopefully, I will be back within a couple of years. Last, but not least, there are some additional people who I would like to thank. I thank Jos Brouwers, Jeroen Jansen and Bas Vaandrager for performing and analyzing lipidomics. I also would like to thank Jeannette Wolfswinkel for running a well-organized laboratory.

References

1. Dyce KM, Sack WO, Wensing CJG. The adrenal glands. In: *Textbook of veterinary anatomy*. 4th ed. St. Louis; United States of America: Saunders Elsevier; 2010:221-222.
2. Bragulla H, Budras KD, Forstenpointner G, König HE, Liebich HG, Maierl J, Mülling C, Probst A, Reese S, Ruberte J. Endocrine glands (glandulae endocrinae). In: König HE, Liebich HG, eds. *Veterinary anatomy of domestic mammals: Textbook and colour atlas*. Stuttgart; Germany: Schattauer; 2004:542-543.
3. Yates R, Katugampola H, Cavlan D, Cogger K, Meimaridou E, Hughes C, Metherell L, Guasti L, King P. Adrenocortical development, maintenance, and disease. In: Forrest D, Tsai S, eds. *Current Topics in Developmental Biology*. St. Louis; United States of America: Saunders Elsevier; 2013:239-312.
4. Galac S, Reusch CE, Kooistra HS, Rijnberk A. Adrenals. In: Rijnberk A, Kooistra HS, eds. *Clinical endocrinology of dogs and cats: An illustrated text*. Hannover; Germany: Schlütersche; 2010:93-140.
5. Behrend EN, Kooistra HS, Nelson R, Reusch CE, Scott-Moncrieff JC. Diagnosis of spontaneous canine hyperadrenocorticism: 2012 acvim consensus statement (small animal). *Journal of Veterinary Internal Medicine*. 2013;27(6):1292-1304. Accessed 16 January 2017. doi: 10.1111/jvim.12192.
6. Galac S. Selecting the best treatment option for a dog with cushing's syndrome. *Acta Veterinaria-Beograd*. 2015;65(1):1-19. Accessed 20 August 2017. doi: 10.1515/acve-2015-0001.
7. Schwartz P, Kovak JR, Koprowski A, Ludwig LL, Monette S, Bergman PJ. Evaluation of prognostic factors in the surgical treatment of adrenal gland tumors in dogs: 41 cases (1999-2005). *Journal of the American Veterinary Medical Association*. 2008;232(1):77-84. Accessed 18 August 2017. doi: 10.2460/javma.232.1.77.
8. van Sluijs FJ, Sjollem BE, Voorhout G, van den Ingh TS, Rijnberk A. Results of adrenalectomy in 36 dogs with hyperadrenocorticism caused by adrenocortical tumour. *The Veterinary Quarterly*. 1995;17(3):113-116. Accessed 18 August 2017. doi: 10.1080/01652176.1995.9694547.
9. Jiménez Peláez M, Bouvy BM, Dupré GP. Laparoscopic adrenalectomy for treatment of unilateral adrenocortical carcinomas: Technique, complications, and results in seven dogs. *Veterinary Surgery*. 2008;37(5):444-453. Accessed 18 August 2017. doi: 10.1111/j.1532-950X.2008.00410.x.
10. Mayhew PD, Culp WTN, Hunt GB, Steffey MA, Mayhew KN, Fuller M, Della-Maggiore A, Nelson RW. Comparison of perioperative morbidity and mortality rates in dogs with noninvasive adrenocortical masses undergoing laparoscopic versus open adrenalectomy. *Journal of the American Veterinary Medical Association*. 2014;245(9):1028-1035. Accessed 18 August 2017. doi: 10.2460/javma.245.9.1028.
11. Sbiera S, Leich E, Liebisch G, Sbiera I, Schirbel A, Wiemer L, Matysik S, Eckhardt C, Gardill F, Gehl A, Kendl S, Weigand I, Bala M, Ronchi CL, Deutschbein T, Schimitz G, Rosenwald A, Allolio B, Fassnacht M, Kross M. Mitotane inhibits sterol-o-acyl transferase 1 triggering lipid-mediated endoplasmic reticulum stress and apoptosis in adrenocortical carcinoma cells. *Endocrinology*. 2015;156(11):3895-3908. Accessed 11 November 2016. doi: 10.1210/en.2015-1367.

12. Reid LE, Behrend EN, Martin LG, Kempainen RJ, Ward CR, Lurye JC, Donovan TC, Lee HP. Effect of trilostane and mitotane on aldosterone secretory reserve in dogs with pituitary-dependent hyperadrenocorticism. *Journal of Veterinary Internal Medicine*. 2014;28(2):443-450. Accessed 19 August 2017. doi: 10.1111/jvim.12276.
13. Kintzer PP, Peterson ME. Mitotane treatment of 32 dogs with cortisol-secreting adrenocortical neoplasms. *Journal of the American Veterinary Medical Association*. 1994;205(1):54-61. Accessed 18 August 2017.
14. Kintzer PP, Peterson ME. Mitotane (o, p'-DDD) treatment of 200 dogs with pituitary-dependent hyperadrenocorticism. *Journal of Veterinary Internal Medicine*. 1991;5(3):182-190. Accessed 10 December 2016. doi: 10.1111/j.1939-1676.1991.tb00945.x.
15. Hogan TF, Citrin DL, Johnson BM, Nakamura S, Davis TE, Borden EC. O,p'-DDD (mitotane) therapy of adrenal cortical carcinoma. observations on drug dosage, toxicity, and steroid replacement. *Cancer*. 1978;42(5):2177-2181. Accessed 19 August 2017. doi: 10.1002/1097-0142(197811)42:53.0.CO;2-X.
16. Ramsey IK. Trilostane in dogs. *Veterinary Clinics of North America: Small Animal Practice*. 2010;40(2):269-283. Accessed 10 December 2016. doi: 10.1016/j.cvsm.2009.10.008.
17. Neiger R, Ramsey I, O'Connor J, Hurley KJ, Mooney CT. Trilostane treatment of 78 dogs with pituitary-dependent hyperadrenocorticism. *Veterinary Record*. 2002;150(26):799-804. Accessed 19 August 2017. doi 10.1136/vr.150.26.799.
18. Chapman PS, Kelly DF, Archer J, Brockman DJ, Neiger R. Adrenal necrosis in a dog receiving trilostane for the treatment of hyperadrenocorticism. *Journal of Small Animal Practice*. 2004;45(6):307-310. Accessed 10 December 2016. doi: 10.1111/j.1748-5827.2004.tb00241.x.
19. Chang TY, Chang CCY, Cheng D. Acyl-coenzyme A: Cholesterol acyltransferase. *Annual Review of Biochemistry*. 1997;66:613-638. Accessed 2 August 2017. doi: 10.1146/annurev.biochem.66.1.613.
20. Chang T, Chang CCY, Lin S, Yu C, Li B, Miyazaki A. Roles of acyl-coenzyme A: Cholesterol acyltransferase-1 and -2. *Current Opinion in Lipidology*. 2001;12(3):289-296. Accessed 19 August 2017. doi: 10.1097/00041433-200106000-00008.
21. Warner GJ, Stoudt G, Bamberger M, Johnson WJ, Rothblat GH. Cell toxicity induced by inhibition of acyl coenzyme A:Cholesterol acyltransferase and accumulation of unesterified cholesterol. *The Journal of Biological Chemistry*. 1995;270(11):5772-5778. Accessed 2 October 2017. doi: 10.1074/jbc.270.11.5772.
22. Lee RG, Willingham MC, Davis MA, Skinner KA, Rudel LL. Differential expression of ACAT1 and ACAT2 among cells within liver, intestine, kidney, and adrenal of nonhuman primates. *The Journal of Lipid Research*. 2000;41(12):1991-2001. Accessed 30 March 2017.
23. Kraemer FB, Shen W, Harada K, Patel S, Osuga J, Ishibashi S, Azhar S. Hormone-sensitive lipase is required for high-density lipoprotein cholesteryl ester-supported adrenal steroidogenesis. *Molecular Endocrinology*. 2004;18(3):549-557. Accessed 10 December 2016. doi: 10.1210/me.2003-0179.
24. Lin D, Sugawara T, Strauss III JF, Clark BJ, Stocco DM, Saenger P, Rogol A, Miller WL. Role of steroidogenic acute regulatory protein in adrenal and gonadal steroidogenesis. *Science*. 1995;267(5205):1828-1831. Accessed 10 December 2016. doi: 10.1126/science.7892608.

25. Sanders K, Mol JA, Kooistra HS, Slob A, Galac S. New insights in the functional zonation of the canine adrenal cortex. *Journal of Veterinary Internal Medicine*. 2016;30(3):741-750. Accessed 10 December 2016. doi: 10.1111/jvim.13946.
26. LaPensee CR, Mann JE, Rainey WE, Crudo V, Hunt SW, Hammer GD. ATR-101, a selective and potent inhibitor of acyl-CoA acyltransferase 1, induces apoptosis in H295R adrenocortical cells and in the adrenal cortex of dogs. *Endocrinology*. 2016;157(5):1775-1788. Accessed 14 November 2016. doi: 10.1210/en.2015-2052.
27. Brewer JW. Regulatory crosstalk within the mammalian unfolded protein response. *Cellular and Molecular Life Sciences*. 2014;71(6):1067-1079. Accessed 1 February 2017. doi: 10.1007/s00018-013-1490-2.
28. Chakrabarti A, Chen AW, Varner JD. A review of the mammalian unfolded protein response. *Biotechnology and Bioengineering*. 2011;108(12):2777-2793. Accessed 31 January 2017. doi: 10.1002/bit.23282.
29. Shen J, Chen X, Hendershot L, Prywes R. ER stress regulation of ATF6 localization by dissociation of BiP/GRP78 binding and unmasking of golgi localization signals. *Developmental Cell*. 2002;3(1):99-111. Accessed 2 February 2017. doi: 10.1016/S1534-5807(02)00203-4.
30. Ye J, Rawson RB, Komuro R, Chen X, Davé UP, Prywes R, Brown MS, Goldstein JL. ER stress induces cleavage of membrane-bound ATF6 by the same proteases that process SREBPs. *Molecular Cell*. 2000;6(6):1355-1364. Accessed 2 February 2017. doi: 10.1016/S1097-2765(00)00133-7.
31. Adachi Y, Yamamoto K, Okada T, Yoshida H, Harada A, Mori K. ATF6 is a transcription factor specializing in the regulation of quality control proteins in the endoplasmic reticulum. *Cell Structure and Function*. 2008;33(1):75-89. Accessed 2 February 2017. doi: 10.1247/csf.07044.
32. Okada T, Yoshida H, Akazawa R, Negishi M, Mori K. Distinct roles of activating transcription factor 6 (ATF6) and double-stranded RNA-activated protein kinase-like endoplasmic reticulum kinase (PERK) in transcription during the mammalian unfolded protein response. *Biochemical Journal*. 2002;366(2):585-594. Accessed 2 February 2017. doi: 10.1042/BJ20020391.
33. Yamamoto K, Sato T, Matsui T, Sato M, Okada T, Yoshida H, Harada A, Mori K. Transcriptional induction of mammalian ER quality control proteins is mediated by single or combined action of ATF6a and XBP1. *Developmental Cell*. 2007;13(3):365-376. Accessed 14 August 2017. doi: 10.1016/j.devcel.2007.07.018.
34. Yoshida H, Matsui T, Hosokawa N, Kaufman RJ, Nagata K, Mori K. A time-dependent phase shift in the mammalian unfolded protein response. *Developmental Cell*. 2003;4(2):265-271. Accessed 1 February 2017. doi: 10.1016/S1534-5807(03)00022-4.
35. Yoshida H, Matsui T, Yamamoto A, Okada T, Mori K. XBP1 mRNA is induced by ATF6 and spliced by IRE1 in response to ER stress to produce a highly active transcription factor. *Cell*. 2001;107(7):881-891. Accessed 1 February 2017. doi: 10.1016/S0092-8674(01)00611-0.
36. Bertolotti A, Zhang Y, Hendershot LM, Harding HP, Ron D. Dynamic interaction of BiP and ER stress transducers in the unfolded-protein response. *Nature Cell Biology*. 2000;2(6):326-332. Accessed 1 February 2017. doi: 10.1038/35014014.

37. Lee K, Tirasophon W, Shen X, Michalak M, Prywes R, Okada T, Yoshida H, Mori K, Kaufman RJ. IRE1-mediated unconventional mRNA splicing and S2P-mediated ATF6 cleavage merge to regulate XBP1 in signaling the unfolded protein response. *Genes and Development*. 2002;16(4):452-466. Accessed 1 February 2017. doi: 10.1101/gad.964702.
38. Calton M, Zeng H, Urano F, Till JH, Hubbard SR, Harding HP, Clark SG, Ron D. IRE1 couples endoplasmic reticulum load to secretory capacity by processing the XBP-1 mRNA. *Nature*. 2002;415(6867):92-96. Accessed 1 February 2017. doi: 10.1038/415092a.
39. Lee AH, Iwakoshi NN, Glimcher LH. XBP-1 regulates a subset of endoplasmic reticulum resident chaperone genes in the unfolded protein response. *Molecular and Cellular Biology*. 2003;23(21):7448-7459. Accessed 1 February 2017. doi: 10.1128/MCB.23.21.7448-7459.2003.
40. Harding HP, Zhang Y, Ron D. Protein translation and folding are coupled by an endoplasmic-reticulum-resident kinase. *Nature*. 1999;397(6716):271-274. Accessed 3 February 2017. doi: 10.1038/16729.
41. Harding HP, Zhang Y, Zeng H, Novoa I, Lu PD, Calton M, Sadri N, Yun C, Popko B, Paules R, Stojdl DF, Bell JC, Hetmann T, Leiden JM, Ron D. An integrated stress response regulates amino acid metabolism and resistance to oxidative stress. *Molecular Cell*. 2003;11(3):619-633. Accessed 1 February 2017. doi: 10.1016/S1097-2765(03)00105-9.
42. Fawcett TW, Martindale JL, Guyton KZ, Hai T, Holbrook NJ. Complexes containing activating transcription factor (ATF)/cAMP-responsive-element-binding protein (CREB) interact with the CCAAT/enhancer-binding protein (C/EBP)-ATF composite site to regulate Gadd153 expression during the stress response. *Biochemical Journal*. 1999;339(1):135-141. Accessed 3 February 2017. doi: 10.1042/0264-6021:3390135.
43. Harding HP, Zhang Y, Zeng H, Novoa I, Lu PD, Calton M, Sadri N, Yun C, Popko B, Paules R, Stojdl DF, Bell JC, Hettmann T, Leiden JM, Ron D. Regulated translation initiation controls stress-induced gene expression in mammalian cells. *Molecular Cell*. 2000;6(5):1099-1108. Accessed 3 February 2017. doi: 10.1016/S1097-2765(00)00108-8.
44. Ma Y, Brewer JW, Alan Diehl J, Hendershot LM. Two distinct stress signaling pathways converge upon the CHOP promoter during the mammalian unfolded protein response. *Journal of Molecular Biology*. 2002;318(5):1351-1365. Accessed 3 February 2017. doi: 10.1016/S0022-2836(02)00234-6.
45. Yoshida H, Okada T, Haze K, Yanagi H, Yura T, Negishi M, Mori K. ATF6 activated by proteolysis binds in the presence of NF-Y (CBF) directly to the cis-acting element responsible for the mammalian unfolded protein response. *Molecular and Cellular Biology*. 2000;20(18):6755-6767. Accessed 3 February 2017. doi: 10.1128/MCB.20.18.6755-6767.2000.
46. Tabas I, Ron D. Integrating the mechanisms of apoptosis induced by endoplasmic reticulum stress. *Nature Cell Biology*. 2011;13(3):184-190. Accessed 7 April 2017. doi: 10.1038/ncb0311-184.
47. Xiaoping Z, Fajun Y. Regulation of SREBP-mediated gene expression. *Sheng Wu Wu Li Hsueh Bao*. 2012;28(4):287-294. Accessed 24 February 2017. doi: 10.3724/SP.J.1260.2012.20034.
48. Galac S, Kars VJ, Klarenbeek S, Teerds KJ, Mol JA, Kooistra HS. Expression of receptors for luteinizing hormone, gastric-inhibitory polypeptide, and vasopressin in normal adrenal glands and cortisol-

- secreting adrenocortical tumors in dogs. *Domestic Animal Endocrinology*. 2010;39(1):63-75. Accessed 30 August 2017. doi: 10.1016/j.domaniend.2010.02.003.
49. Labelle P, Kyles AE, Farver TB, De Cock HEV. Indicators of malignancy of canine adrenocortical tumors: Histopathology and proliferation index. *Veterinary Pathology*. 2004;41(5):490-497. Accessed 19 August 2017. doi: 10.1354/vp.41-5-490.
50. Brinkhof B, Spee B, Rothuizen J, Penning LC. Development and evaluation of canine reference genes for accurate quantification of gene expression. *Analytical Biochemistry*. 2006;356(1):36-43. Accessed 14 August 2017. doi: 10.1016/j.ab.2006.06.001.
51. Stassen QEM, Riemers FM, Reijmerink H, Leegwater PAJ, Penning LC. Reference genes for reverse transcription quantitative PCR in canine brain tissue. *BMC Research Notes*. 2015;8(1). Accessed 14 August 2017. doi: 10.1186/s13104-015-1628-4.
52. Livak KJ, Schmittgen TD. Analysis of relative gene expression data using real-time quantitative PCR and the $2^{-\Delta\Delta CT}$ method. *Methods*. 2001;25(4):402-408. Accessed 14 August 2017. doi: 10.1006/meth.2001.1262.
53. Meijer JC, De Bruijne JJ, Rijnberk A, Crougths RJM. Biochemical characterization of pituitary-dependent hyperadrenocorticism in the dog. *Journal of Endocrinology*. 1978;77(1):111-118. Accessed 18 January 2017. doi: 10.1677/joe.0.0770111.
54. Bligh EG, Dyer WJ. A rapid method of total lipid extraction and purification. *Canadian Journal of Biochemistry and Physiology*. 1959;37(8):911-917. Accessed 22 February 2017. doi: 10.1139/o59-099.
55. Retra K, Bleijerveld O, van Gestel R, Tielens AGM, van Hellemond J, Brouwers J. A simple and universal method for the separation and identification of phospholipid molecular species. *Rapid Communications in Mass Spectrometry*. 2008;22(12):1853-1862. Accessed 22 February 2017. doi: 10.1002/rcm.3562.
56. Tuohetahuntala M, Molenaar MR, Spee B, Brouwers JF, Houweling M, Vaandrager AB, Helms JB. ATGL and DGAT1 are involved in the turnover of newly synthesized triacylglycerols in hepatic stellate cells. *The Journal of Lipid Research*. 2016;57(7):1162-1174. Accessed 22 February 2017. doi: 10.1194/jlr.M066415.
57. Hook B, Schagat T. Profiling compound effects on cell health in a time course using a multiplexed same-well assay. <http://nld.promega.com/resources/pubhub/profiling-compound-effects-on-cell-health-in-a-time-course-using-a-multiplexed-same-well-assay/>. Updated 2012. Accessed 29 July 2017.
58. Niles AL, Moravec RA, Eric Hesselberth P, Scurria MA, Daily WJ, Riss TL. A homogeneous assay to measure live and dead cells in the same sample by detecting different protease markers. *Analytical Biochemistry*. 2007;366(2):197-206. Accessed 21 August 2017. doi: 10.1016/j.ab.2007.04.007.
59. Marusyk A, Polyak K. Tumor heterogeneity: Causes and consequences. *BBA Reviews on Cancer*. 2010;1805(1):105-117. Accessed 20 August 2017. doi: 10.1016/j.bbcan.2009.11.002.
60. Lee O, Chang CCY, Lee W, Chang T. Immunodepletion experiments suggest that acyl-coenzyme A:Cholesterol acyltransferase-1 (ACAT-1) protein plays a major catalytic role in adult human liver, adrenal gland, macrophages, and kidney, but not in intestines. *The Journal of Lipid Research*. 1998;39(8):1722-1727. Accessed 30 March 2017.

61. Smith JL, Rangaraj K, Simpson R, Maclean DJ, Nathanson LK, Stuart KA, Scott SP, Ramm GA, de Jersey J. Quantitative analysis of the expression of ACAT genes in human tissues by real-time PCR. *The Journal of Lipid Research*. 2004;45(4):686-696. Accessed 14 March 2017. doi: 10.1194/jlr.M300365-JLR200.
62. Chang CCY, Chen J, Thomas MA, Cheng D, Veronica DP, Newton RS, Pape ME, Chang T. Regulation and immunolocalization of acyl-coenzyme A:Cholesterol acyltransferase in mammalian cells as studied with specific antibodies. *The Journal of Biological Chemistry*. 1995;270(49):29532-29540. Accessed 20 August 2017. doi: 10.1074/jbc.270.49.29532.
63. Hescot S, Slama A, Lombès A, Paci A, Remy H, Leboulleux S, Chadarevian R, Trabado S, Amazit L, Young J, Baudin E, Lombès M. Mitotane alters mitochondrial respiratory chain activity by inducing cytochrome c oxidase defect in human adrenocortical cells. *Endocrine-Related Cancer*. 2013;20(3):371-381. Accessed 11 November 2016. doi: 10.1530/ERC-12-0368.
64. Stigliano A, Cerquetti L, Borro M, Gentile G, Bucci B, Misiti S, Piergrossi P, Brunetti E, Simmaco M, Toscano V. Modulation of proteomic profile in H295R adrenocortical cell line induced by mitotane. *Endocrine-Related Cancer*. 2008;15(1):1-10. Accessed 11 November 2016. doi: 10.1677/ERC-07-0003.
65. Lin CW, Chang YH, Pu HF. Mitotane exhibits dual effects on steroidogenic enzymes gene transcription under basal and cAMP-stimulating microenvironments in NCI-H295 cells. *Toxicology*. 2012;298(1-3):14-23. Accessed 9 August 2017. doi: 10.1016/j.tox.2012.04.007.
66. Jamal Z, Suffolk RA, Boyd GS, Suckling KE. Metabolism of cholesteryl ester in monolayers of bovine adrenal cortical cells. effect of an inhibitor of acyl-CoA : Cholesterol acyltransferase. *BBA Lipids and Lipid Metabolism*. 1985;834(2):230-237. Accessed 9 August 2017. doi: 10.1016/0005-2760(85)90160-2.
67. Burns V, Kerppola T. ATR-101 inhibits cholesterol efflux and cortisol secretion by ABC transporters, causing cytotoxic cholesterol accumulation in adrenocortical carcinoma cells. *British Journal of Pharmacology*. 2017. Accessed 18 April 2017. doi: 10.1111/bph.13951.
68. Wolfgang GHI, Verneti LA, MacDonald JR. Isolation and use of primary adrenocortical cells from guinea pigs, dogs and monkeys for in vitro toxicity studies. *Toxicology Methods*. 1994;4(3):149-160. Accessed 18 April 2017. doi: 10.3109/15376519409041600.
69. Dominick MA, Bobrowski WA, Macdonald JR, Gough AW. Morphogenesis of a zone-specific adrenocortical cytotoxicity in guinea pigs administered PD 132301-2, an inhibitor of acyl-CoA: Cholesterol acyltransferase. *Toxicologic Pathology*. 1993;21(1):54-62. Accessed 18 April 2017. doi: 10.1177/019262339302100107.
70. Dominick MA, Mcguire EJ, Reindel JF, Bobrowski WF, Bocan TMA, Gough AW. Subacute toxicity of a novel inhibitor of acyl-CoA: Cholesterol acyltransferase in beagle dogs. *Toxicological Sciences*. 1993;20(2):217-224. Accessed 18 April 2017. doi: 10.1093/toxsci/20.2.217.
71. Poli G, Guasti D, Rapizzi E, Rossella F, Letizia C, Baninelli A, Cini N, Bani D, Mannelli M, Luconi M. Morphofunctional effects of mitotane on mitochondria in human adrenocortical cancer cells. *Endocrine-Related Cancer*. 2013;20(4):537-550. Accessed 11 November 2016. doi: 10.1530/ERC-13-0150.

72. Hescot S, Amazit L, Lhomme M, Travers S, DuBow A, Battini S, Boulate G, Namer IJ, Lombes A, Kontush A, Imperiale A, Baudin E, Lombes M. Identifying mitotane-induced mitochondria-associated membranes dysfunctions: Metabolomic and lipidomic approaches. *Oncotarget*. 2017. Accessed 9 August 2017. doi: 10.18632/oncotarget.18968.
73. Verneti LA, Macdonald JR, Wolfgang GHI, Dominick MA, Pegg DG. ATP depletion is associated with cytotoxicity of a novel lipid regulator in guinea pig adrenocortical cells. *Toxicology and Applied Pharmacology*. 1993;118(1):30-38. Accessed 18 April 2017. doi: 10.1006/taap.1993.1005.
74. Cheng Y, Kerppola RE, Kerppola TK. ATR-101 disrupts mitochondrial functions in adrenocortical carcinoma cells and in vivo. *Endocrine-Related Cancer*. 2016;23(4):1-19. Accessed 14 November 2016. doi: 10.1530/ERC-15-0527.
75. Verneti LA, MacDonald JR, Pegg DG. Differential toxicity of an inhibitor of mitochondrial respiration in canine hepatocytes and adrenocortical cell cultures. *Toxicology in vitro*. 1996;10(1):51-57. Accessed 18 April 2017. doi: 10.1016/0887-2333(95)00102-6.
76. Reindel JF, Dominick MA, Bocan TMA, Gough AW, McGuire EJ. Toxicologic effects of a novel acyl-CoA:Cholesterol acyltransferase inhibitor in cynomolgus monkeys. *Toxicologic Pathology*. 1994;22(5):510-518. Accessed 18 April 2017. doi: 10.1177/019262339402200505.
77. Ferraz-De-Souza B, Hudson-Davies RE, Lin L, Parnaik R, Hubank M, Dattani MT, Achermann JC. Sterol O-acyltransferase 1 (SOAT1, ACAT) is a novel target of steroidogenic factor-1 (SF-1, NR5A1, Ad4BP) in the human adrenal. *The Journal of Clinical Endocrinology and Metabolism*. 2011;96(4):E663-E668. Accessed 11 August 2017. doi: 10.1210/jc.2010-2021.
78. Scheidt HA, Haralampiev I, Theisgen S, Schirbel A, Sbiera S, Huster D, Kross M, Müller P. The adrenal specific toxicant mitotane directly interacts with lipid membranes and alters membrane properties depending on lipid composition. *Molecular and Cellular Endocrinology*. 2016;428:68-81. Accessed 9 August 2017. doi: 10.1016/j.mce.2016.03.022.
79. Li Y, Ge M, Ciani L, Kuriakose g, Westover EJ, Dura M, Covey DF, Freed JH, Maxfield FR, Lytton J, Tabas I. Enrichment of endoplasmic reticulum with cholesterol inhibits sarcoplasmic-endoplasmic reticulum calcium ATPase-2b activity in parallel with increased order of membrane lipids: Implications for depletion of endoplasmic reticulum calcium stores and apoptosis in cholesterol-loaded macrophages. *The Journal of Biological Chemistry*. 2004;279(35):37030-37039. Accessed 2 February 2017. doi: 10.1074/jbc.M405195200.
80. Millendo Therapeutics I. A study of ATR-101 for the treatment of congenital adrenal hyperplasia. <https://clinicaltrials.gov/ct2/show/NCT02804178>. Updated 2017. Accessed 2 August 2017.

Appendix

Appendix 1: Animals

Table 13: Data of the normal adrenals (NAs), adrenocortical adenomas (ACAs) and adrenocortical carcinomas (ACCs) used for quantitative real-time polymerase chain reaction (RT-qPCR) of sterol-O-acyl transferase 1 (SOAT1). The median age of the dogs of which the NAs were obtained from was 777 days (IQR = 1102.). For the ACAs it was 3408 days (IQR = 1186) and for the ACCs it was 3711 days (IQR = 854). F = female, FC = castrated female, M = male, MC = castrated male, * = dog of which metastases were obtained from.

Type of tissue	Dog breed	Gender	Age at time of adrenalectomy (days)
NA	Unknown	Unknown	Unknown
NA	Unknown	Unknown	Unknown
NA	Unknown	Unknown	Unknown
NA	Mixed-breed	F	453
NA	Unknown	M	475
NA	Beagle	M	1773
NA	Unknown	Unknown	Unknown
NA	Mixed-breed	F	691
NA	Mixed-breed	F	Unknown
NA	Mixed-breed	F	863
NA	Unknown	Unknown	Unknown
NA	Unknown	F	1504
ACA	Mixed-breed	M	2958
ACA	Tibetan Terrier	M	4838
ACA	Mixed-breed	FC	4209
ACA	Miniature Wirehaired Dachshund	FC	3364
ACA	Mixed-breed	FC	3981
ACA	Maltese Dog	FC	3379
ACA	Mixed-breed	MC	4196
ACA	West Highland White Terrier	FC	3408
ACA	Miniature Wirehaired Dachshund	MC	2944
ACA	Schnauzer	FC	4883
ACA	Yorkshire Terrier	FC	4113
ACA	Jack Russell Terrier	F	3023
ACA	Jack Russell Terrier	MC	4923
ACA	Golden Retriever	MC	2119
ACA	Polish Lowland Sheepdog	M	3253
ACC	Dutch Decoy Dog	FC	4197
ACC	Chihuahua	F	774
ACC	Maltese Dog	F	4017
ACC	Mixed-breed	F	3592
ACC	Labrador Retriever	FC	2593
ACC	American Staffordshire Terrier	MC	2967
ACC	Mixed-breed	FC	3845
ACC	Mixed-breed	F	2786
ACC	Schnauzer	MC	3462
ACC	Belgian Malinois	F	3662

ACC	Scotch Collie	MC	3967
ACC	Shih Tzu	MC	4132
ACC	White Swiss Shepherd	M	3382
ACC	Labrador Retriever	F	2203
ACC	Jack Russell Terrier	FC	2331
ACC	White Swiss Shepherd	M	3192
ACC	Miniature Schnauzer	M	3983
ACC	Labrador Retriever	FC	3936
ACC	French Bulldog	MC	4182
ACC	Labrador Retriever	MC	4442
ACC	Maltese Dog	FC	3896
ACC	German Pointer	M	4043
ACC	Fox Terrier	M	3996
ACC	Labrador Retriever	FC	3439*
ACC	Basenji	F	4011*
ACC	Welsh Terrier	MC	3179
ACC	Miniature Wirehaired Dachshund	FC	2541
ACC	Jack Russell Terrier	FC	3681*
ACC	Weimaraner	M	2974
ACC	Lhasa Apso	M	3451
ACC	Maltese Dog	F	4354
ACC	Scottish Terrier	MC	2903
ACC	Briard	FC	3254
ACC	Mixed-breed	MC	4215
ACC	Dutch Sheepdog	MC	4210
ACC	Golden Retriever	FC	2806
ACC	Mixed-breed	F	3297
ACC	West Highland White Terrier	FC	3740
ACC	Jack Russell Terrier	M	4066
ACC	Shepherd	M	3830
ACC	Labrador Retriever	FC	3861
ACC	Mixed-breed	MC	4701
ACC	Golden Retriever	FC	4348
ACC	Jack Russell Terrier	M	3496

Table 14: Data of normal adrenals (NAs), adrenocortical adenomas (ACAs) and adrenocortical carcinomas (ACCs) used for immunohistochemistry (IHC) of SOAT1. The median age of the dogs of which the NAs were obtained from was 576 days (IQR: -). For the ACAs it was 3658 days (IQR: 817) and for the ACCs it was 3845 days (IQR: 838). F = female, FC = castrated female, M = male, MC = castrated male, * = dog of which metastases were obtained from.

Type of tissue	Dog breed	Gender	Age at time of adrenalectomy (days)
NA	Beagle	M	1594
NA	Mixed-breed	F	576
NA	Mixed-breed	F	576
NA	Unknown	Unknown	Unknown
ACA	Mixed-breed	M	2958
ACA	Fox Terrier	FC	3402
ACA	Tibetan Terrier	M	4838
ACA	Mixed-breed	FC	4209
ACA	Mixed-breed	M	4094
ACA	Miniature Wirehaired Dachshund	FC	3364
ACA	Mixed-breed	FC	3981
ACA	Maltese Dog	FC	3379
ACA	Mixed-breed	MC	4196
ACA	West Highland White Terrier	FC	3408
ACA	Shepherd	FC	3658
ACC	Unknown	M	Unknown
ACC	Dutch Decoy Dog	FC	4197
ACC	Chihuahua	F	774
ACC	Maltese Dog	F	4017
ACC	Mixed-breed	F	3592
ACC	Beagle	F	3887
ACC	Bouvier des Flandres	FC	4015
ACC	Labrador Retriever	FC	3329
ACC	Labrador Retriever	FC	2593
ACC	American Staffordshire Terrier	MC	2967
ACC	Mixed-breed	FC	3845
ACC	Standard long-haired Dachshund	MC	4529
ACC	Mixed-breed	F	2786
ACC	Schnauzer	MC	3462
ACC	Belgian Malinois	F	3662
ACC	Scotch Collie	MC	3967
ACC	Shih Tzu	MC	4132
ACC	White Swiss Shepherd	M	3382
ACC	Newfoundlander	M	3018
ACC	Mixed-breed	M	3761
ACC	Labrador Retriever	F	2203
ACC	Australian Terrier	FC	4418
ACC	Jack Russell Terrier	FC	2331
ACC	White Swiss Shepherd	M	3192
ACC	Miniature Schnauzer	M	3983
ACC	Labrador Retriever	FC	3936
ACC	French Bulldog	MC	4182

ACC	Labrador Retriever	MC	4442
ACC	Labrador Retriever	FC	4083
ACC	Maltese Dog	FC	3896
ACC	German Pointer	M	4043
ACC	Fox Terrier	M	3996
ACC	Labrador Retriever	FC	3439*
ACC	Basenji	F	4011
ACC	Welsh Terrier	MC	3179
ACC	Miniature Wirehaired Dachshund	FC	2541

Table 15: Data of the normal adrenals (NAs) and adrenocortical carcinoma (ACC) used for our *in vitro* studies. The median age of the dogs of which the NAs were obtained from was 468 days (IQR = 87). F = female, FC = castrated female, M = male.

Type of tissue	Dog breed	Gender	Age at time of adrenalectomy (days)	Purpose
NA	Mixed-breed	F	488	Primer testing
NA	Mixed-breed	F	457	Pilot study 1, lipidomics
NA	Mixed-breed	M	478	Primer testing
NA	Mixed-breed	M	482	Fluorescent imaging of lipid droplets
NA	Beagle	F	621	Pilot study 2, Western Blot UPR
NA	Beagle	F	623	Pilot study 2, Apo-Tox Glo™ Triplex mitotane and ethanol
NA	Mixed-breed	M	426	Follow-up cortisol, Alamar Blue Assay
NA	Mixed-breed	M	437	Follow-up cortisol, Alamar Blue Assay, Caspase-Glo® 3/7 Assay
NA	Mixed-breed	M	428	Follow-up cortisol, Alamar Blue Assay
NA	Mixed-breed	M	453	Follow-up cortisol, Alamar Blue Assay, Caspase-Glo® 3/7 Assay
ACC	Cairn Terrier	FC	4206	Follow-up cortisol, Alamar Blue Assay, Caspase-Glo® 3/7 Assay

Appendix 2: SOAT1 protein expression

Appendix 2.1: ACAs

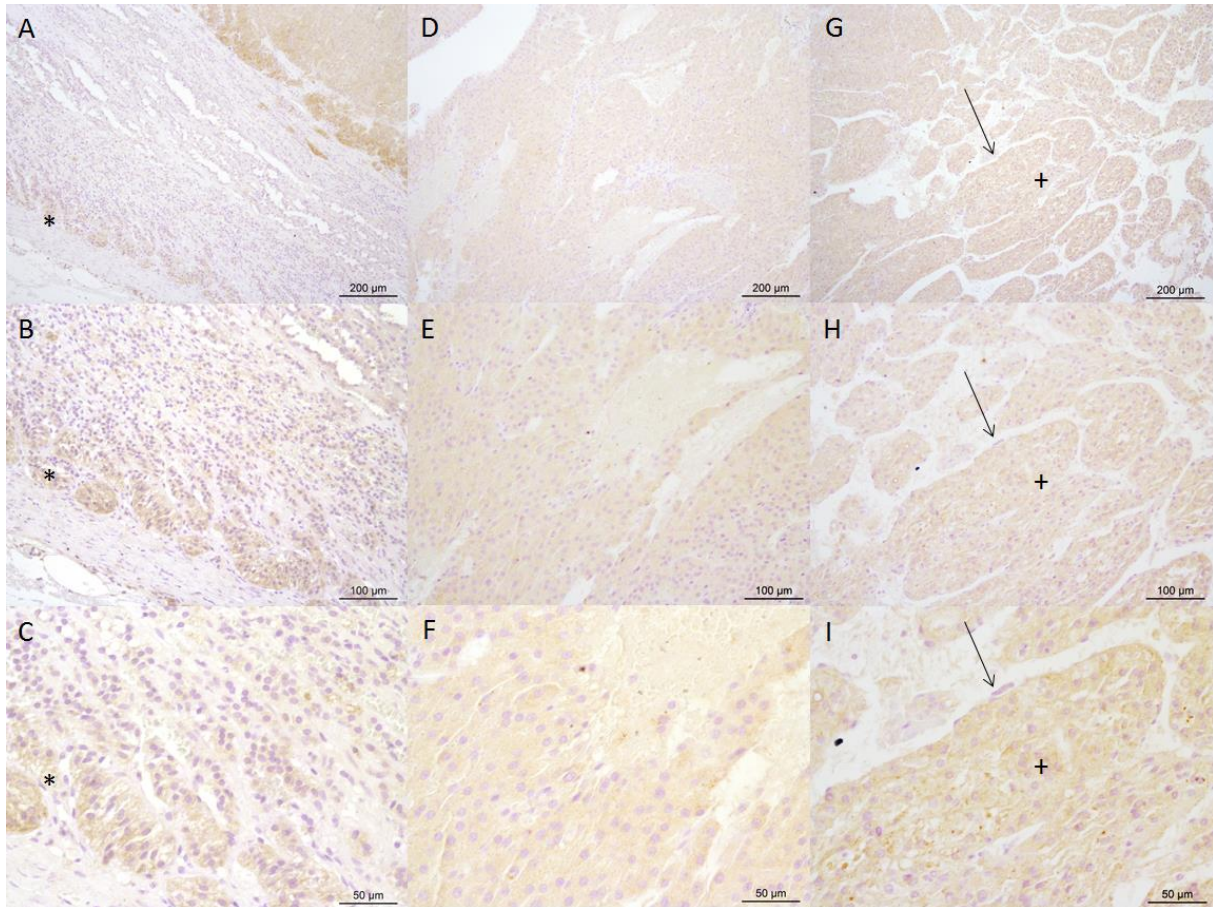


Figure 30: Sterol-O-acyl transferase 1 (SOAT1) protein expression of an adrenocortical adenoma (ACA) with an H-score of 2.1. The ACA shows some zona glomerulosa remnants (asterisk) (A, B and C). The ACA is intense vascularized (arrow) and shows a more equal (D, E and F) and lobulated pattern (plus) (G, H and I). Scale bar represents 200 μ M (A, D and G), 100 μ M (B, E and H) or 50 μ M (C, F and I).

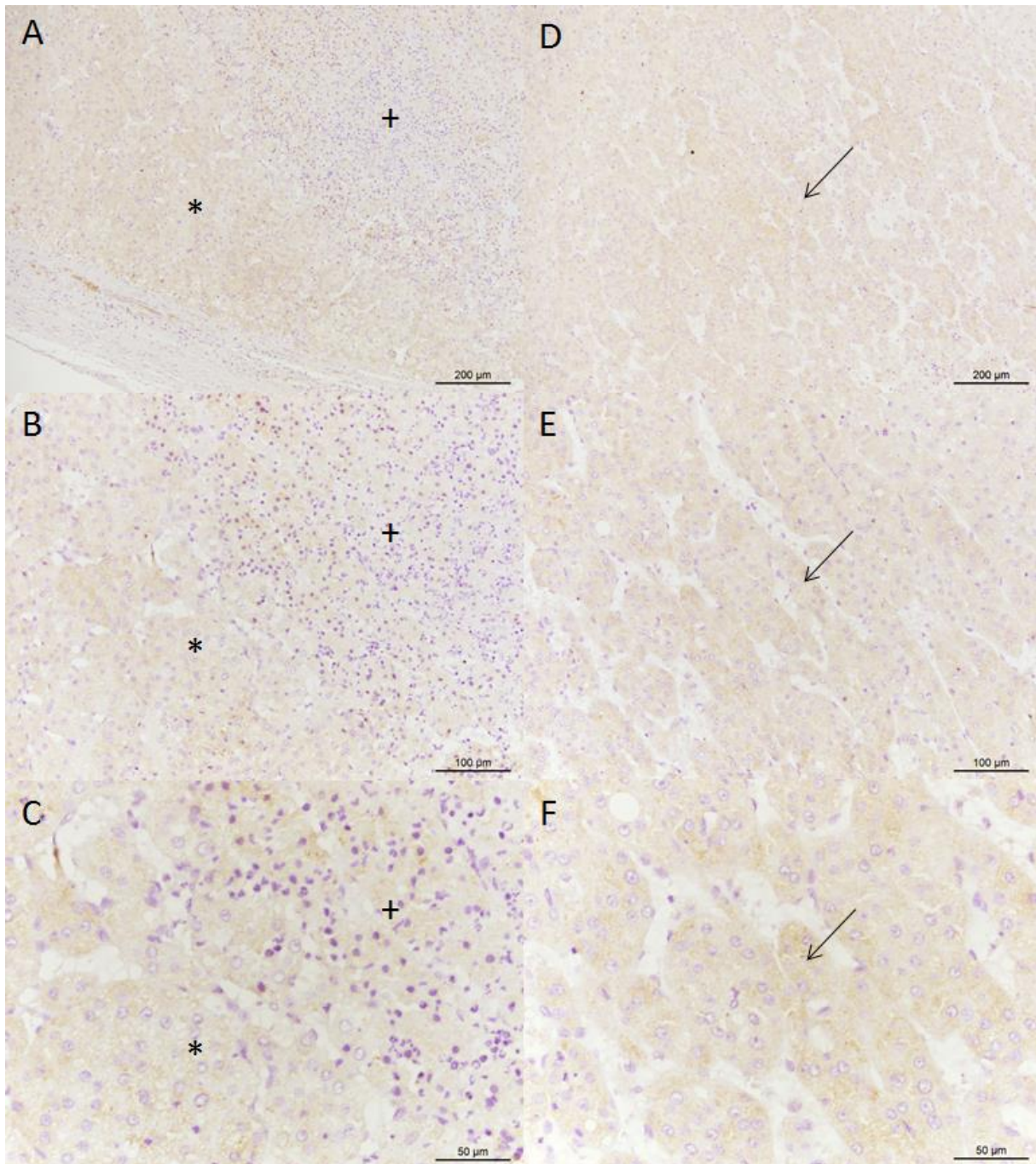


Figure 31: Sterol-O-acyl transferase 1 (SOAT1) protein expression of an adrenocortical adenoma (ACA) with an H-score of 2.4. The ACA shows infiltration of polymorph nuclear cells (asterisk and plus) (A, B and C). The ACA shows a lobulated pattern (arrow) (D, E and F). Scale bar represents 200 μM (A and D), 100 μM (B and E) or 50 μM (C and F).

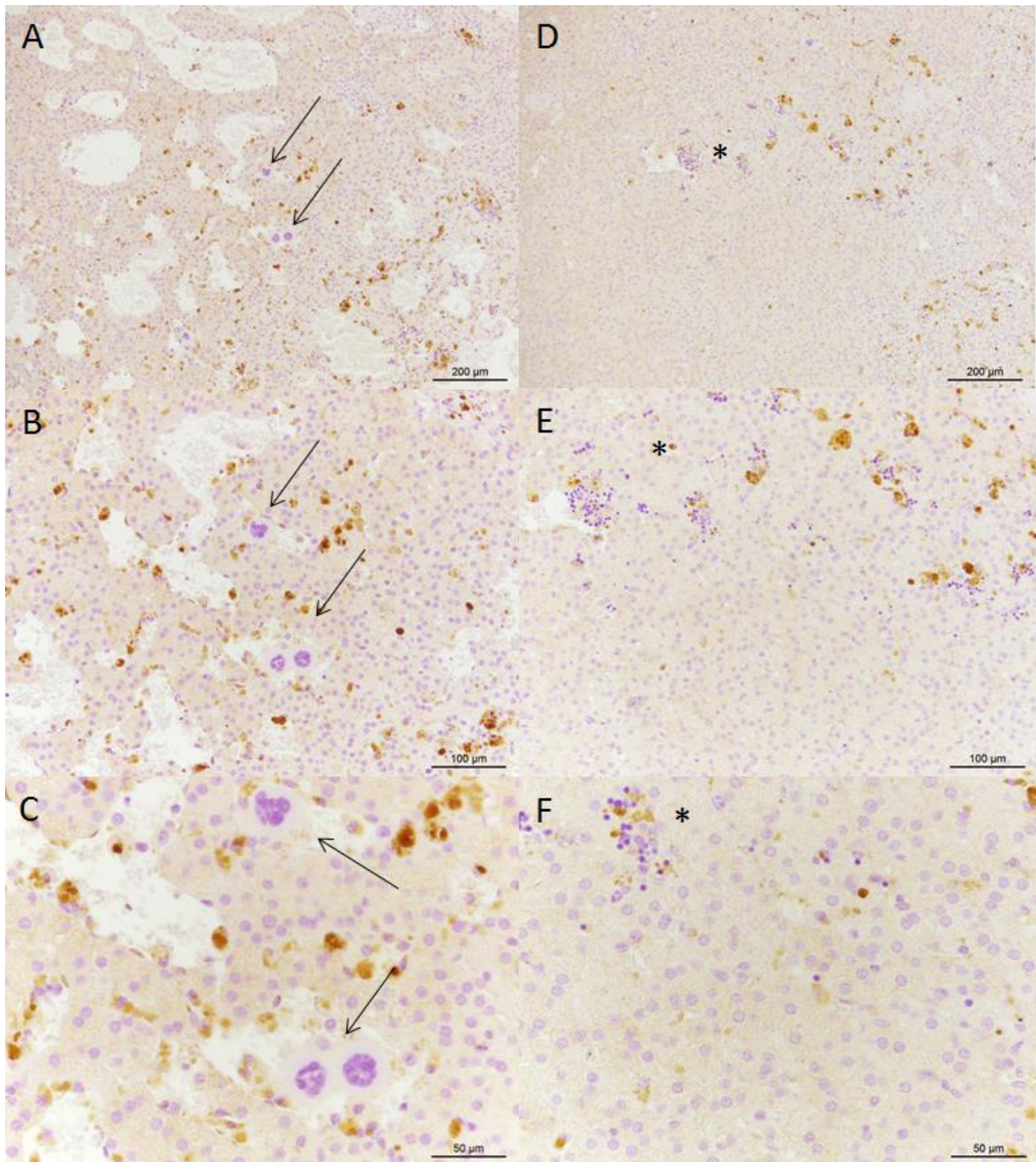


Figure 32: Sterol-O-acyl transferase 1 (SOAT1) protein expression in an adrenocortical adenoma (ACA) with an H-score of 5.0. The ACA shows megakaryocytes (arrow) and haematopoiesis (asterisk). Scale bar represents 200 μm (A and D), 100 μm (B and E) or 50 μm (C and F).

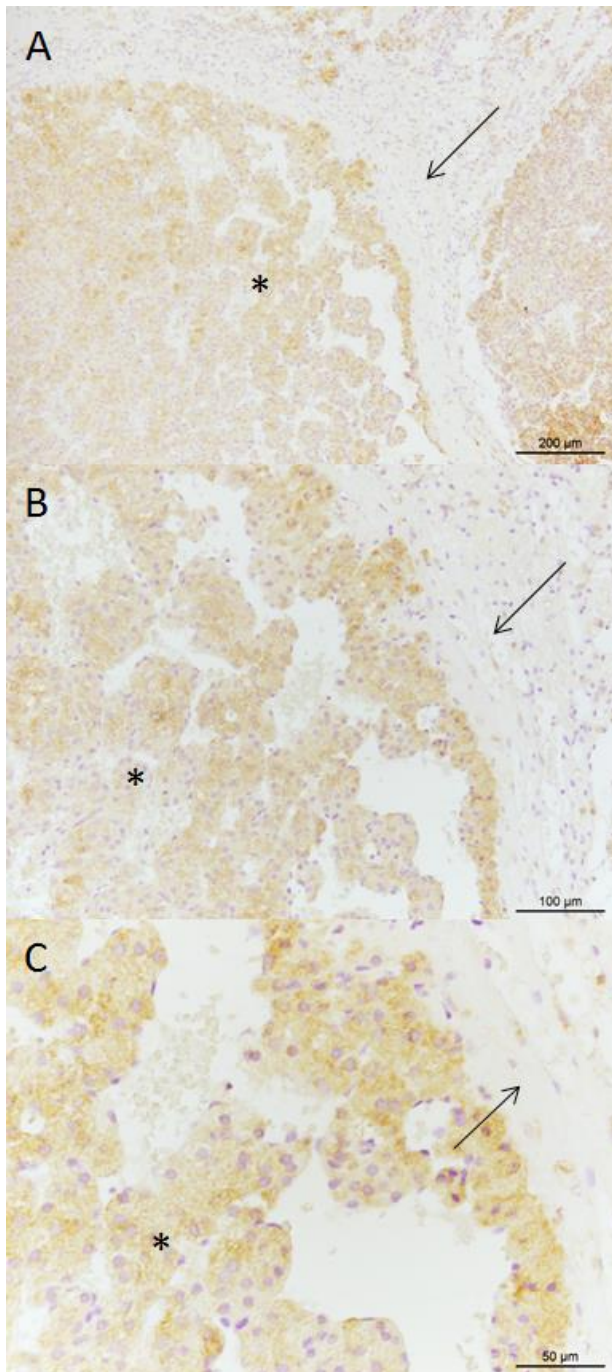


Figure 33: Sterol-O-acyl transferase 1 (SOAT1) protein expression in an adrenocortical adenoma (ACA) with an H-score of 5.0. The ACA shows a fine lobulated structure (asterisk) and a septum (arrow). Scale bar represents 200 μM (A), 100 μM (B) or 50 μM (C).

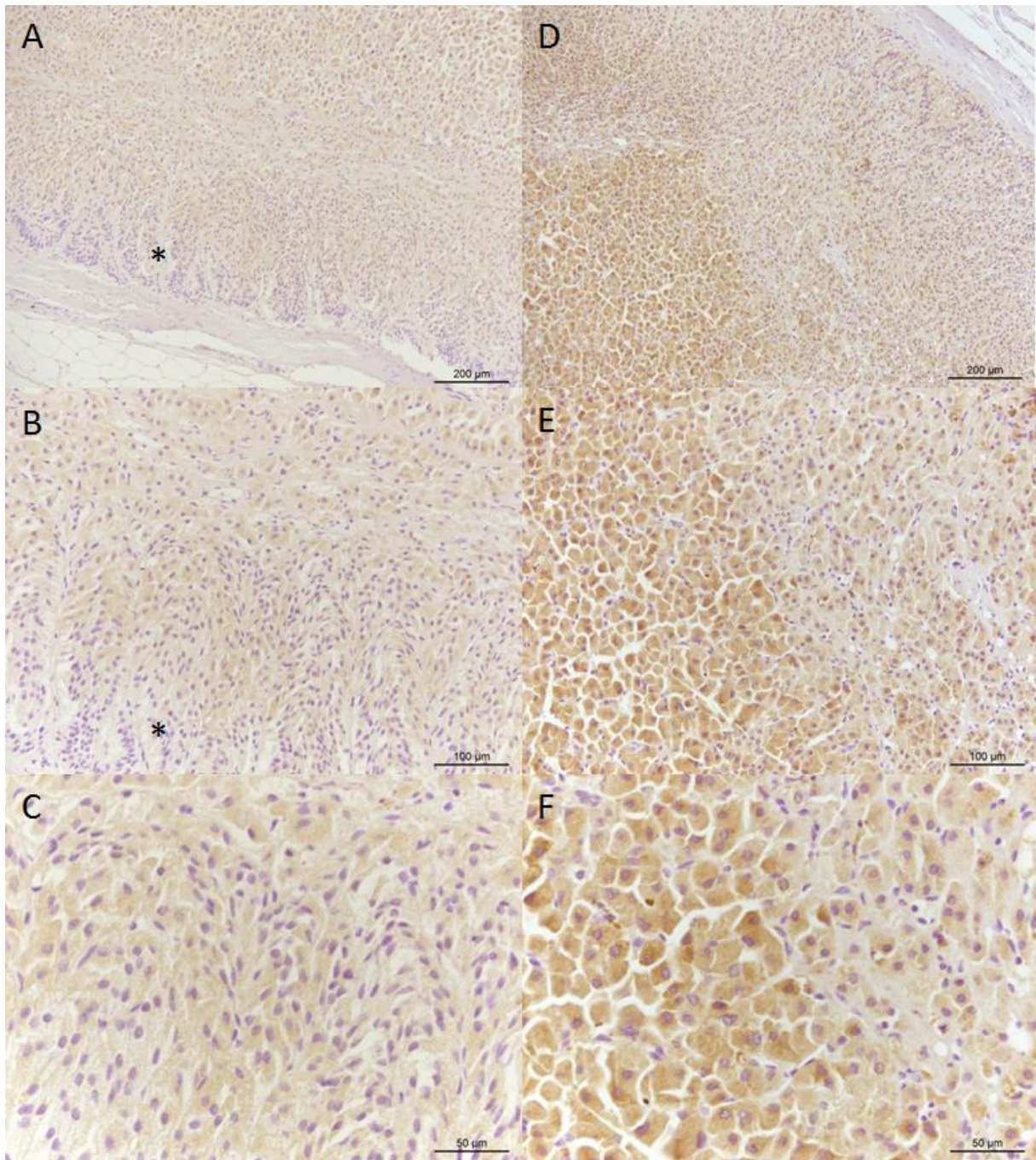


Figure 34: Sterol-O-acyl transferase 1 (SOAT1) protein expression in an adrenocortical adenoma (ACA) with an H-score of 7.6. Some zona glomerulosa remnants are visible (asterisk) (A and B). Part of the ACA stained stronger (D, E and F) than the other part (A, B and C). Scale bar represents 200 μm (A and D), 100 μm (B and E) or 50 μm (C and F).

Appendix 2.2: ACCs

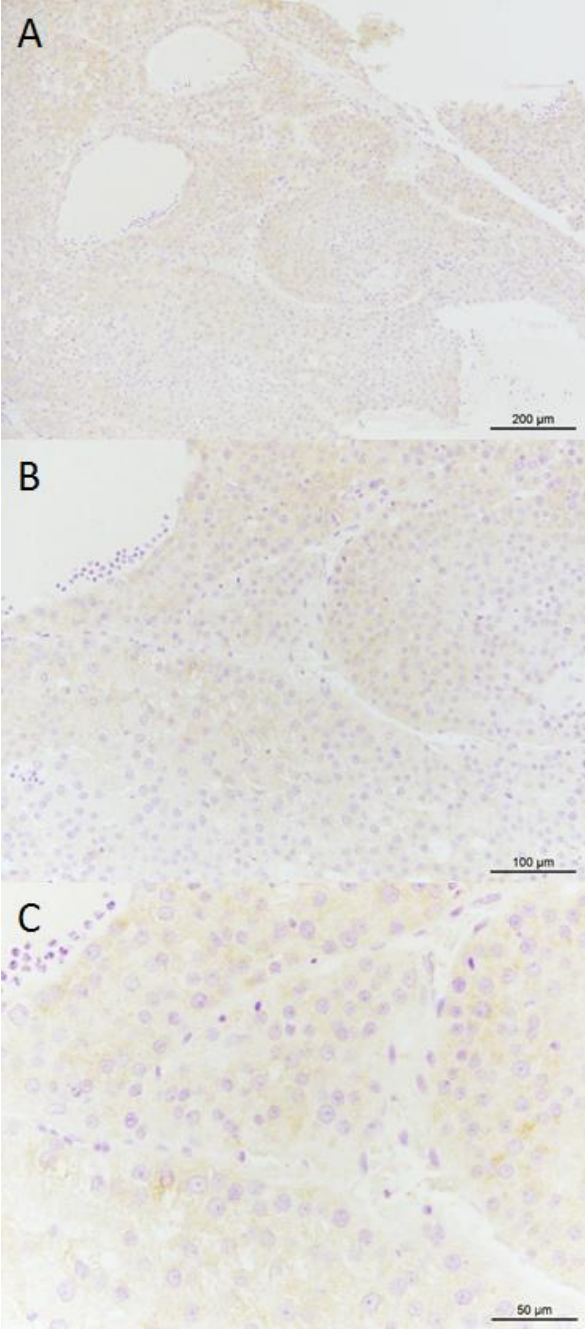


Figure 35: Sterol-O-acyl transferase 1 (SOAT1) protein expression in an adrenocortical carcinoma (ACC) with an H-score of 0.8. Scale bar represents 200 μM (A), 100 μM (B) or 50 μM (C).

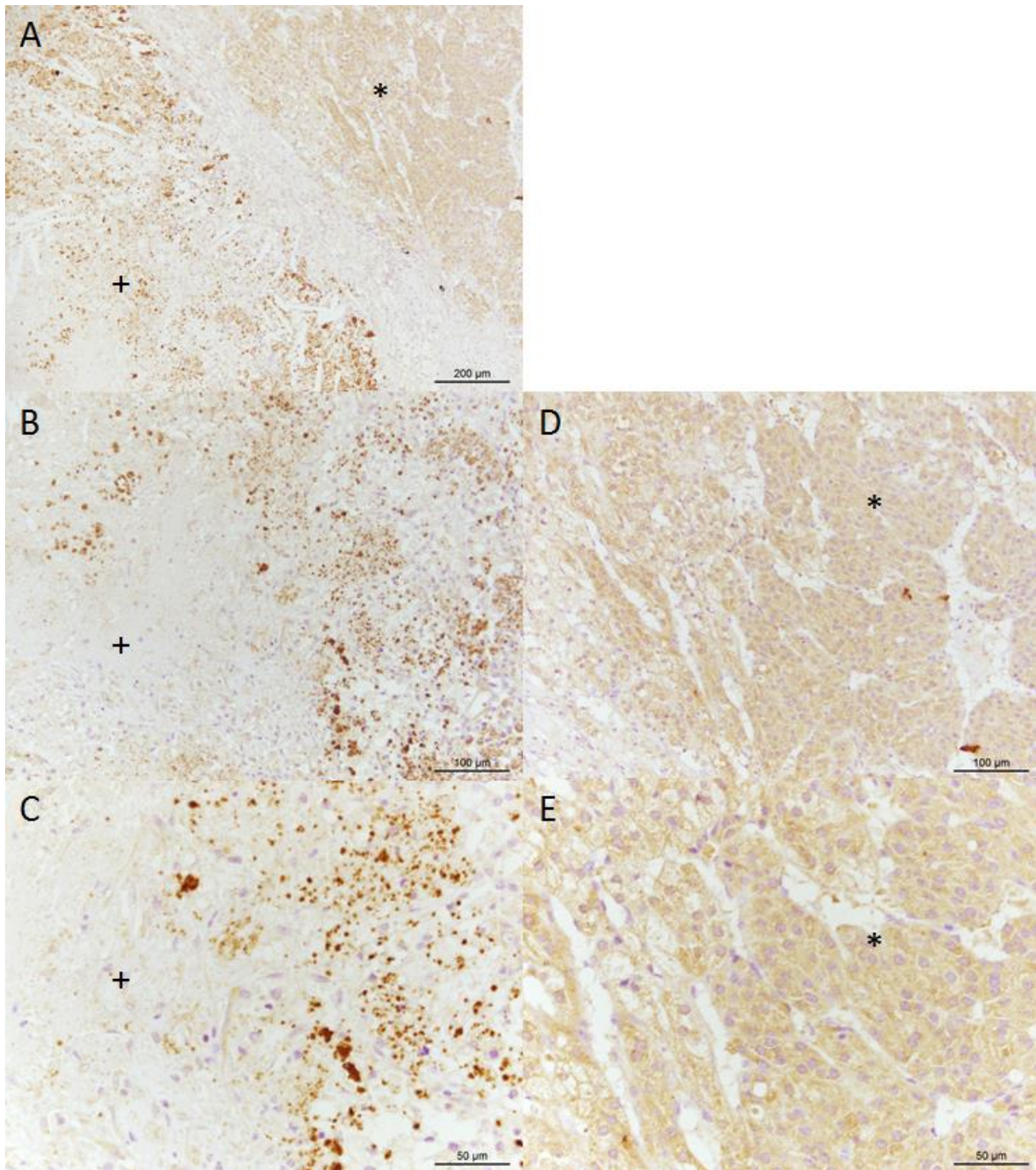


Figure 36: Sterol-O-acyl transferase 1 (SOAT1) protein expression in an adrenocortical carcinoma (ACC) with an H-score of 2.1. The ACC was divided into two parts. One part of the ACC showed a lobulated pattern (asterisk), while the other part showed no structure with some cells (plus). Scale bar represents 200 μ m (A), 100 μ m (B and D) or 50 μ m (C and E).

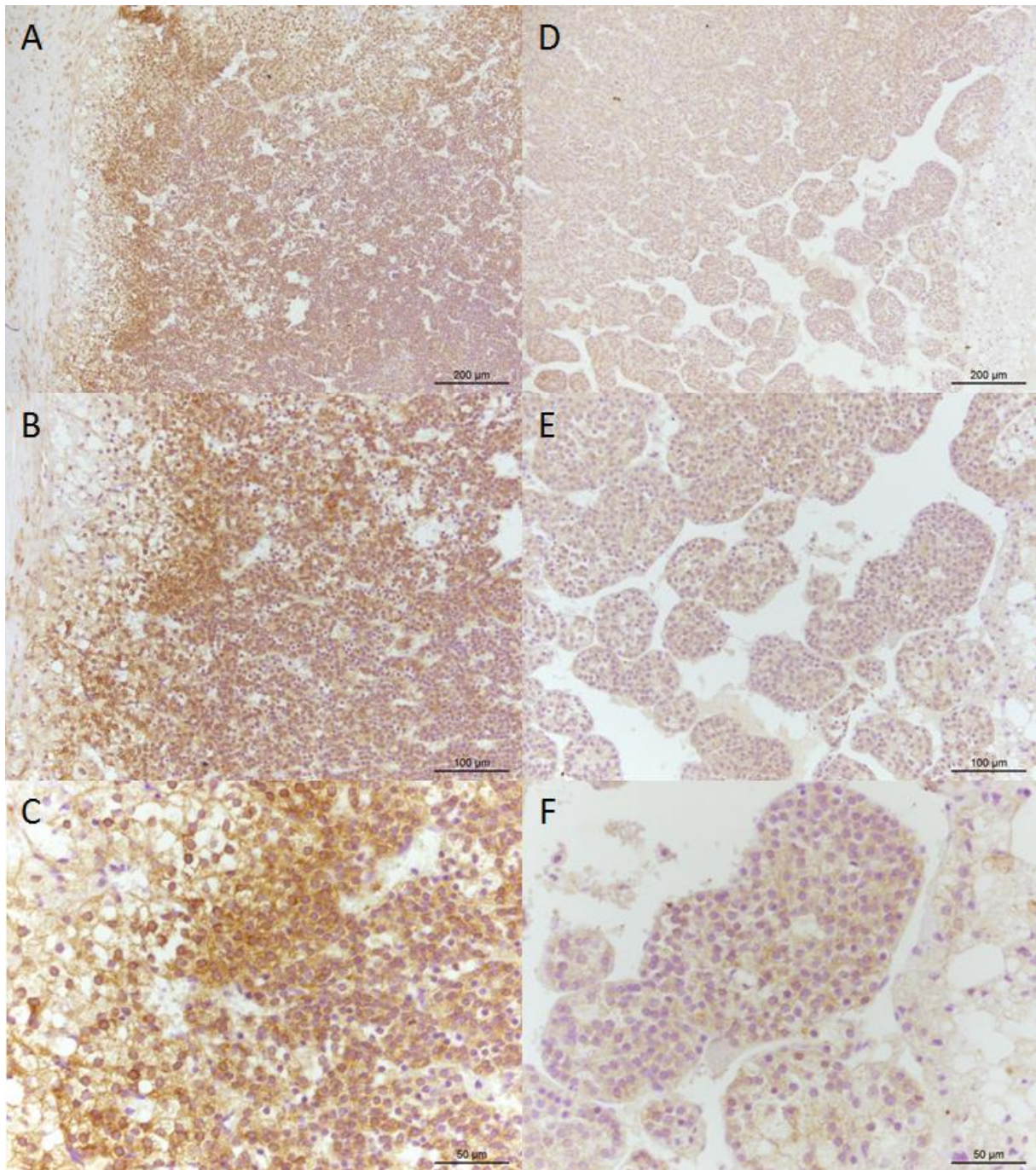


Figure 37: Sterol-O-acyl transferase 1 (SOAT1) protein expression in an adrenocortical carcinoma (ACC) with an H-score of 9.4. Part of the ACC stained stronger (A, B and C) than the other part (D, E and F). The ACC showed a lobulated pattern. Scale bar represents 200 μ M (A and D), 100 μ M (B and E) or 50 μ M (C and F).

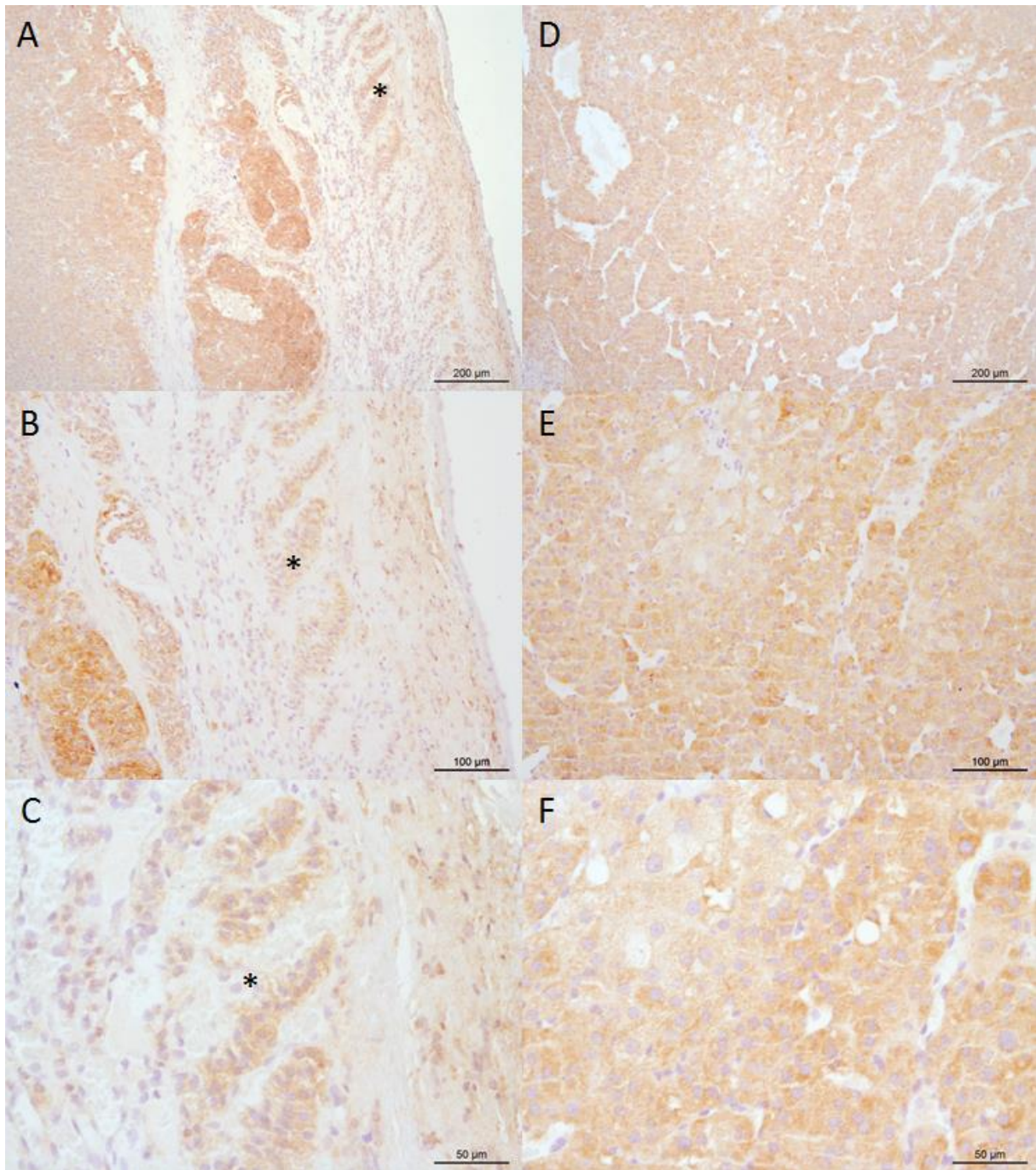


Figure 38: Sterol-O-acyl transferase 1 (SOAT1) protein expression in an adrenocortical carcinoma (ACC) with an H-score of 10.8. The ACC showed zona glomerulosa remnants (asterisk) (A, B and C) and a fine lobulated pattern (D, E and F). Scale bar represents 200 μM (A and D), 100 μM (B and H) or 50 μM (C and F).

Appendix 2.3: Control tissues

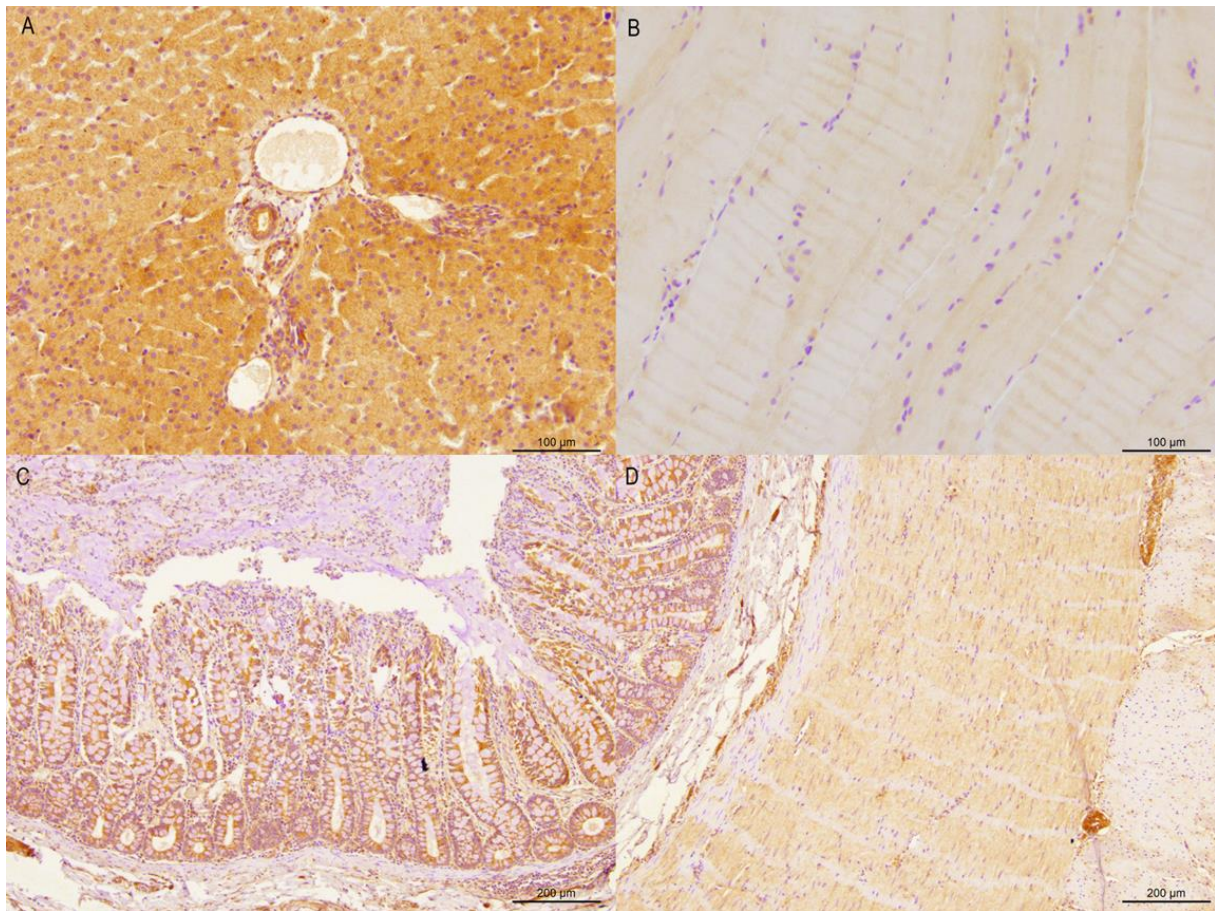


Figure 39: Sterol-O-acyl transferase 1 (SOAT1) protein expression in control tissues. *SOAT1* protein was present in all control tissues. The intensity of staining was the strongest in the liver (A), followed by colon (C and D) and muscle (B). Scale bar represents 200 μM (A and B) or 100 μM (C and D).

Appendix 3: Primers

Table 16: Primer pairs for quantitative real-time polymerase chain reaction (RT-qPCR). *Primer pairs of BAX, Bcl-2, Casp3, CYP17, ERP72, HPRT, RPS5, RPS19, SDHA, SOAT1, SREBF1, SRPR and YWHAZ were developed before the start of this research project. The remaining primer pairs were developed during this research project. In case of multiple transcript variants, all accession numbers are mentioned.* ATF4 = activating transcription factor 4, BAX = Bcl-2 associated X, Bcl-2 = B-cell lymphoma 2, bp = base pairs, Casp3 = caspase 3, CHOP = CCAAT/enhancer-binding protein homologous protein, CYP17 = 17 α -hydroxylase, EDEM1 = ER degradation enhancing α -mannosidase like protein 1, ERP72 = ER protein 72, For = forward primer, GRP78 = glucose-regulated protein 78, HERPUD1 = homocysteine inducible endoplasmic reticulum protein with ubiquitin like domain 1, HPRT = hypoxanthine-guanine phosphoribosyltransferase, p58^{ipk} = DnaJ heat shock protein family member C3, Rev = reverse primer, RPS5 = ribosomal protein S5, RPS19 = ribosomal protein S19, SDHA = succinate dehydrogenase complex subunit A, SOAT1 = sterol-O-acyl transferase 1, SREBF1/2 = sterol regulatory element-binding transcription factor 1/2, SRPR = signal recognition particle receptor, sXBP1 = spliced X-box binding protein, Ta = annealing temperature, uXBP1 = unspliced X-box binding protein, YWHAZ = tyrosin-3-monooxygenase/tryptophan 5-monooxygenase.

Target gene	Sequence (5'→3')	Ta (°C)	Accession number	Length of product (bp)
ATF4	For CTA-GGT-CTC-TTA-GAC-GAC-TAC-C Rev AGG-CAT-CCT-CCT-TTC-CG	61.6	XM_854584.4	144
BAX	For CCT-TTT-GCT-TCA-GGG-TTT-CA Rev CTC-AGC-TTC-TTG-GTG-GAT-GC	58-59	NM_001003011.1	108
Bcl-2	For TGG-AGA-GCG-TCA-ACC-GGG-AGA-TGT Rev AGG-TGT-GCA-GAT-GCC-GGT-TCA-GGT	62	NM_001002949.1	87
Casp3	For CGG-ACT-TCT-TGT-ATG-CTT-ACT-C Rev CAC-AAA-GTG-ACT-GGA-TGA-ACC	61	NM_001003042.1	89
CHOP	For GGG-AGC-TGG-AAG-CCT-G Rev TTT-GAT-TCT-TCC-TCC-TTG-TTT-CC	62.7	XM_014117187.1 XM_005625542.2	102
CYP17	For CCT-GCG-GCC-CCT-ATG-CTC Rev GGC-CGG-TAC-CAC-TCC-TTC-TCA	60	XM_535000.3	134
EDEM1	For TAC-TAC-GCC-ATC-TGG-AAA-CG Rev TTC-TTG-GTT-GCC-TGG-TAG-AG	59.4	XM_533753.4	136
ERP72	For AGG-ACT-CAG-GAA-GAA-ATC-GT Rev GAA-CTC-CAC-CAG-AAT-GAT-GTC	64.9	XM_843145.5	140
GRP78	For GGA-AAG-AAG-GTA-ACC-CAT-GC Rev CCA-AGC-CGT-AAG-CAA-TAG-C	60.5	XM_858292.4	150
HERPUD1	For ATC-TCA-AGG-CCT-GAA-GCT-G Rev TGC-ATG-TAG-TAC-TGC-CGC	64.4	XM_845948.4 XM_014109341.1 XM_005617538.2 XM_005617539.2	127
HPRT	For AGC-TTG-CTG-GTG-AAA-AGG-AC Rev TTA-TAG-TCA-AGG-GCA-TAT-CC	56 and 58	NM_001003357.2	104
P58^{ipk}	For CAG-AGA-TGG-CAG-ATA-CAC-AG Rev CTT-CAA-CAG-GCT-TCT-CAT-CC	62.7	XM_005634019.2	136
RPS5	For TCA-CTG-GTG-AGA-ACC-CCC-T Rev CCT-GAT-TCA-CAC-GGC-GTA-G	62.5	XM_533568.5	141
RPS19	For CCT-TCC-TCA-AAA-AGT-CTG-GG Rev GTT-CTC-ATC-GTA-GGG-AGC-AAG	61 and 63	XM_005616513.2	95
SDHA	For GCCTGGATCTCTTGATGGA Rev TTCTGGCTCTTATGCGATG	61	DQ402985.1	92
SOAT1	For CAA-CTA-TCC-TAG-GAC-TCC-CAG Rev CAT-AGG-ACC-AGA-ACG-CGA	60.3	XM_005622465.2	164
SREBF1	For CAC-TGA-AGC-AAA-GCT-GAA-TAA-GTC Rev TTC-TCC-TGC-TTG-AGC-TTC-TG	61-66	XM_014113166.1	95

SREBF2	For TTG-AGA-AGC-GGT-ATC-GTT-CC Rev CTT-GTG-CAT-CTT-GGC-ATC-TG	61.6	XM_843994.4 XM_014117321.1	85
SRPR	For GCT-TCA-GGA-TCT-GGA-CTG-C Rev GTT-CCC-TTG-GTA-GCA-CTG-G	61.2	XM_546411.5	81
sXBP1	For TGA-GAA-CCA-GGA-GTT-AAG-AC Rev GCT-GCG-GAC-TCA-GCA-GAC-C	62.7	Unknown	120
uXBP1	For CTC-ATG-GCC-TTG-TAG-TTG-AG Rev CAC-GTA-GTC-TGA-GTG-CTG	59.4	XM_849540.4	149
YWHAZ	For CGA-AGT-TGC-TGC-TGG-TGA Rev TTG-CAT-TTC-CTT-TTT-GCT-GA	58	XM_843951.5	94

Appendix 4: Absolute data

Appendix 4.1: Pilot study 1

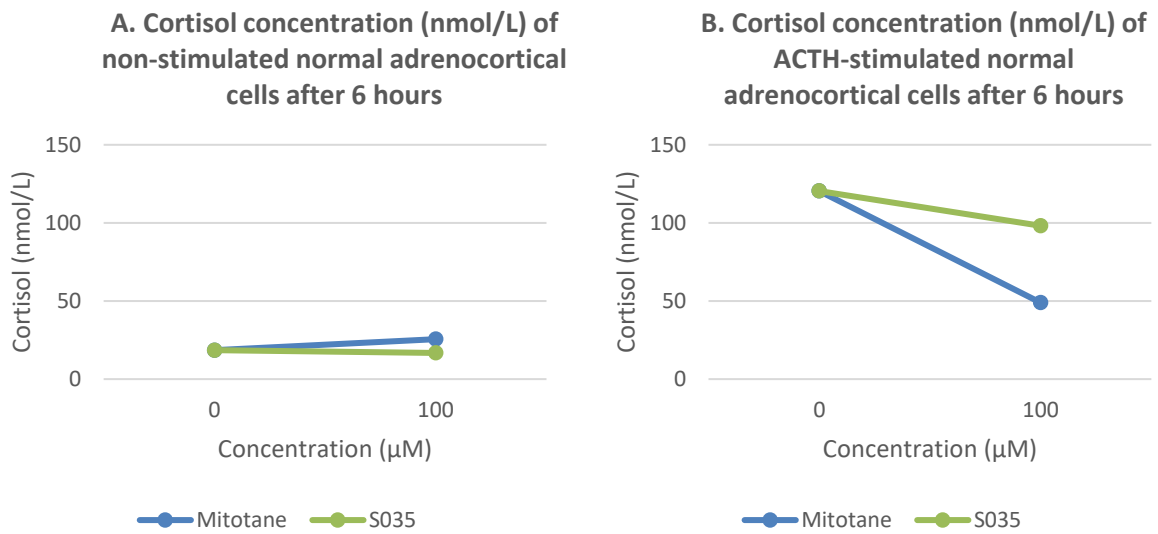


Figure 40: Effects of mitotane and Sandoz 58-035 (S035) on the cortisol concentration (nmol/L) of non-stimulated (A) and ACTH-stimulated (B) normal adrenocortical cells (n=1) after 6 hours.

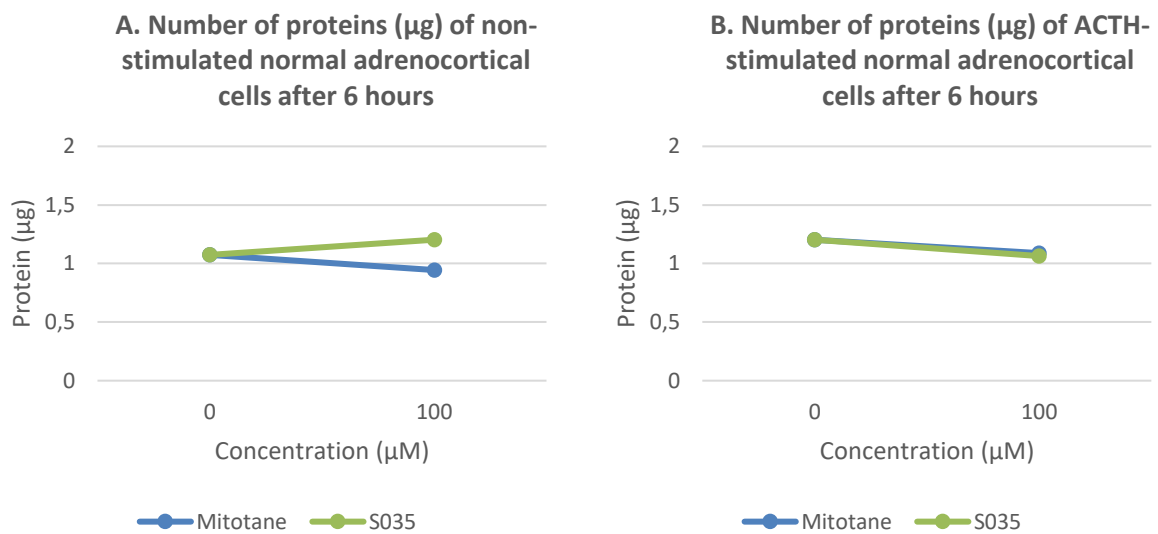


Figure 41: Effects of mitotane and Sandoz 58-035 (S035) on the amount of protein (µg) of non-stimulated (A) and ACTH-stimulated (B) normal adrenocortical cells (n=1) after 6 hours.

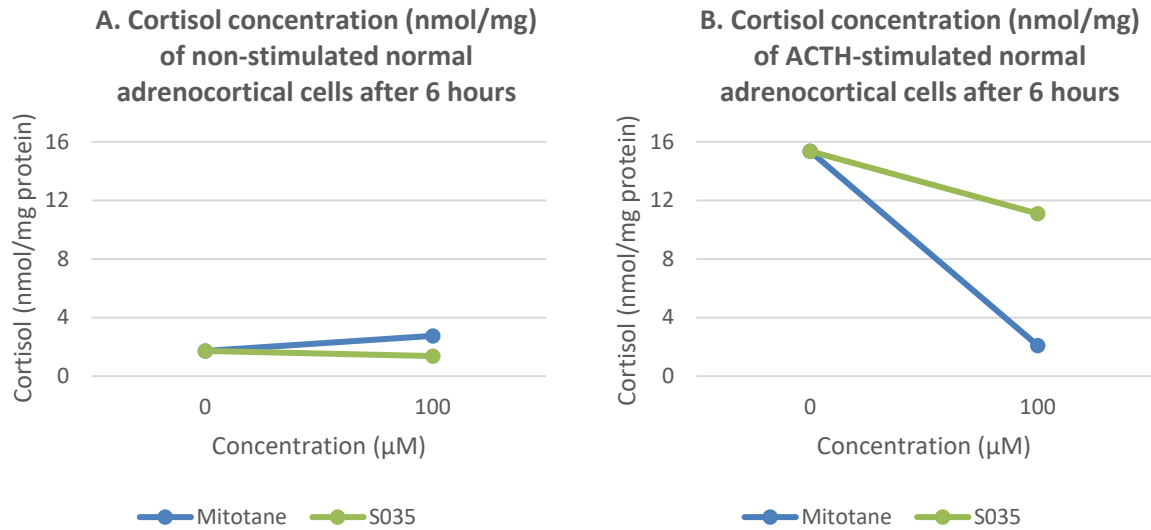


Figure 42: Effects of mitotane and Sandoz 58-035 (S035) on the cortisol concentration (nmol/mg protein) of non-stimulated (A) and stimulated (B) normal adrenocortical cells (n=1) after 6 hours.

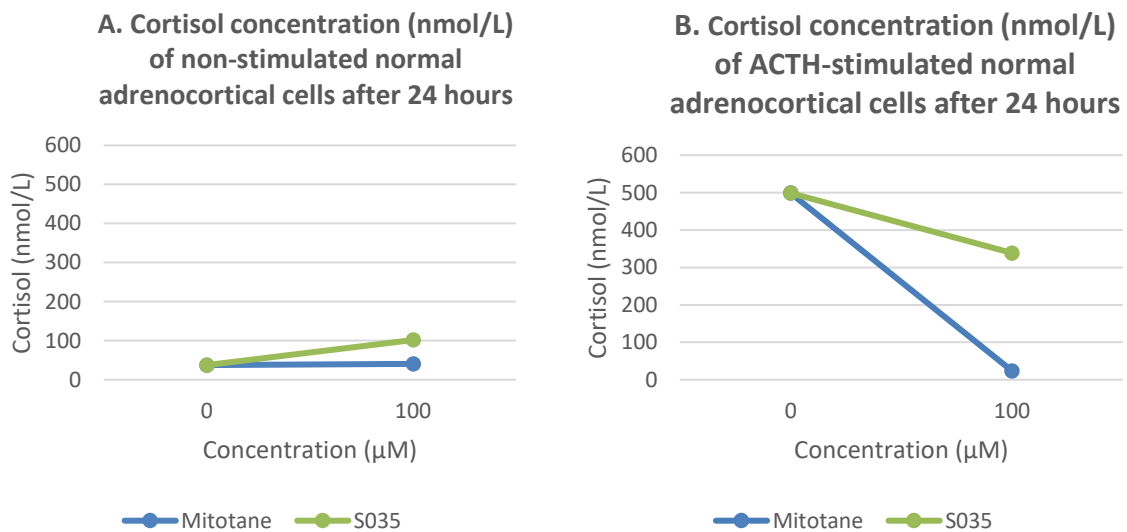


Figure 43: Effects of mitotane and Sandoz 58-035 (S035) on the cortisol concentration (nmol/L) of non-stimulated (A) and ACTH-stimulated (B) normal adrenocortical cells (n=1) after 24 hours.

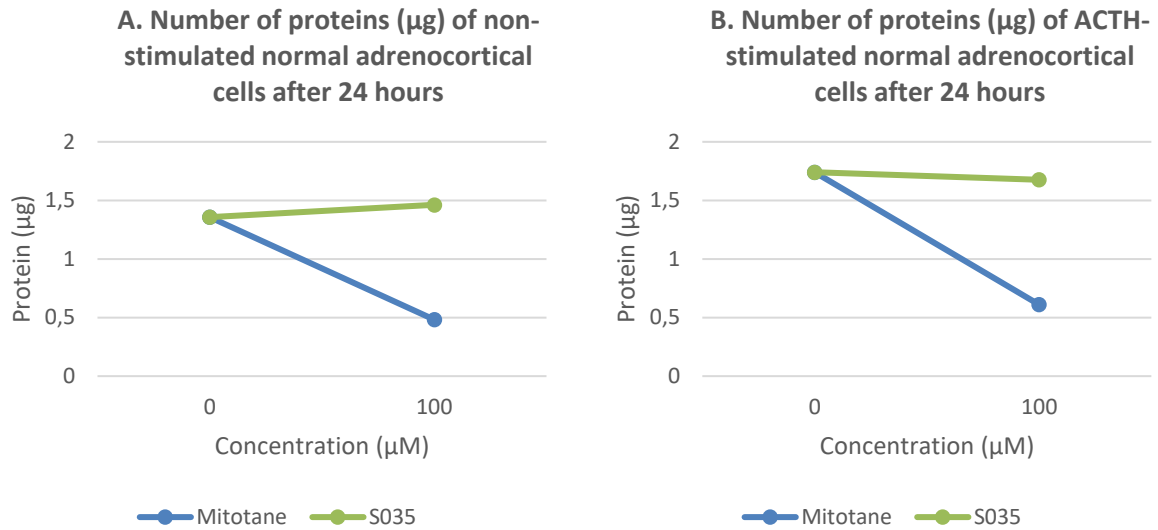


Figure 44: Effects of mitotane and Sandoz 58-035 (S035) on the amount of protein (µg) of non-stimulated (A) and ACTH-stimulated (B) normal adrenocortical cells (n=1) after 24 hours.

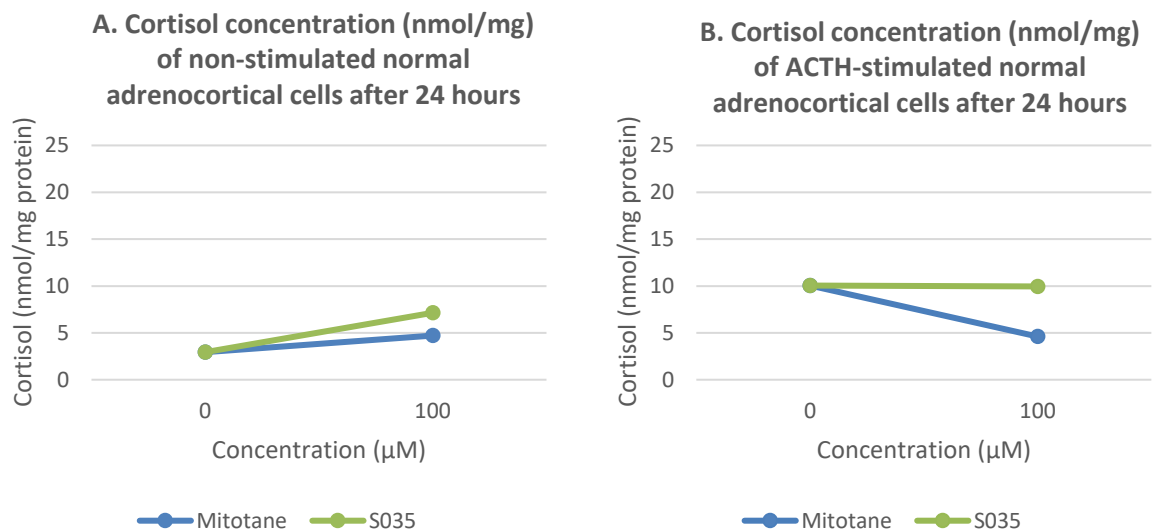


Figure 45: Effects of mitotane and Sandoz 58-035 (S035) on the cortisol concentration (nmol/mg protein) of non-stimulated (A) and ACTH-stimulated (B) normal adrenocortical cells (n=1) after 24 hours.

Appendix 4.2: Pilot study 2

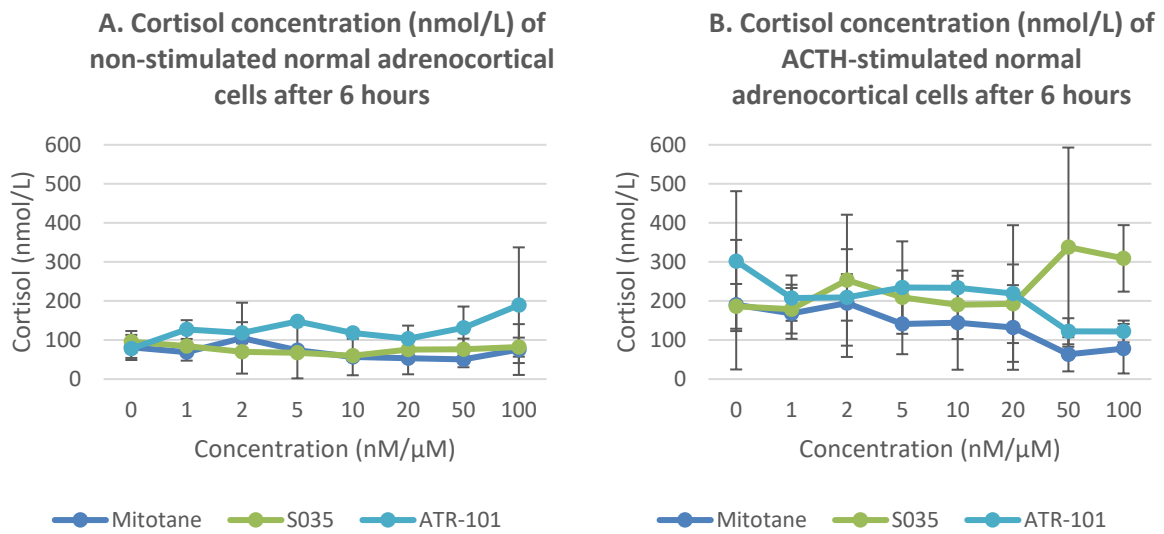


Figure 46: Effects of mitotane, Sandoz 58-035 (S035) and ATR-101 on the cortisol concentration (nmol/L) of non-stimulated (A) and ACTH-stimulated (B) normal adrenocortical cells (n=2) after 6 hours.

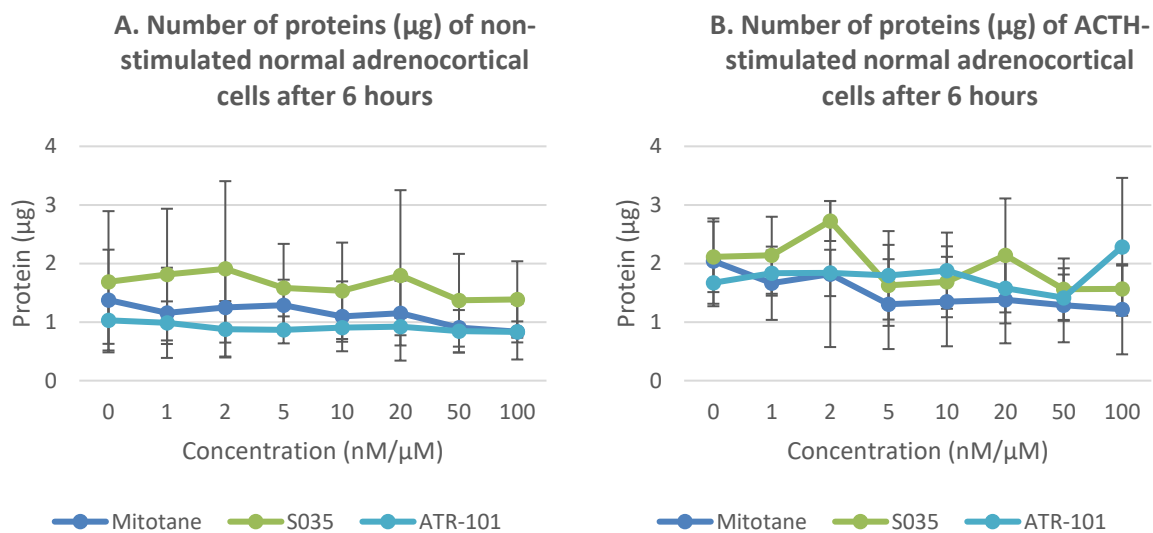


Figure 47: Effects of mitotane, Sandoz 58-035 (S035) and ATR-101 on the amount of protein (μg) of non-stimulated (A) and ACTH-stimulated (B) normal adrenocortical cells (n=2) after 6 hours.

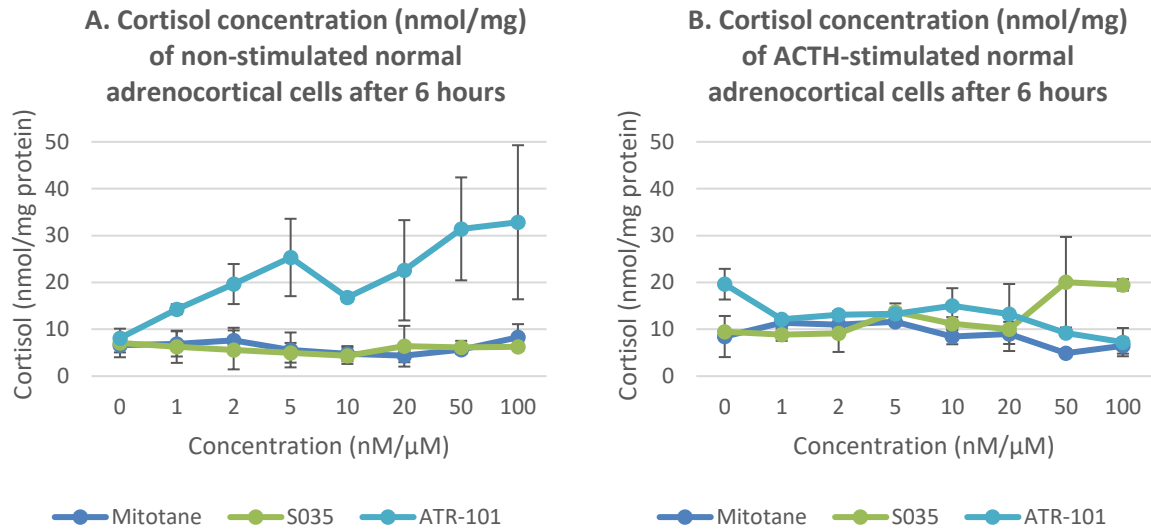


Figure 48: Effects of mitotane, Sandoz 58-035 (S035) and ATR-101 on the cortisol concentration (nmol/mg protein) of non-stimulated (A) and ACTH-stimulated (B) normal adrenocortical cells (n=2) after 6 hours.

Appendix 4.3: Follow-up cortisol

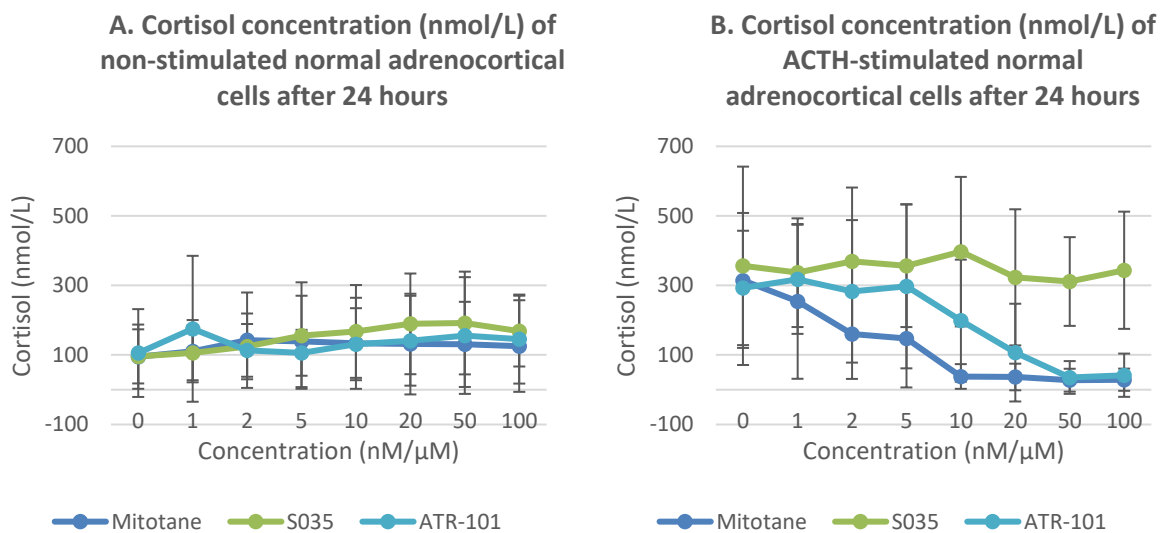


Figure 49: Effects of mitotane, Sandoz 58-035 (S035) and ATR-101 on the cortisol concentration (nmol/L) of non-stimulated (A) and ACTH-stimulated (B) normal adrenocortical cells (n=4) after 24 hours.

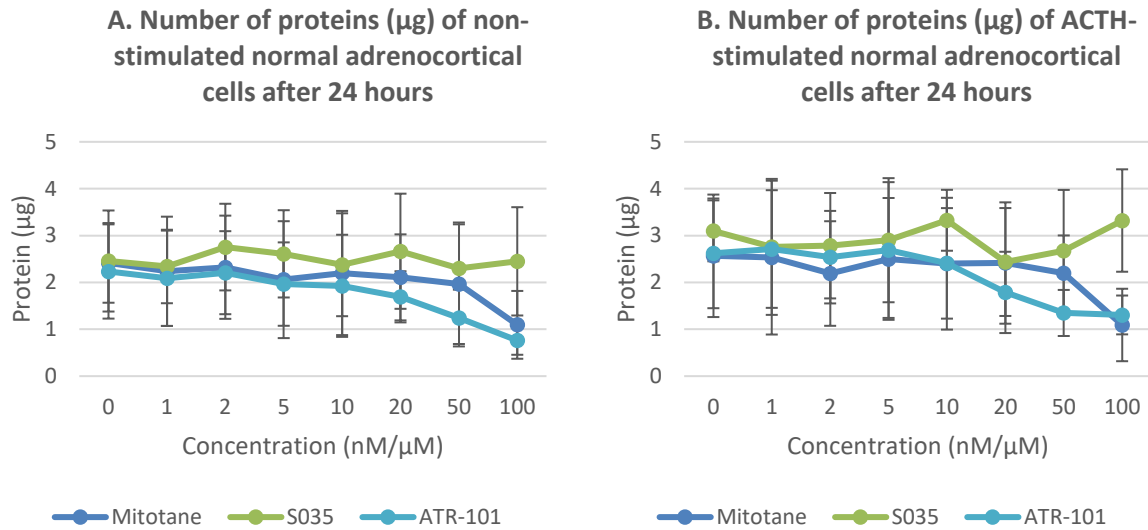


Figure 50: Effects of mitotane, Sandoz 58-035 (S035) and ATR-101 on the amount of protein (μg) of non-stimulated (A) and ACTH-stimulated (B) normal adrenocortical cells (n=4) after 24 hours.

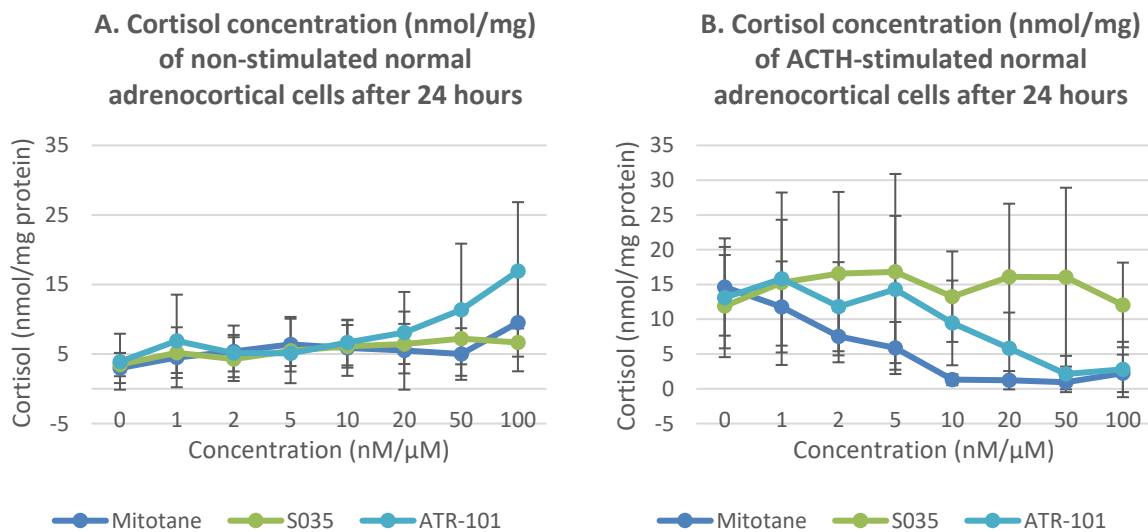


Figure 51: Effects of mitotane, Sandoz 58-035 (S035) and ATR-101 on the cortisol concentration (nmol/mg protein) of non-stimulated (A) and ACTH-stimulated (B) normal adrenocortical cells (n=4) after 24 hours.

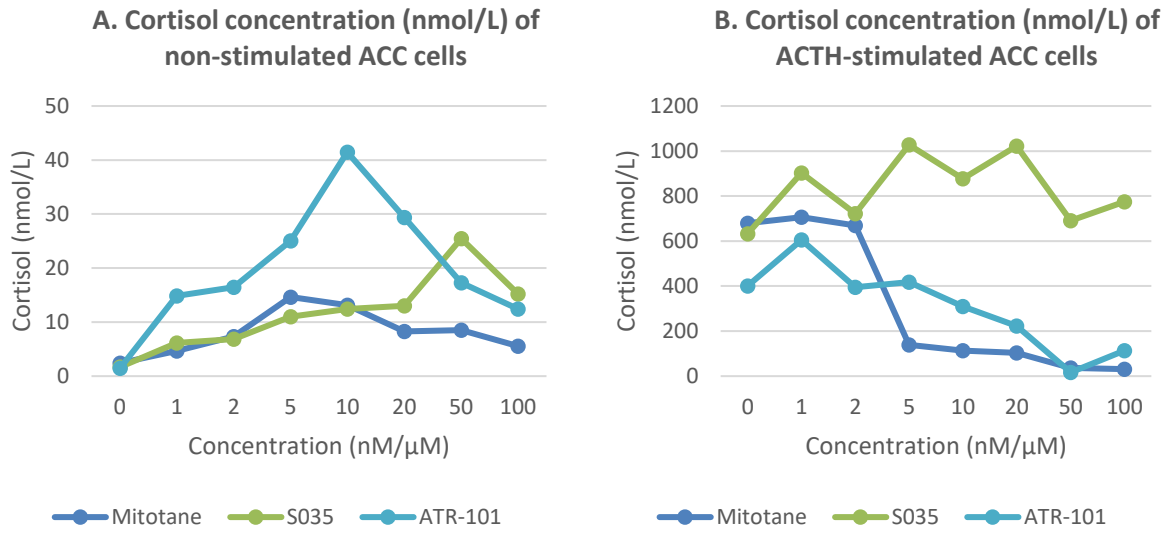


Figure 52: Effects of mitotane, Sandoz 58-035 (S035) and ATR-101 on the cortisol concentration (nmol/L) of non-stimulated (A) and ACTH-stimulated (B) adrenocortical carcinoma (ACC) cells (n=1) after 24 hours.

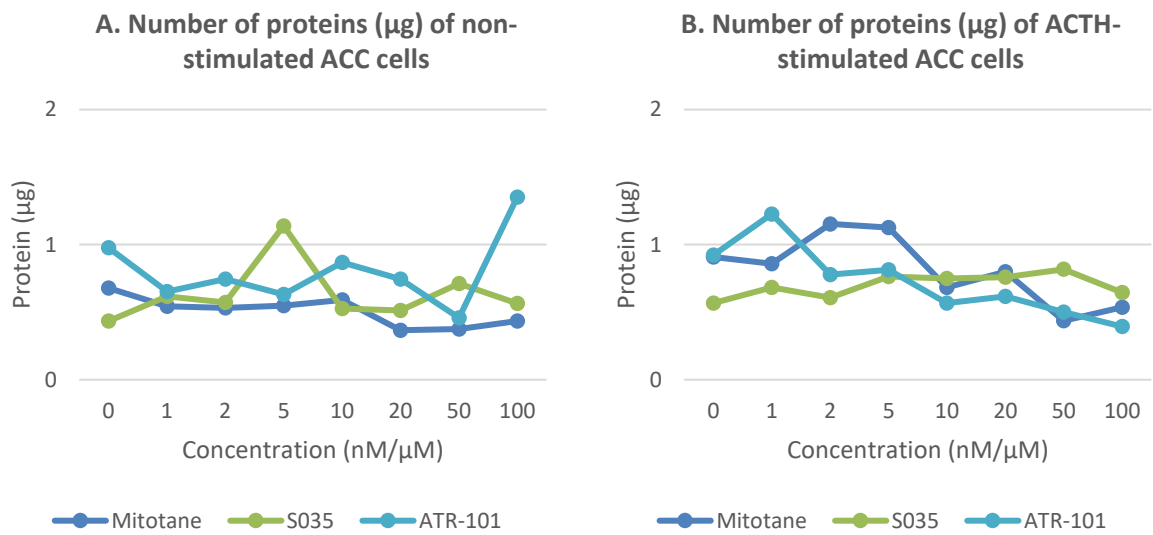


Figure 53: Effects of mitotane, Sandoz 58-035 (S035) and ATR-101 on the amount of protein (μ g) of non-stimulated (A) and ACTH-stimulated (B) adrenocortical carcinoma (ACC) cells (n=1) after 24 hours.

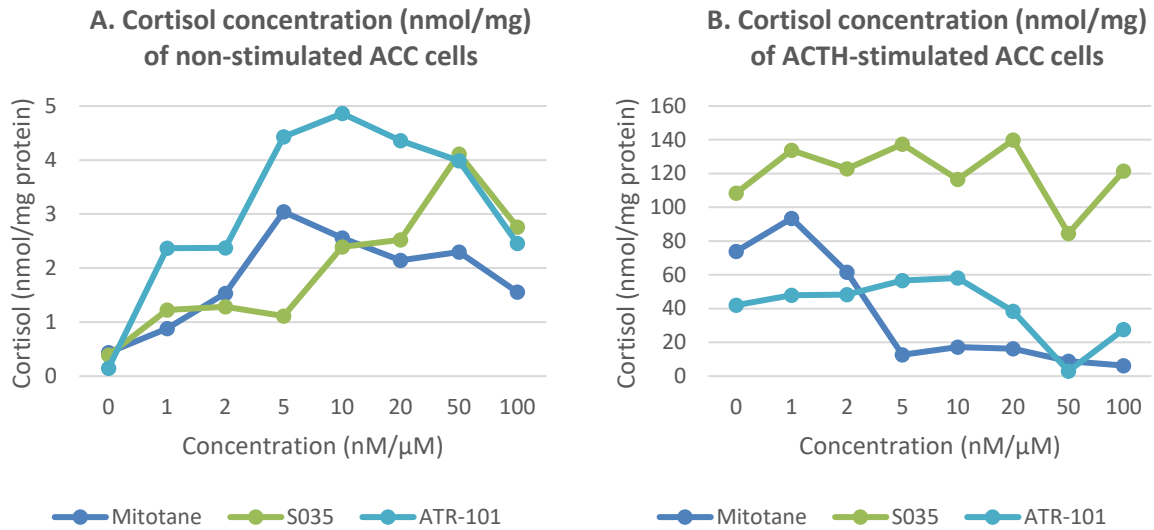


Figure 54: Effects of mitotane, Sandoz 58-035 (S035) and ATR-101 on the cortisol concentration (nmol/mg protein) of non-stimulated (A) and ACTH-stimulated (B) adrenocortical carcinoma (ACC) cells (n=1) after 24 hours.

Appendix 4.4: ApoTox-Glo™ Triplex Assay

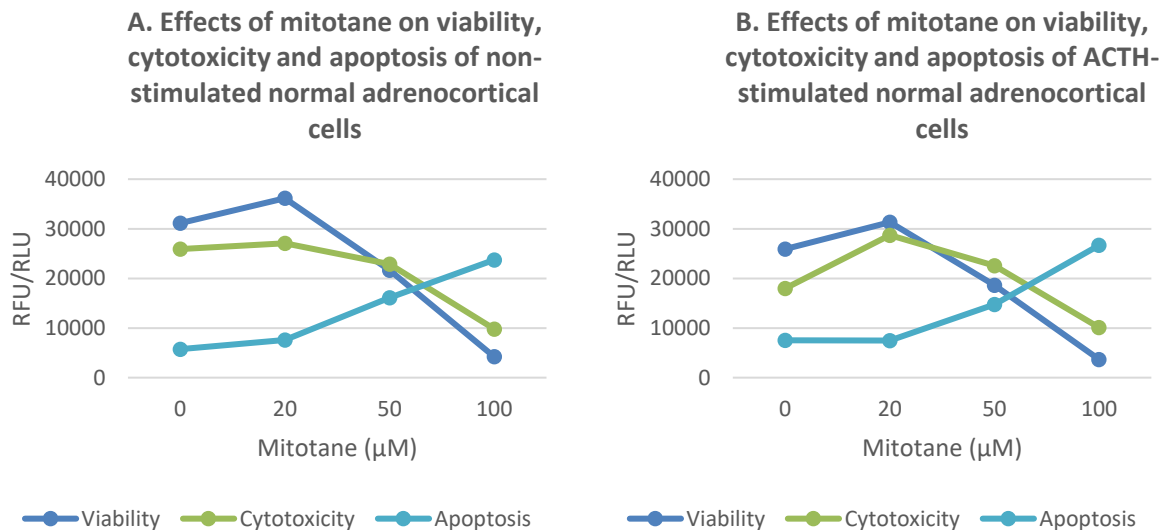


Figure 55: Effects of mitotane on viability, cytotoxicity and apoptosis of non-stimulated (A) and ACTH-stimulated (B) normal adrenocortical cells (n=1) after 24 hours measured by the ApoTox-Glo™ Triplex Assay. RFU = relative fluorescence units, RLU = relative luminescence units.

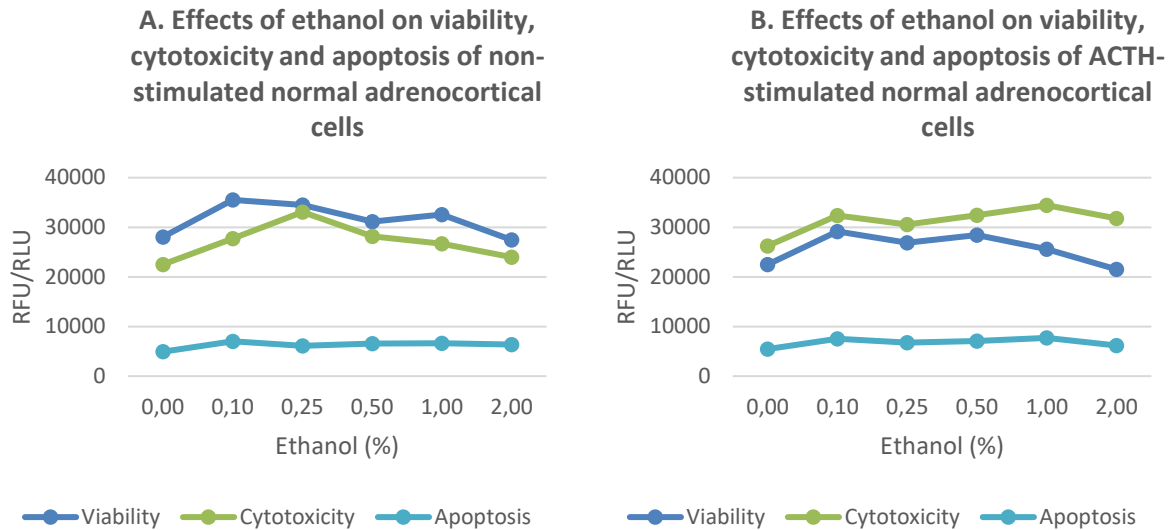


Figure 56: Effects of ethanol on viability, cytotoxicity and apoptosis of non-stimulated (A) and ACTH-stimulated (B) normal adrenocortical cells (n=1) after 24 hours measured by the ApoTox-Glo™ Triplex Assay. RFU = relative fluorescence units, RLU = relative luminescence units.

Appendix 4.5: Follow-up apoptosis and viability

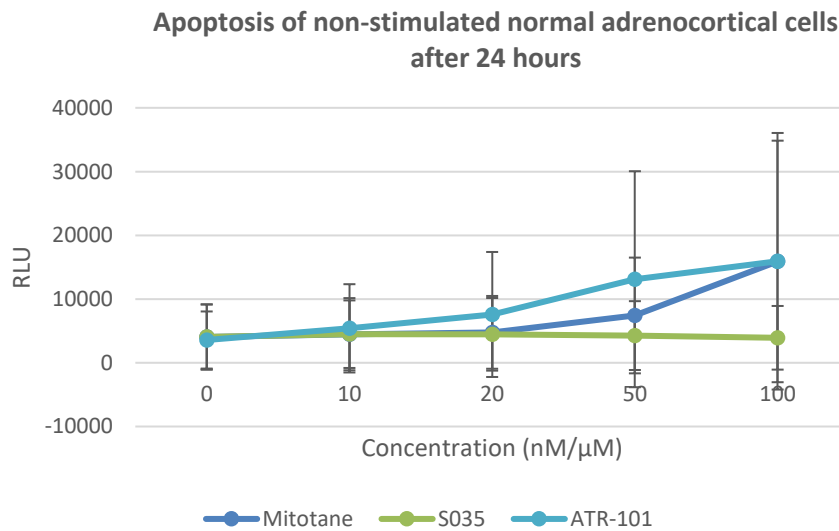


Figure 57: Effects of mitotane, Sandoz 58-035 (S035) and ATR-101 on apoptosis of non-stimulated normal adrenocortical cells (n=2) after 24 hours measured by the Caspase-Glo® 3/7 Assay. RLU = relative luminescence units.

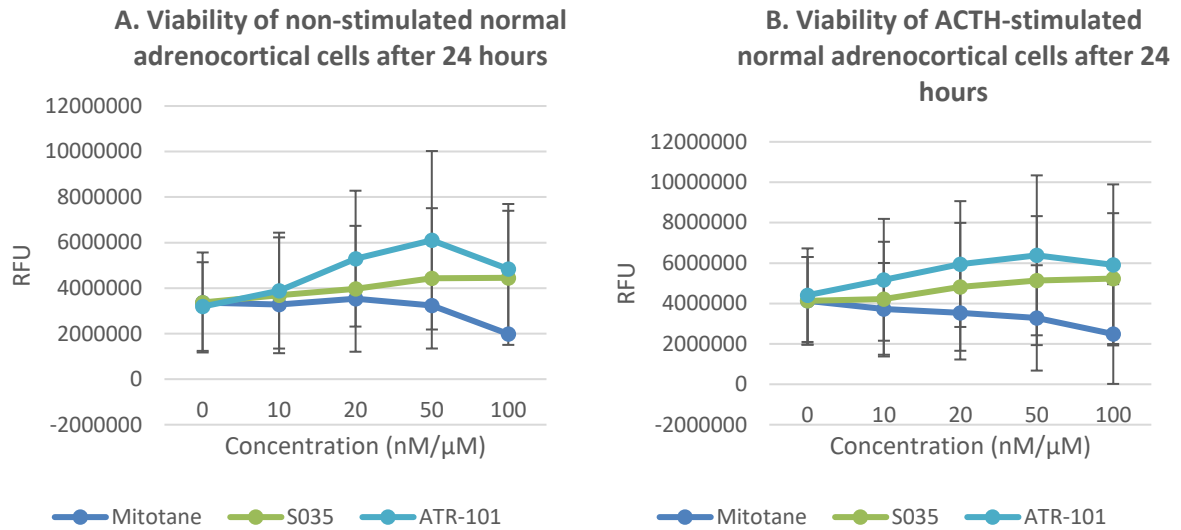


Figure 58: Effects of mitotane, Sandoz 58-035 (S035) and ATR-101 on viability of non-stimulated (A) and ACTH-stimulated (B) normal adrenocortical cells (n=4) after 24 hours measured by the alamarBlue® Assay. RFU = relative fluorescence units.

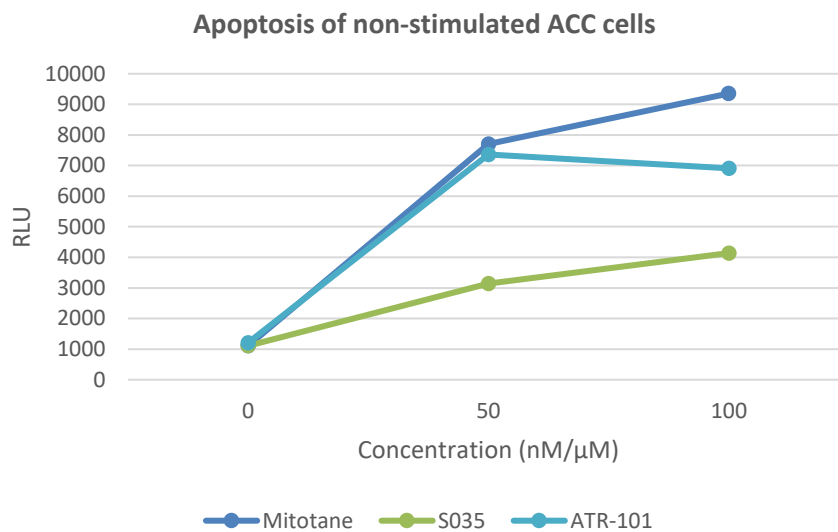


Figure 59: Effects of mitotane, Sandoz 58-035 (S035) and ATR-101 on apoptosis of non-stimulated adrenocortical carcinoma (ACC) cells (n=1) after 24 hours measured by the Caspase-Glo® 3/7 Assay. RLU = relative luminescence units.

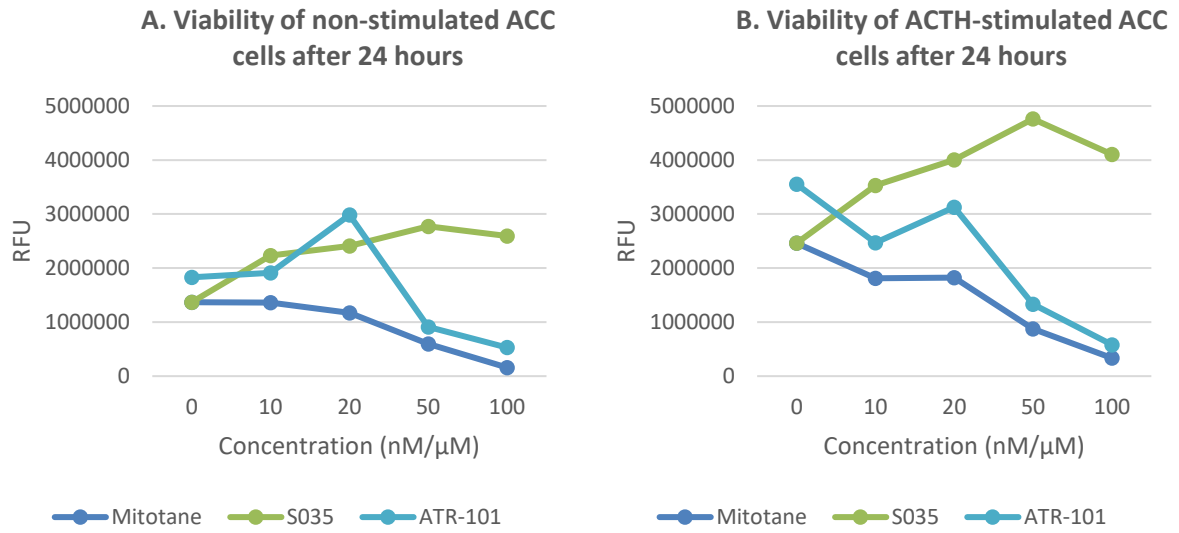


Figure 60: Effects of mitotane, Sandoz 58-035 (S035) and ATR-101 on viability of non-stimulated (A) and ACTH-stimulated (B) adrenocortical carcinoma (ACC) cells (n=1) after 24 hours measured by the alamarBlue® Assay. RFU = relative fluorescence units.

Appendix 5: Lipidomics

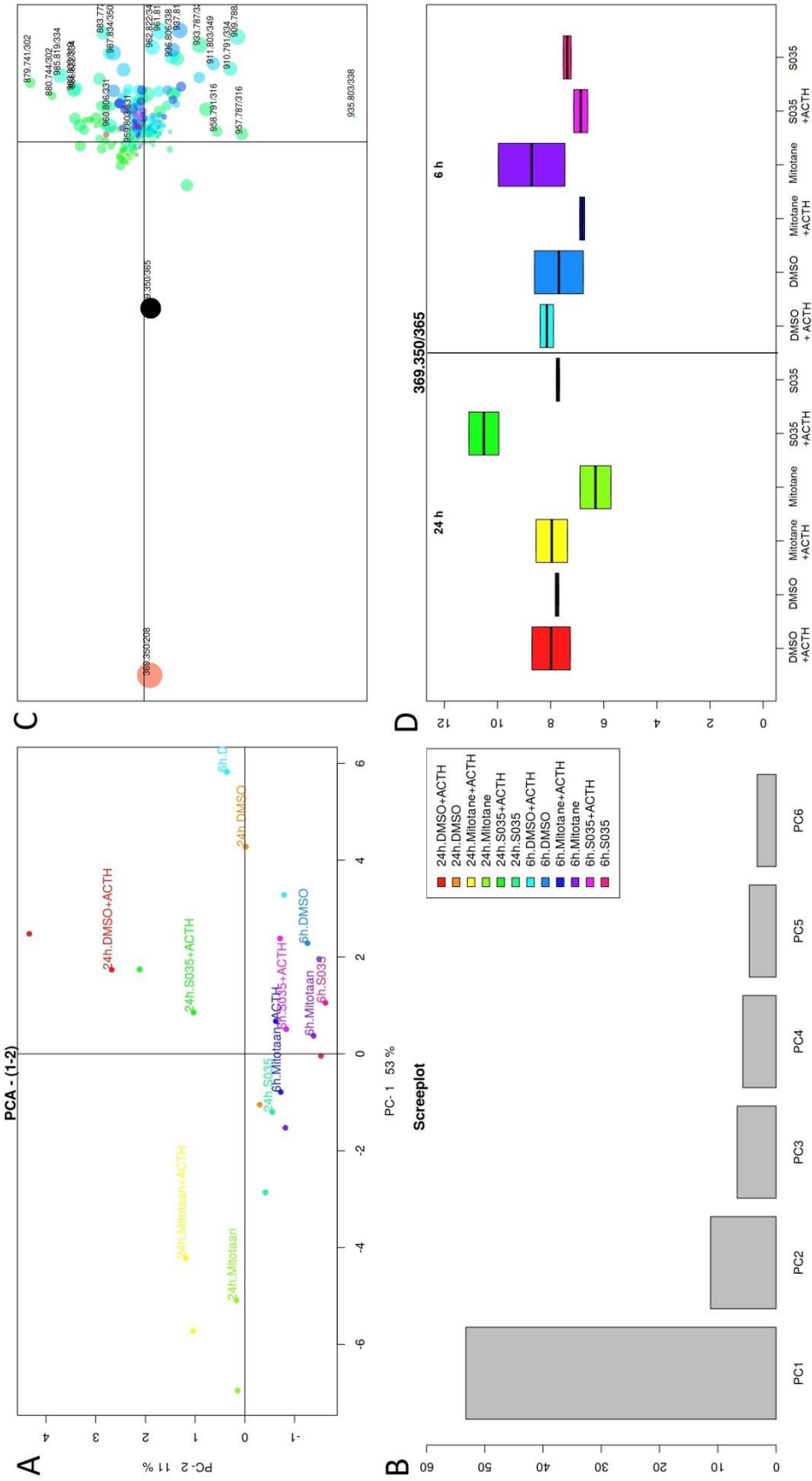


Figure 61: Effects of mitotane and Sandoz 58-035 (S035) on lipid metabolism of non-stimulated and ACTH-stimulated normal adrenocortical cells (n=1) after 6 and 24 hours.